



THESIS
2
2010



This is to certify that the
thesis entitled

INVESTIGATION OF TRACTION DRIVE SYSTEMS FOR
SERIES HYBRID ELECTRIC BUSES

presented by

Craig B. Rogers

has been accepted towards fulfillment
of the requirements for the

 M.S. degree in Electrical Engineering

Major Professor's Signature

 Nov. 11, 2009

Date

PLACE IN RETURN BOX to remove this checkout from your record.
TO AVOID FINES return on or before date due.
MAY BE RECALLED with earlier due date if requested.

DATE DUE	DATE DUE	DATE DUE

**INVESTIGATION OF TRACTION DRIVE SYSTEMS FOR SERIES HYBRID
ELECTRIC BUSES**

By

Craig B. Rogers

A THESIS

Submitted to

Michigan State University

in partial fulfillment of the requirements

for the degree of

MASTER OF SCIENCE

Electrical Engineering

2009

ABSTRACT

INVESTIGATION OF TRACTION DRIVE SYSTEMS FOR SERIES HYBRID ELECTRIC BUSES.

By

Craig B. Rogers

Abstract—This paper presents a comparison of power electronics topology designs for implementation in a Series Hybrid Electric Bus project. This specific hybrid vehicle design uses an internal combustion diesel engine (ICE), an ac electric generator, a passive/active rectifier/inverter, power storage, a traction motor inverter, and a traction motor/brake. The value of the hybrid vehicle comes from its increased efficiencies. The hybrid system decouples the ICE's power and speed from that of the bus. This decoupling is accomplished by replacing the traditional mechanical or hydro mechanical transmission with power electronics and energy storage facilities. This decoupling allows ICE operation at its most efficient power versus speed point. During normal operation, the energy storage system can be used to handle the dynamic loads and the internal combustion engine can handle the steady loading. This hybrid system also recaptures braking energy which is lost with conventional bus systems. The power electronics facilitate the process via control of power flow, battery management, motor control and generator control. There are two presently existing inverter/converter configurations that can be designed to implement these power electronics solutions. There is also a new solution using the novel Z-Source inverter as a current source inverter. Each of these designs have specific operation modes, control methods and features that are analyzed and discussed in this paper. The advantages and disadvantages of each are discussed. The concepts are then demonstrated via simulation and experimental results.

DEDICATION

Dedicated to my Brother

John Russell Rogers

June 09, 1961 – February 24, 2008

ACKNOWLEDGEMENTS

I would like to thank my parents for their guidance love and support throughout the years. Without them and their instilled values of perseverance, this work would not have been possible.

I would further like to thank my advisor Dr. Peng for his support, guidance and encouragement. Thank you for all that you have taught me in the years that I have known you.

I would also like to thank Dr. Strangas for the guidance and education that he has bestowed upon me.

Thank you to my children Nicole, Angela, and Brian for their love, understanding, and being a part of the best parts of my life.

And finally, thank you to my colleagues at Michigan State University's Power Electronics and Motor Drives Laboratory. I have greatly enjoyed your friendship and appreciate your shared knowledge.

TABLE OF CONTENTS

LIST OF FIGURES	vii
1. INTRODUCTION	1
1.2 Conventional Vehicles	1
1.3 Alternative Vehicles	4
1.4 Fuel Cell Vehicles.....	14
1.5 Outline of Thesis	16
2. HYBRID ELECTRIC VEHICLE Power Electronics Review.....	18
2.1 Voltage Source Inverter	18
2.1.1 Switching Analysis of the Voltage Source Inverter	21
2.1.2 Voltage Source Inverter Control.....	25
2.2 Current Source Inverter	32
2.3 Z-source Inverter	34
2.3.2 Maximum Boost Control.....	44
2.3.3 Maximum Constant Boost Control	48
2.4 Input/Output Equations of the Z-source Inverter	55
3. INTRODUCTION TO POWER ELECTRONICS TOPOLOGIES AND THEIR OPERATING PRINCIPLES	57
3.1. Traditional Input Rectifier/VSI to Output VSI	68
3.1.1 Battery & Traction Motor Mode.....	68
3.1.2 Battery, Starter Motor, Traction Motor Mode.....	69
3.1.3 Generator, Battery Discharge, Traction Motor Mode	71
3.1.4 Generator, Battery Charging, Traction Motor Mode	72
3.1.5 Regenerative Braking and Battery Charging Mode.....	72
3.1.6 High voltage battery	75
3.1.7 Low voltage battery with DC/DC converter.....	75
3.1.8 Comparison of the high voltage battery vs. the low voltage battery..	77
3.2 Input Rectifier/VSI to Output CSI with Z-Source impedance network	

(battery in parallel with Z's capacitor)	82
3.2.1 High voltage battery	85
3.2.2 Low voltage battery with DC/DC converter	86
3.3 Input Rectifier/CSI to Output VSI with Z-Source impedance network (battery in parallel with Z's capacitor)	86
3.3.1 High voltage & Low voltage battery options	89
3.4 Input Rectifier/VSI to Output CSI with Z-Source impedance network (battery in parallel with Input Converter)	89
3.4.1 High voltage	93
3.4.2 Low voltage battery with DC/DC converter	93
3.5 Summary	94
4. COMPARISON OF POWER ELECTRONICS TOPOLOGIES	95
4.2 Description of Switching Device Power Comparison	95
4.3 DC/DC Boost – Buck Converter	97
4.4 Traditional VSI with PWM	100
4.5 Traditional Z-Source Inverter [the Voltage Fed Z-Source Inverter (VF-ZSI)] with PWM	102
4.6 Current Fed Z-Source Inverter (CF-ZSI).	105
4.7 Application of Equations to the Back to Back Topologies	117
4.7.1 Back to Back VSI-to-VSI Network Topology	117
4.7.2 Back to Back VSI-to-CSI Z-Network Topology (VSI-Z-CSI)	119
4.7.3 Back to Back CSI-to-VSI Z-Network Topology	125
4.7.4 Comparison of Circuit Topologies	129
4.8 Future Work	138

LIST OF FIGURES

Figure 1 Typical Internal Combustion Engine (ICE) Vehicle.....	3
Figure 2 Typical Electric Vehicle (EV).....	5
Figure 3 Typical Series HEV [5].....	9
Figure 4 Typical Parallel HEV [5]	12
Figure 5 Typical Series-Parallel HEV [6]	13
Figure 6 Typical Series-Parallel HEV with Planetary Gear Set [6].....	14
Figure 7 Typical Fuel Cell Vehicle [7]	15
Figure 8 (A) IGBT Module Example [7] (B) IGBT Module Example [7]	19
Figure 9 Traditional voltage source inverter	20
Figure 10 Single phase half-bridge inverter	21
Figure 11 Single Phase Inverter Voltage Output.....	22
Figure 12 Single Phase Inverter Voltage Output – Zoomed In	23
Figure 13 Single Phase Inverter Voltage Output at Zero Crossing	24
Figure 14 Typical Three Phase Voltage Source Inverter.....	25
Figure 15 Simple pulse width modulator [12]	26
Figure 16 SPWM generation	27
Figure 17 Saturated Pulse Width Modulation	28
Figure 18 Standard sine wave reference signal at 100% modulation index [14].....	30
Figure 19 Reference signal modified with third harmonics, equivalent to standard sine wave reference signal at 100% modulation index [14]	31

Figure 20 Reference signal modified with third harmonics at 100% modulation index [14]	31
Figure 21 Traditional current source inverter.....	32
Figure 22 Current Source Inverter with Gate Turn Off Thyristors.....	33
Figure 23 Z-source inverter	34
Figure 24 Illustration of the 100 switching vector	36
Figure 25 Illustration of the 011 switching vector	36
Figure 26 Illustration of the V_{111} switching vector	37
Figure 27 Traditional PWM Control Method.....	38
Figure 28 ZSI During SCZ State.....	40
Figure 29 Modified PWM with shoot through zero states [9]	40
Figure 30 Voltage gain of the simple boost control [16].....	42
Figure 31 Z-Source Inverter in Open Circuit Zero Mode	43
Figure 32 Maximum boost control strategy [16].....	45
Figure 33 Voltage gain of the maximum boost control strategy [16]	46
Figure 34 Maximum boost control with third harmonic injection strategy [16]	47
Figure 35 Voltage gain of the maximum boost control with third harmonic injection [16].....	48
Figure 36 Maximum constant boost control strategy [17]	49
Figure 37 Voltage gain of the maximum constant boost control strategy [17]	51
Figure 38 Third Harmonic Injection into Reference Signals	52
Figure 39 Third Harmonic Injection with Max. Constant Boost PWM [17]	53
Figure 40 Voltage gain of the maximum constant boost control with third harmonic injection [17]	54

Figure 41 Voltage stress comparison of different control methods [17].....	55
Figure 42 Traditional Input Rectifier/VSI to Output VSI.....	61
Figure 43 Input Rectifier/VSI to Output CSI with Z-Source impedance network (battery in parallel with Z's capacitor).....	63
Figure 44 Input Rectifier/CSI to Output VSI with Z-Source impedance network (battery in parallel with Z's capacitor).....	65
Figure 45 Input Rectifier/VSI to Output CSI with Z-Source impedance network (battery in parallel with Input Converter)	67
Figure 46 A single phase model of the Voltage Source Inverter and the Generator	70
Figure 47 Voltage Phase Angle Control.....	73
Figure 48 Voltage Phase Angle Control.....	74
Figure 49 DC/DC Converter	76
Figure 50 Series Combination of Battery Cells;See Note.....	79
Figure 51 Back to Back VSI, CSI with Z-Source Network.....	82
Figure 52 Back to Back VSI topology	83
Figure 53 Back to Back VSI, CSI Z-Source Topology	84
Figure 54 VSI-Z-CSI Regenerative Mode with VSI in SCZ.....	85
Figure 55 CSI-Z-VSI Topology	86
Figure 56 Shoot-Through Duty Cycle vs. DC Voltage Across Inverter.....	89
Figure 57 Input VSI/Rectifier to Output CSI topology.....	90
Figure 58 Regenerative Braking with VSI-Z-CSI and Battery Parallel to VSI Active State.....	91
Figure 59 Regenerative Braking with VSI-Z-CSI and Battery Parallel to VSI Open Circuit Zero State	92
Figure 60 Regenerative Braking with VSI-Z-CSI and Battery Parallel to VSI, Short Circuit Zero State	92

Figure 61 Input VSI to Output CSI with Z-Source DC Link	93
Figure 62 DC/DC Boost-Buck Converter	98
Figure 63 Traditional VSI	100
Figure 64 Traditional Z-Source Inverter	102
Figure 65 Current Fed ZSI	105
Figure 66 IGBT Module Schematic	106
Figure 67 Reverse Blocking IGBT Module Schematic (RB-IGBT)	106
Figure 68 RB-IGBT Symbol	106
Figure 70 SCZ Switch States of VF-ZSI	109
Figure 71 SCZ Regions of the CF-ZSI	111
Figure 72 SCZ Switch States of CF-ZSI detail	115
Figure 73 Back to Back VSI-to-VSI Network Topology	117
Figure 74 VSI-Z-CSI	120
Figure 75 VSI-Z-CSI; CSI in OCZ State	121
Figure 76 VSI-Z-CSI; CSI in SCZ State	121
Figure 77 CSI-Z-VSI	125
Figure 78 ILZ Average	131
Figure 79 SDP Comparison	135
Figure 80 SDP (Normalized) Comparison	121
Figure 81 Proposed Topology	134
Figure 82 Possible Implementation of the Proposed Topology (1)	134
Figure 83 Possible Implementation of the Proposed Topology (2)	135
Figure 84 Possible Implementation of the Proposed Topology (3)	135

KEYS TO SYMBOLS OR ABBREVIATIONS

ac voltage at the traction motor

-peak (\hat{V}_{TM})

-RMS (V_{TM})

-Line to Line (V_{TM-LL})

ac voltage at the generator/starter motor

-peak (\hat{V}_G)

-RMS (V_G)

-Line to Line (V_{G-LL})

Average Line Current (I_{AV} or I_{av})

Battery terminal voltage (V_{BAT})

Boost factor (B)

Buck–boost factor (B_B)

Capacitor voltage (V_C)

Constant power speed ratio (CPSR)

Current Fed Z-Source Inverter (CF-ZSI)

Current Source Inverter (CSI)

dc-link voltage across the generator inverter bridge (V_d) or (V_{DC-G})

dc-link voltage across the traction motor inverter bridge (V_{DC-TM})

Electric vehicle (EV)

Electro Magnetic Interference (EMI)

Fuel cell (FC)

Fuel cell hybrid electric vehicle (FC HEV)

Fuel cell vehicle (FCV)

Generator Power, Three Phase ($P_{3\phi}$)

Hybrid electric vehicle (HEV)

Hybrid Vehicle (HV)

Hybrid vehicle (HV)

Insulated Gate Bi-Polar Junction Transistor Module (IGBT)

Internal combustion engine (ICE)

Lower shoot-through envelope (V_n)

Lower shoot-through envelope reference signal (V_{nref})

Modulation index (M)

Open Circuit Zero Switching Period (T_{OCZ}) or (T_I)

Peak Line Current (\hat{I}_{LINE})

Phase A Lower switch gate control signal (S_{an})

Phase A upper switch gate control signal (S_{ap})

Phase A voltage reference (V_a^*)

Phase angle between phase voltage and line current (Θ)

Phase B Lower switch gate control signal (S_{bn})

Phase B upper switch gate control signal (S_{bp})

Phase B voltage reference (V_b^*)

Phase C Lower switch gate control signal (S_{cn})

Phase C upper switch gate control signal (S_{cp})

Phase C voltage reference (V_c^*)

Pulse width modulation (PWM)

Reverse Blocking Insulated Gate Bi-Polar Junction Transistor Module (RB-IGBT)

Series Hybrid Electric Vehicle (SHEV)

Shoot-through duty cycle (D_0)

Short Circuit Zero Switching Period (T_{scz})

Sinusoidal pulse width modulation (SPWM)

State of charge (SOC)

Switching cycle interval (T)

Switching Device Power (SDP)

Time during shoot through (T_0)

Traction Motor Power, Three Phase ($P_{3\phi-TM}$)

Upper shoot-through envelope (V_p)

Upper shoot-through envelope reference signal (V_{pref})

Voltage Fed Z-Source Inverter (VF-ZSI)

Voltage gain (MB)

Voltage Source Inverter (VSI)

Zero emission vehicle (ZEV)

Z-Source Inductor Current (I_{Lz})

Z-Source Inverter (ZSI)

1. INTRODUCTION

Alternatively powered vehicles are becoming of great importance. Several factors are causing the need for change from traditional vehicles. As the population of the planet continues to grow, and as the industrialization of these populations continue to grow, the rate of depletion of traditional fuel sources (fossil fuels – oil, and coal primarily) is also increasing. Along with this increased global demand for power comes the increased pollution from consuming fuels. Both the decreasing supply of fossil fuels and the increasing level of pollutants in our environment are becoming very significant concerns. As a result, there is a growing search for ways in which these problems may be reduced or solved. Both alternative fuels and ways to increase efficiency in the use of fuels are being sought after. One such approach is the development of hybrid vehicles which are much more fuel efficient and which produce much less pollutants. This introduction will provide a discussion of traditional vehicle, electric vehicles, fuel cell vehicles, hybrid vehicles. The hybrid vehicle discussion is broken down into parallel, series, series/parallel, and finally a discussion of the series hybrid electric bus is presented.

1.2 Conventional Vehicles

The tradition of fuel power vehicles started in 1769 with a self propelled military tractor invented by the French engineer and mechanic, Nicolas Joseph Cugnot (1725-1804). Much before this date, conceptual designs had been made by both Leonardo Da Vinci and Isaac Newton. [1] In 1823, Samuel Brown patented the first internal combustion engine to be applied industrially. It was compression-less and based on the "Leonardo

cycle," In 1838, a patent was granted to William Barnet (English) for an engine using in-cylinder compression. In 1854, the Italians Eugenio Barsanti and Felice Matteucci patented the first working efficient internal combustion engine in London but did not go into production with it. It was similar in concept to the successful Otto Langen indirect engine, but not so well worked out in detail. [2]. Various fuels were used over these years. By far the most prevalent designs today use gasoline or diesel fuel. Present day buses are primarily users of diesel fuel. The typical road vehicle in use today is based upon a standard platform. That is a gasoline or diesel fueled internal combustion compression engine. The engine is coupled to the remainder of the drive train through a multiple gear ratio transmission. From the transmission, power is delivered to the drive wheels through a drive shaft/s and a differential gear box. The engines are of the cylindrical compression type, and the transmission usually has three to five discrete gear ratios. The function of the differential gear box is to allow one of the drive wheels to rotate at a different speed than the other drive wheel while both are delivering power to the road. Each of these drive train components is mechanical. See Ffigure 1 for a schematic of the typical conventional vehicle.

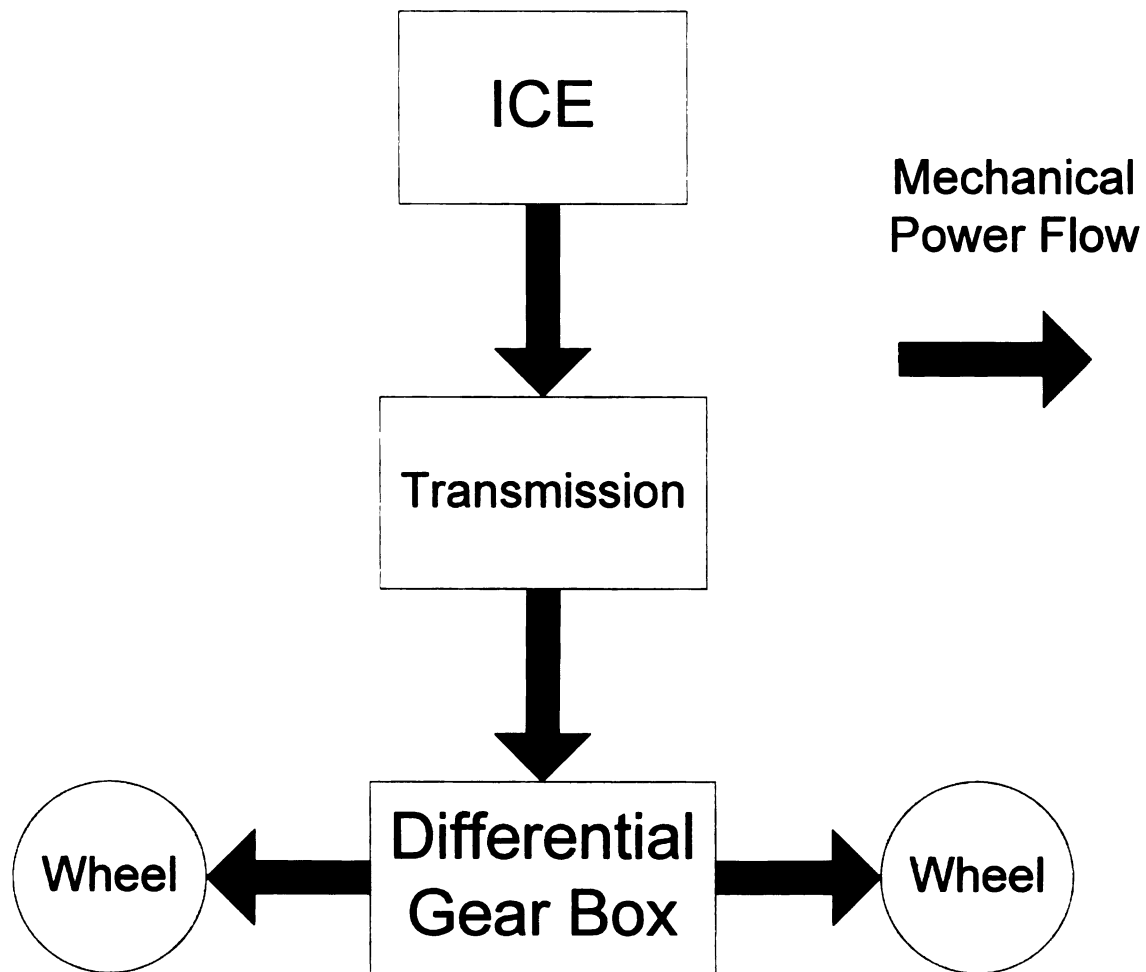


Figure 1 Typical Internal Combustion Engine (ICE) Vehicle

Hybrid vehicles use some combination of these mechanical components as well as electrical components to drive the vehicle. Hybrid busses, due to their use in urban areas and due to their particular drive cycles, are excellent candidates for use of hybrid technology.

1.3 Alternative Vehicles

Various countries and governments across the globe are trying to foster the development of alternative vehicles that mitigate some of these concerns. Alternatives are necessary to eventually create vehicles that do not further deplete crude oil reserves and that produce pollutants at a much reduced rate. The population of the world continues to grow, more nations are becoming industrialized, and burning of fossil fuels is believed to contribute to global warming. There are many reasons to turn to alternative that would alleviate some or all of these concerns. One such alternative is the electric vehicle (EV). This vehicle does not have an internal combustion engine and does not burn any fuels on board. Its power is usually received from the electric utility and stored in batteries that are on board the vehicle.

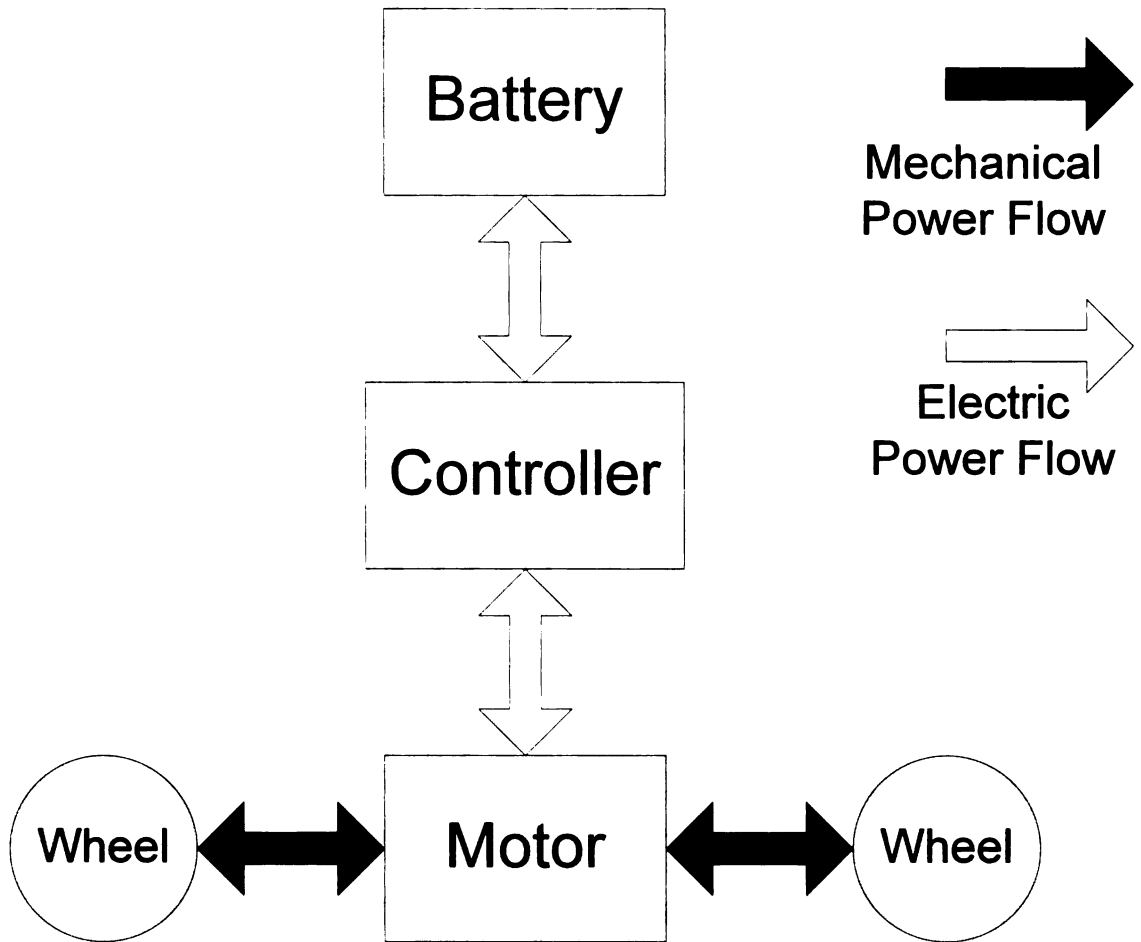


Figure 2 Typical Electric Vehicle (EV)

The stored power is then applied to electric motors to drive the vehicle rather than using an ICE. This type of vehicle is very efficient as compared to conventional vehicles.

Presently, the fuel cost per mile (cost per kilo-watt hour (kWhr)) is about 3 cents per mile as compared to 9 cents per mile for gasoline in the conventional vehicle. One of the main advantages of the EV is that it is a zero emission vehicle (ZEV). Although there is some pollution created when the electricity is generated at the power plant, this is insignificant compared to emissions from conventional ICE vehicles. EVs are also very efficient when

compared to conventional ICE vehicles; only about 20% of the chemical energy in gasoline is converted into work at the wheels of an ICE vehicle, 75% or more of the energy from a battery reaches the wheels of an EV [3]. EVs also provide strong performance, due to the fact that electric motors provide nearly peak power even at low speeds. Cost, performance, and convenience of an EV all depend on the battery. There are several types of batteries commonly used in EVs, advanced lead-acid batteries, nickel-metal hydride, and lithium polymer batteries [3]. The draw back to this type of vehicle is that it takes more time to recharge the batteries and recharging stations are not yet commonly available. Because of the limited storage capacity of the batteries, the range of these vehicles is also more limited.

1.3 Hybrid Vehicles

Hybrid vehicles (HV) are growing in popularity for their fuel efficiency and lower emissions. Fuel costs are increasing and the world's fuel reserves are continuing to grow smaller. Since the world's supply of crude oil is based in just a few countries, a nation's dependence on oil also makes it dependent upon the oil producing nation. Also, pollution issues are increasing in weight. These are the main reasons why the demand for HVs is increasing and why governments are encouraging the sales and development of these vehicles.

A HV is any vehicle that combines two or more sources of power to propel the vehicle. Some of the first HVs were busses, trains, and submarines. Hybrid methods are

now being applied to passenger cars and small trucks as well. There are three main configurations of HVs. They are Series Hybrid, Parallel Hybrid, and Series/Parallel Hybrid. They are described and discussed below.

A common type of hybrid electric vehicle (HEV) combines the energy storage of the EV with an energy source such as an ICE. HEVs have higher efficiency levels due to regenerative braking, and due to their ability to control power from the ICE. By controlling the power flow, it is possible to utilize the most efficient points of operation. Regenerative braking takes advantage of the concept that energy can neither be created nor destroyed – it just changes form. The conventional vehicle converts the kinetic energy of the moving vehicle into heat energy when the brakes are applied to slow the vehicle. This radiated heat is lost to the atmosphere. The HEV converts this inertia into electrical energy by using the traction motor as an electric generator. The production of electrical energy by the generator also produces a resistive torque against the free rotation of the drive wheels which slows the vehicle. This electrical energy is stored as potential energy in the vehicle's battery bank and or ultra capacitors. In this way, energy that would have been wasted is saved for later use. Also, the HEV can use a smaller ICE. The ICE only needs to supply the consistent steady state load while the battery and electric motor can provide power for the dynamic load. Some examples of the dynamic load would be the additional power needed to accelerate and to climb hills. The smaller ICE uses less fuel than the larger engines do. The smaller engine requires less fuel into the smaller cylinders to achieve the correct air to fuel ratios. Also, an ICE has moving parts which involve friction. The smaller parts have less surface friction. Also, the engines have linear reciprocating motion components which must undergo four

accelerations for each crank shaft revolution. Obviously, the lower mass components require less energy.

1.3.1 Series Hybrid Vehicle

The series HEV delivers all of the power to the drive wheels via electric power. None of the power is delivered with direct mechanical connections. For example, a typical configuration uses an ICE connected to a generator. The generator is connected to the traction motor through an electric power inverter and conductors. The power inverter is usually connected to power storage devices such as batteries and or ultra capacitors. See Figure 3.

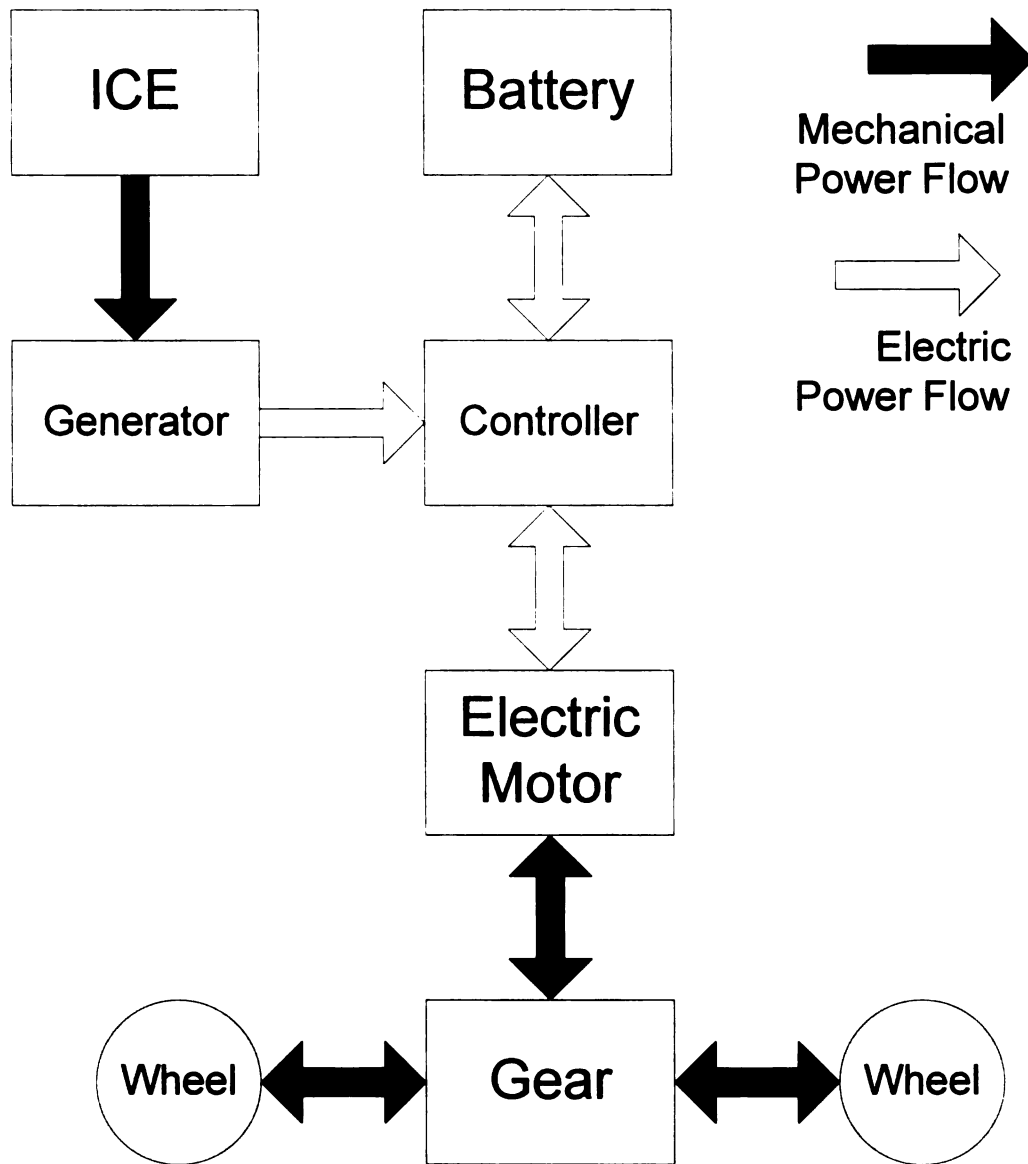


Figure 3 Typical Series HEV [4]

The series HEV uses an ICE which runs for extended periods of time at maximum efficiency, and shuts off when the batteries reach full charge. The ICE is then allowed to operate at the average required power level and the batteries will accept power when this average exceeds instantaneous power demand. The battery likewise provides power when the power required exceeds the average power provided.

In the series HEV configuration the electric motors and power electronics must be

sized for the whole load whereas the parallel case can use a smaller inverter and motor. The ICE is smaller than the conventional vehicle and is comparable to that of the parallel case. Also, this design does not require the additional equipment needed for the parallel case. In higher power applications (buses, freight trains, subway trains), this is a very effective design application.

The series HEV suffers due to the number of energy conversions. The engine converts petroleum potential energy to kinetic energy (rotational motion); the generator converts this kinetic energy to electrical energy. The electrical energy is then converted to chemical energy in the battery and to mechanical (kinetic energy) in the traction motor. However, the series HEV does not require a lossy hydro mechanical transmission. Also, batteries have limited life expectancy. New battery technology has made great improvements with this and there are several batteries that have long life periods when the battery state of charge is maintained within a fairly narrow band and when the charge and discharge rates are maintained within specified limits [3].

1.3.2 Parallel Hybrid Vehicle

The parallel hybrid vehicle has two power flow paths. One is mechanical from the ICE to the wheels, and the other is electrical from the generator and batteries to the electric motor and then mechanically to the wheels. The battery is recharged from regenerative braking and by operating the ICE at a power level in excess of the instantaneous power demand. This excess power is delivered to the batteries through the transmission, to the motor (being operated as a generator), to the power inverter/converter to the battery. The main advantages of this system are that both the engine and the motor size can be

minimized since both can deliver power at the same time to accommodate the peak load requirements. Also, there are potentially less energy conversions for the mechanical power flow path. On the other hand this system typically utilizes a hydro mechanical transmission which has losses, and the control is more complicated than the series HEV. [3].

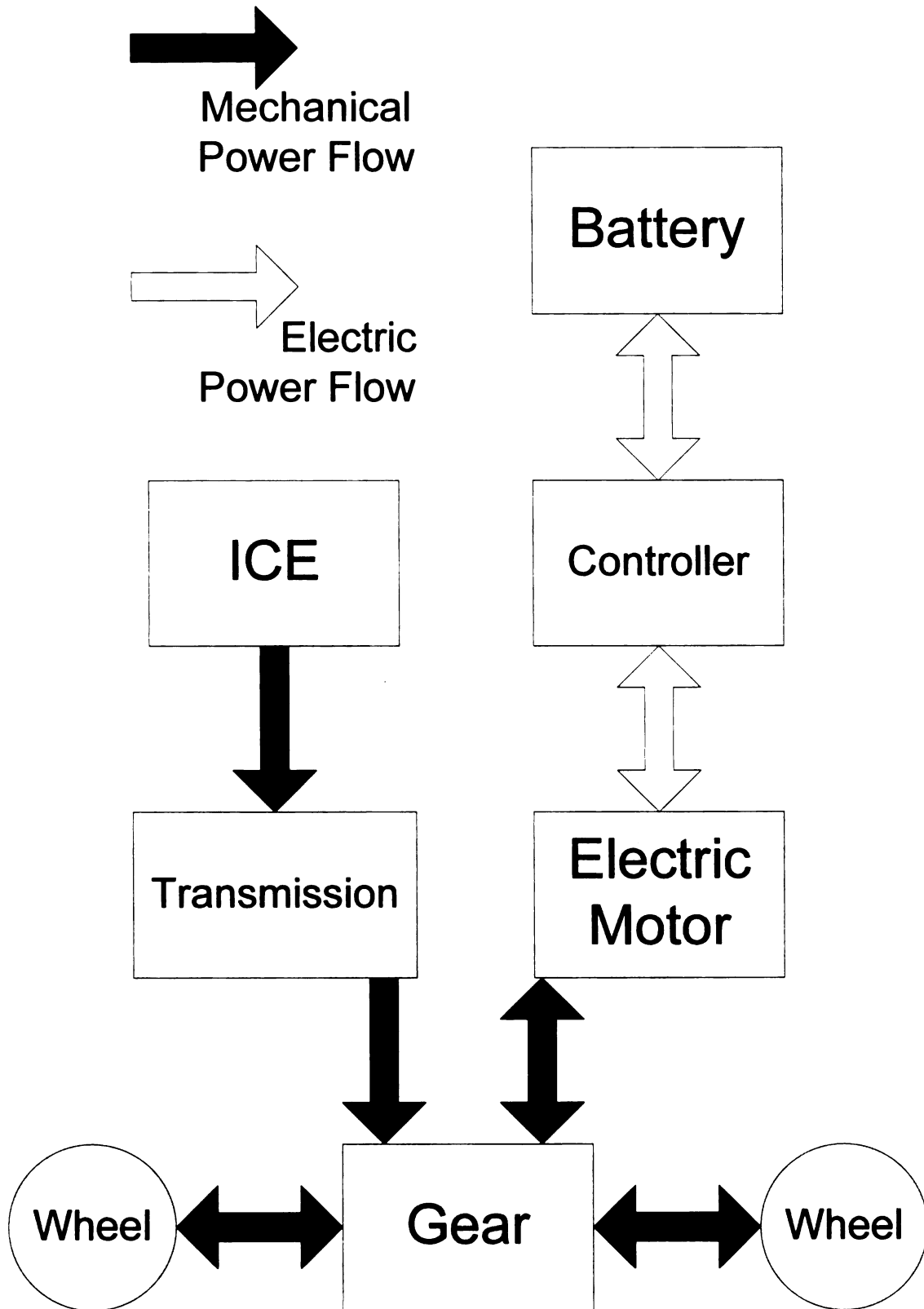


Figure 4 Typical Parallel HEV [4]

1.3.3 Series-Parallel Hybrid Vehicle

The series-parallel HEV combines features from both of the preceding cases. This system can operate in series mechanical mode, series electrical mode, or any combined ratio of the two. As a result, the control system can choose the most advantageous operation mode for the given circumstances. Figure 5. shows a power flow diagram for a series-parallel hybrid. Also notice the planetary component in this figure. This is also a very significant part of the efficiency of the design. The planetary gears (see figure 6. for a diagram) deliver power from the ICE to the wheels or to the generator. It also couples power transfer to or from the generator. The generator is an instrumental part of this control. The generator is used to create either positive or negative torque so that the desired gear ratio is achieved. As a result of the ideal gear ratio, the ICE is continuously operated at its most efficient point for the given power demand. Also, the planetary gear system does not use lossy hydraulic torque converters as the conventional vehicle does.

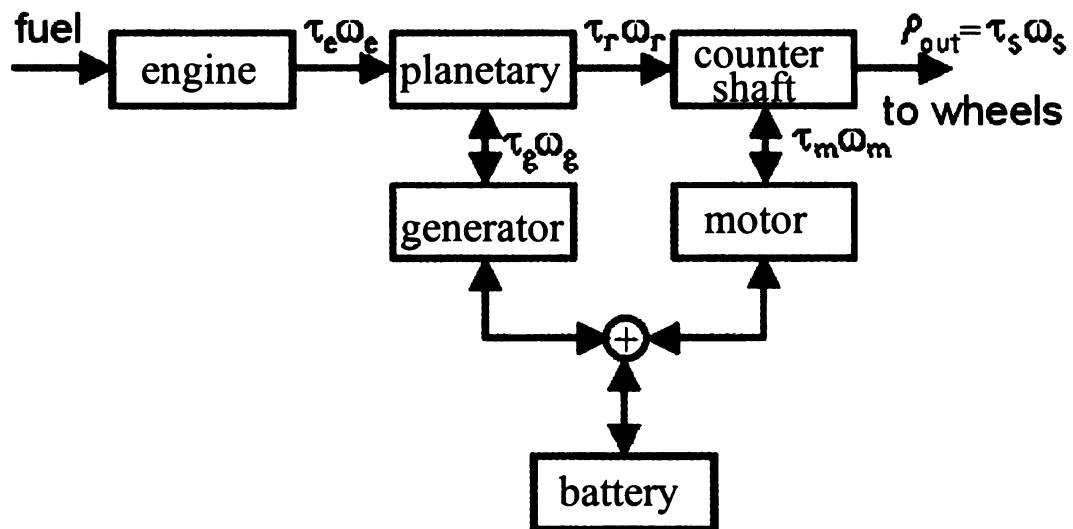


Figure 5 Typical Series-Parallel HEV [5]

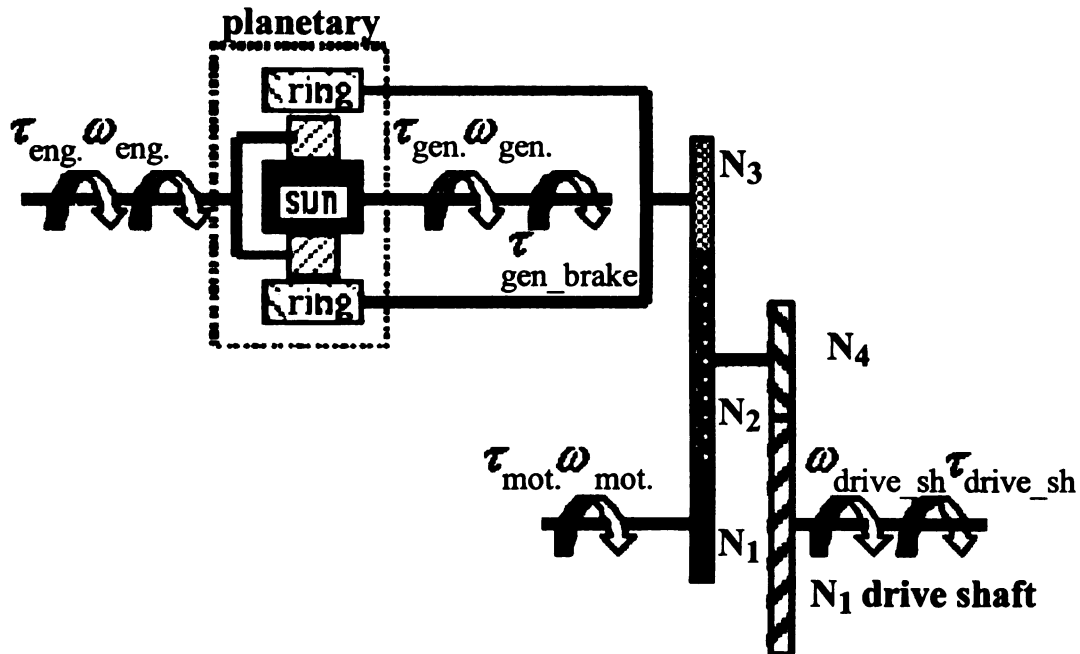


Figure 6 Typical Series-Parallel HEV with Planetary Gear Set [5]

This system benefits from the reduced size ICE, generator, power inverter, and traction motor due to its parallel functionality. Also, the operating system is able to select the most advantageous operation mode for the given circumstances

1.4 Fuel Cell Vehicles

Fuel cell vehicles (FC HEV) are still being developed and have not yet achieved commercial production. However, this type of vehicle offers a great deal of benefits in terms of efficiency, and very low emissions. Its environmental impact is similar to that of an EV, yet the FC HEV has a large range comparable to the conventional EV. The FC

HEV utilizes fuels such as hydrogen, methanol, or gasoline to produce electrical power without combustion. The waste product of the reaction is typically H_2O and CO_2 . The drive train of a FC HEV thus becomes: Fuel Cell, Inverter, and Traction Motor. Most designs will likely include a battery as well. The typical fuel cell does not have the ability to respond quickly to power demand changes. Therefore, the fuel cell can be used to supply average power and the battery can be used to supply or absorb the difference between average power and instantaneous power. Adding regenerative braking to the FC HEV makes the design very fuel efficient. Also, the infrastructure for these fuels does not yet exist. Below is a diagram of the FC HEV structure.

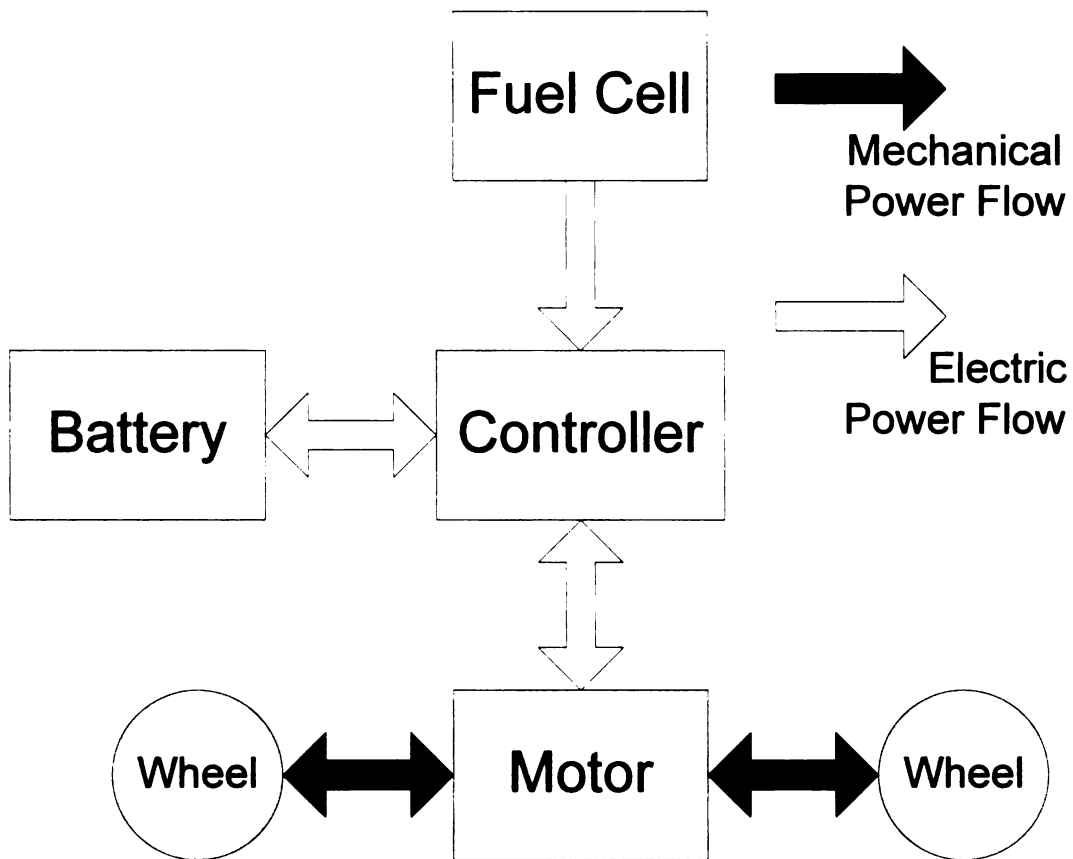


Figure 7 Typical Fuel Cell Vehicle [6]

1.5 Outline of Thesis

The goal of this research is to investigate the feasible options available for the design of traction drive systems for series hybrid electric buses. The traction drive system will deliver power to and from the ICE via a generator and it will deliver power to and from the traction motor. This system will also include interface and control of storage batteries and or ultra capacitors. The following topologies will be considered:

- Back to back voltage source inverters/converters
- Current source inverter (CSI) to Voltage source inverter (VSI) coupled with the Z-Source network -- OR --
- VSI to CSI coupled with the Z-Source network
- High voltage batteries or low voltage batteries with a bi-directional DC-DC buck boost converter
- Each configuration will be analyzed (operating principle, design, and control).
- A comparison of these systems will be included.

Chapter 2: Reviews the current HEV power electronics technologies, and introduces their control strategies. The Z-source inverter and its control strategies are also introduced.

Chapter 3: Introduction to Power Electronics Topologies and their operating principles [delivery of power from the ICE and generator to the traction motor]

3.1. Traditional Input Rectifier/VSI to Output VSI

- i. High voltage battery
- ii. Low voltage battery with DC/DC converter

3.2. Input Rectifier/VSI to Output CSI with Z-Source impedance network
(battery in parallel with Z's capacitor)

- i. High voltage battery
- ii. Low voltage battery with DC/DC converter

3.3. Input Rectifier/CSI to Output VSI with Z-Source impedance network
(battery in parallel with Z's capacitor)

- i. High voltage battery
- ii. Low voltage battery with DC/DC converter

3.4. Input Rectifier/VSI to Output CSI with Z-Source impedance network
(battery in parallel with Input Converter)

- i. High voltage
- ii. Low voltage battery with DC/DC converter

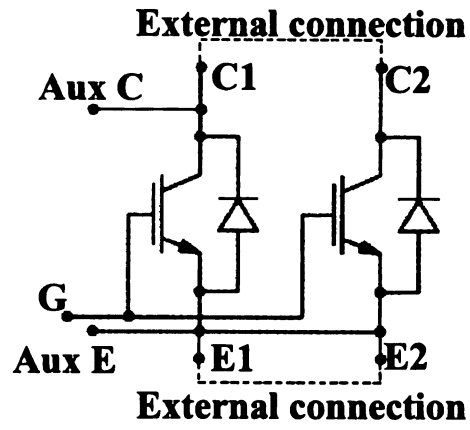
Chapter 4. Comparison of Power Electronics Topologies, Switch Device Power Ratio, Design and Control of the Power Electronics Topologies, Strengths and Weaknesses, Conclusions Related to the Topologies, Future Work

2. HYBRID ELECTRIC VEHICLE Power Electronics Review

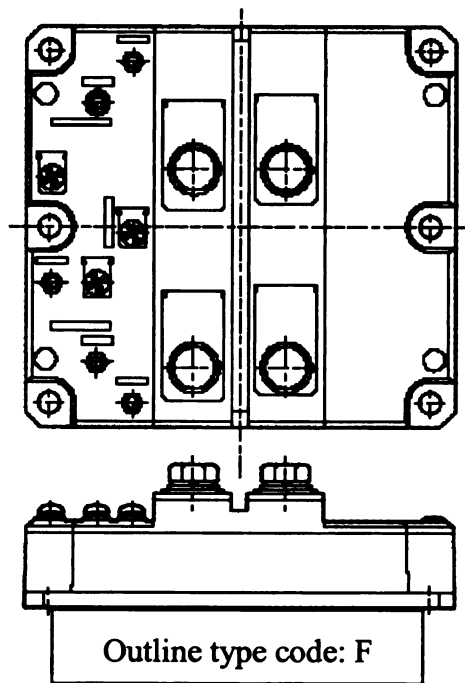
HEVs use an inverter to convert DC voltage and current to AC voltage and current. The AC voltage applied to the traction motor can be varied in frequency to change the motor speed, varied in magnitude to deliver power smoothly at low medium and high power settings, and varied in phase angle to control power flow to the traction motor or from the motor when it is being used as a brake. The traditional method for making this conversion is to use a voltage source inverter or a current source inverter. Another method that is still somewhat new and which offers great features is the use of a Z-source inverter. Each of these topologies will be discussed.

2.1 Voltage Source Inverter

The two traditional topologies are the voltage source inverter and the current source inverter. The voltage source is shown in figure 9. the basic structure uses a dc voltage source connected in parallel with a large capacitor. The capacitor makes up the dc link that connects the voltage source to the three phase bridge inverter. The inverter uses 6 insulated gate bi-polar transistors which include an anti-parallel diode (IGBT module)(fig. 8).



(A)



(B)

Figure 8 (A) IGBT Module Example [7] (B) IGBT Module Example [7]

A characteristic of the voltage source inverter is a smooth voltage supply and a current supply with ripple.[7]. Below is a schematic of a three phase voltage source inverter.

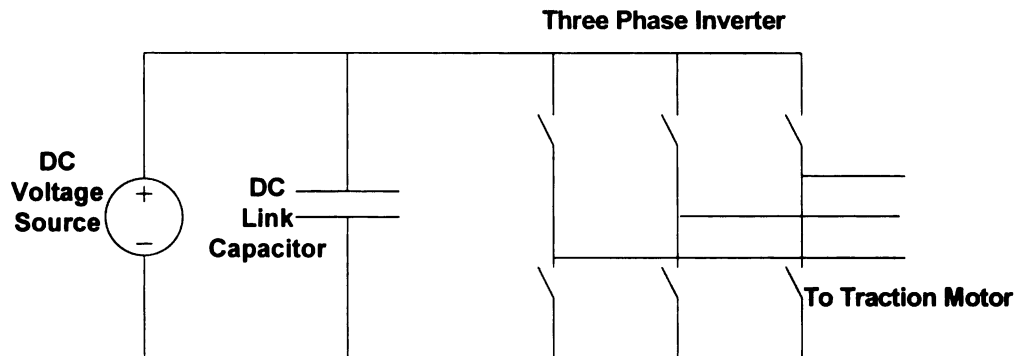


Figure 9 Traditional voltage source inverter

The voltage source inverter has the following limitations: The ac output voltage must be less than the dc link voltage. The voltage source topology can only buck voltage levels. Also, this inverter is not allowed to have a top switch and a bottom switch on simultaneously in the same phase leg. Such an occurrence will cause destructively high short circuit currents through the switching devices. This potential result leaves the inverter vulnerable to electromagnetic interference. Adding a DC-DC converter to the design can resolve the first issue [8]. However, this adds additional cost and complexity to the circuit as well as a decrease in efficiency. The second limitations can be resolved by adding dead time to the switching scheme to create a safety margin between the time that one switch in a phase leg turns off and the next one turns on. However, the addition of dead time adds harmonic distortion to the output wave forms.

2.1.1 Switching Analysis of the Voltage Source Inverter

The three phase voltage source inverter is similar to the single phase version shown in figure 10. The three phase version includes two more switch sets in parallel [9] with the one (T1 and T2) shown below and the switching functions of the other parallel phase legs are phase shifted by 120° from the other. First the single phase version will be discussed.

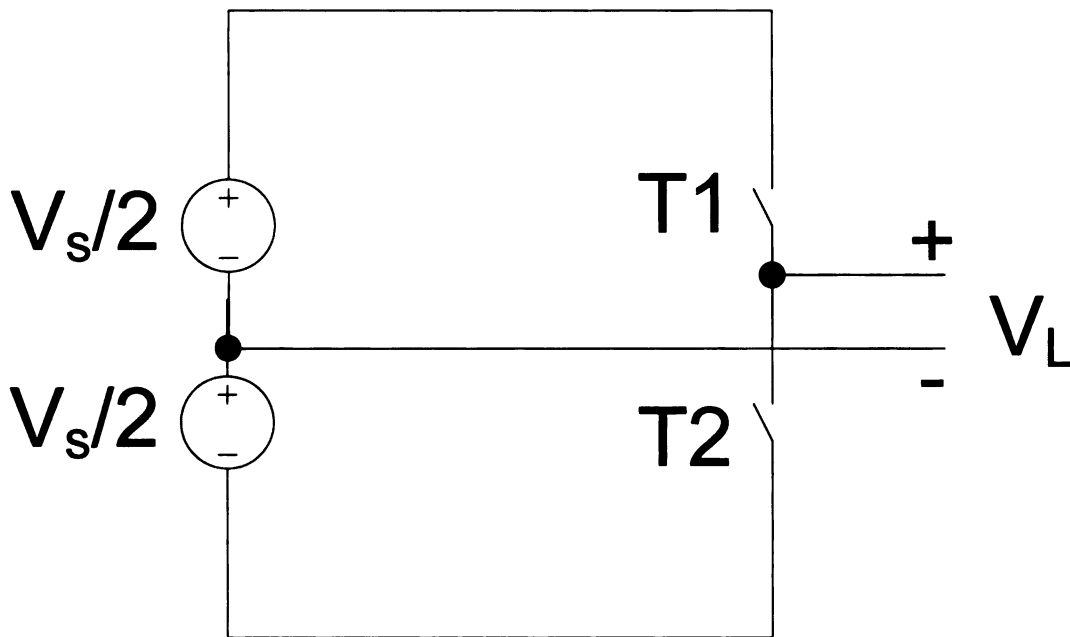


Figure 10 Single phase half-bridge inverter

When the top switch (T1) is gated on, the load has $V_s/2$ impressed across it, while the switch T2 is being gated on impresses a voltage of $-V_s/2$ across the load. By controlling the switches, the average output voltage can be controlled to approximate a sinusoidal wave form. The following three graphs show the output wave forms “Vout” and the sinusoidal approximation “Vout – average”. The first graph shows a whole cycle and the second two graphs are zoomed in at a couple of different points so that the details

of the wave form can be seen.

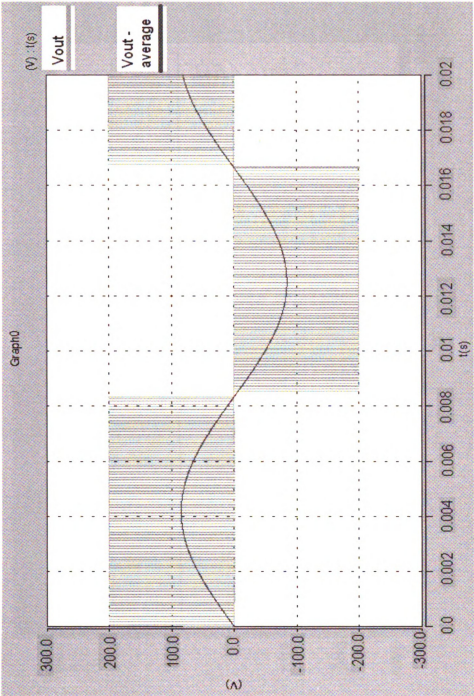


Figure 11 Single Phase Inverter Voltage Output

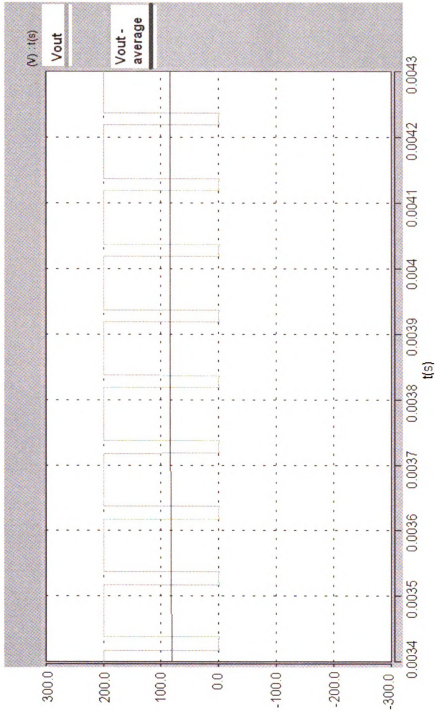


Figure 12 Single Phase Inverter Voltage Output – Zoomed In

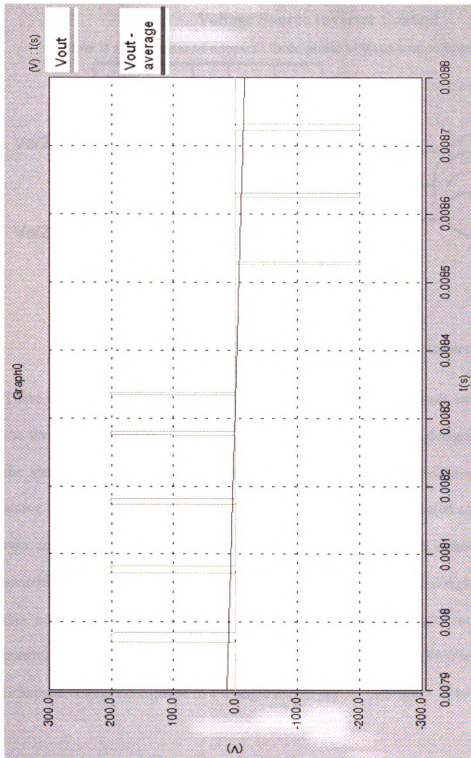


Figure 13 Single Phase Inverter Voltage Output at Zero Crossing

h
c
r

(SF

2.1.2 Voltage Source Inverter Control

Below is a schematic of a typical three phase voltage source inverter.

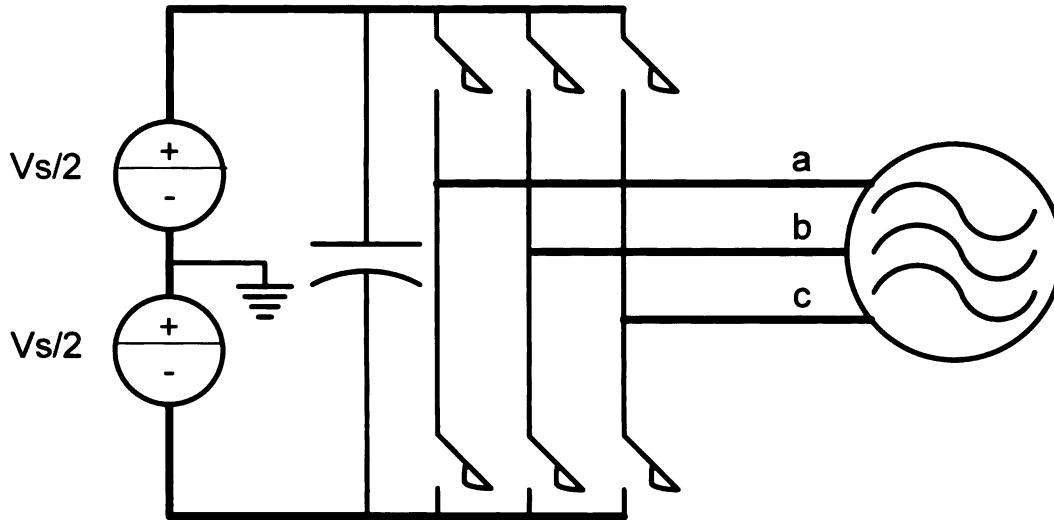


Figure 14 Typical Three Phase Voltage Source Inverter

There are many different pulse width modulation (PWM) methods available to control the three phase inverter. These control methods are algorithms designed for controlling the state of the six switches in the inverter. The traditional V-source inverter has six active vectors (or switching states) when the dc voltage is impressed across the load and two zero vectors when the load terminals are shorted through either the upper three switching devices or the lower three switching devices. The total of eight switching states (six active and two zero) are used in the traditional pulse width modulation (PWM) control methods. One common example of sinusoidal PWM (SPWM) uses sinusoidal reference voltages compared to a triangle carrier wave. See figure 15 below.

The pulse width modulator produces a logic signal, referred to as sinusoidal PWM (SPWM) that is used to command the inverters power transistors to turn on (saturated)

and off (cutoff), in such a way as to produce a sine wave at the inverter's output. As figure 15 shows a simple pulse width modulator can be implemented using a comparator. The comparator is used to compare a reference signal, V_{ref} , and a carrier signal, $V_{carrier}$. The comparator produces a logic-level output as shown in figure 16, which is logic-high whenever V_{ref} is greater than $V_{carrier}$, and logic-low whenever V_{ref} is less than $V_{carrier}$ [10]. This output is used to control the upper switch in a phase leg. To control the lower switch the signal is inverted.

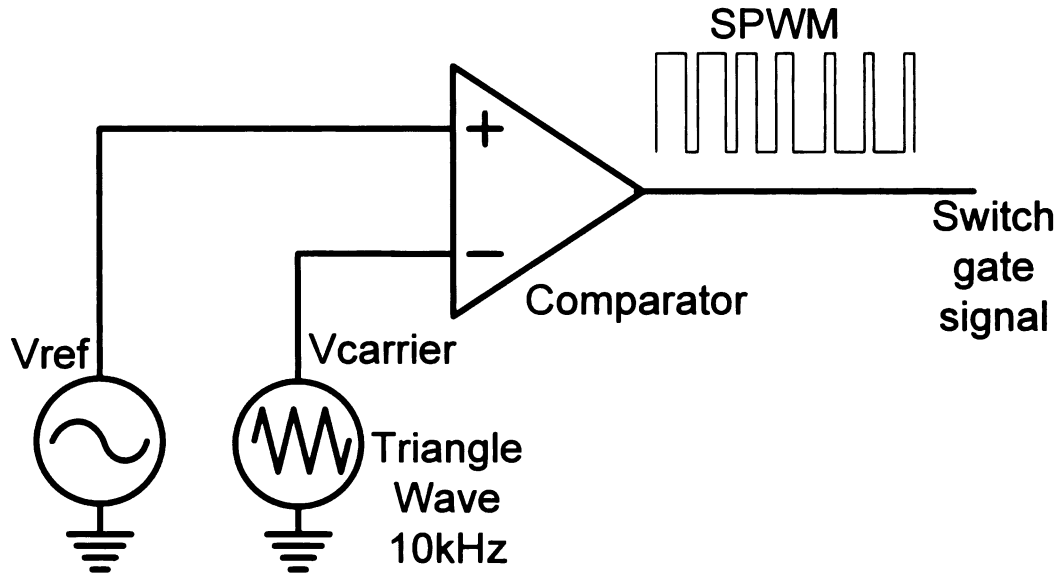


Figure 15 Simple pulse width modulator [10]

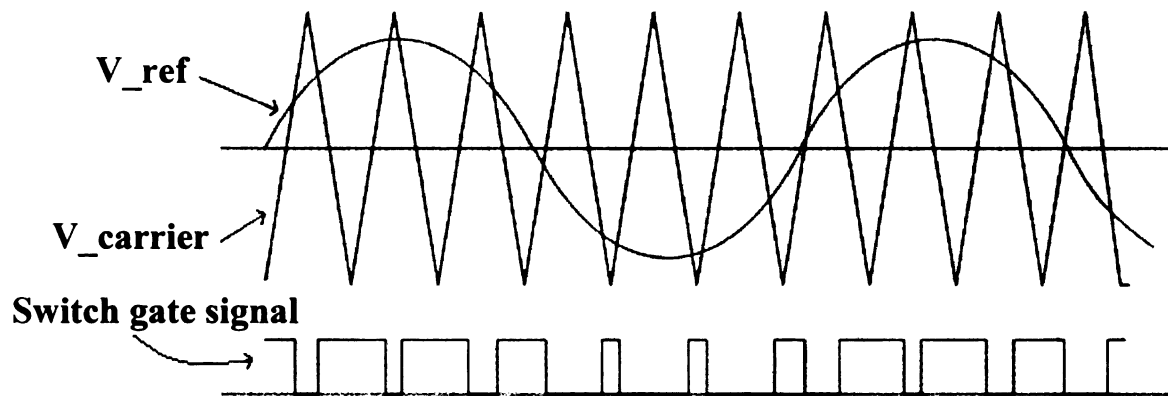


Figure 16 SPWM generation

This comparator output is then connected to the gate driver circuit of the IGBT modules. The logic high output therefore is used to turn on (close the switch) the IGBT and the low logic signal is used to turn it off. By proper control of the V_{ref} signal; frequency, phase angle, and amplitude of the inverter's output can be controlled.

The amplitude of the inverter's output can be controlled by controlling the amplitude of the V_{ref} signal. As the V_{ref} signal is increased in magnitude, V_{ref} will be greater than $V_{carrier}$ for longer periods of time and the IGBT switch will be closed for longer periods of time. As a result, the average magnitude of the inverter's output is higher. The ratio of V_{ref} to $V_{carrier}$ is called the modulation index [9]. When V_{ref} 's peak value is equal to the peak value of $V_{carrier}$, this is called a modulation index of 1 or 100%. At this modulation level, the inverter is outputting the highest amplitude sinusoidal voltage that it can with this particular control method. If the modulation index is increased above 100%, the comparator output would remain at the high logic state for a greater period of time, but the linear relationship between V_{ref} and the average output signal will be lost [11], as shown in figure 17.

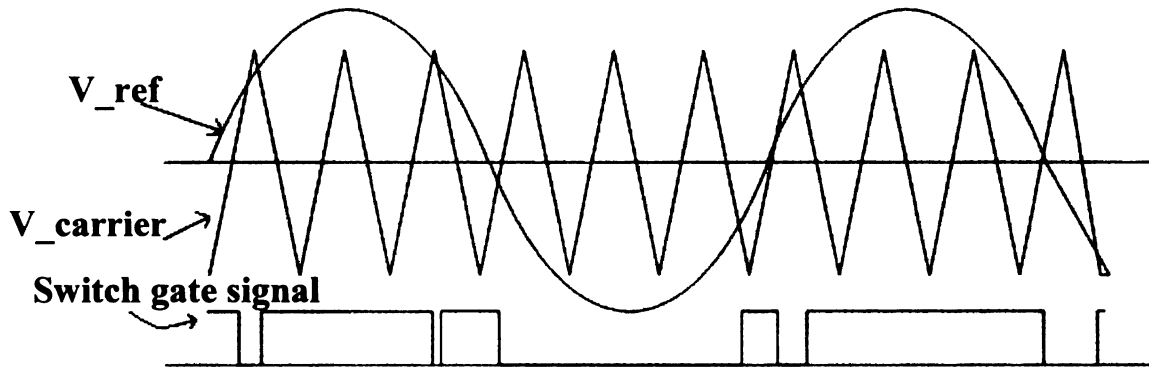


Figure 17 Saturated Pulse Width Modulation

The maximum available voltage on a motor using a standard three-phase power inverter is approximately 86% of the dc link voltage [12]. Figure 18 shows the standard sine wave reference signal, which can achieve 100% (of $V_{carrier}$) maximum modulation index. Third harmonic injection is a method used to increase the modulation index above 100%. With this method, a sinusoidal voltage at three times the frequency of V_{ref} is added to the V_{ref} signal. The resulting reference signal has shorter rise and fall times and a flattened peak. See figure 19. Since the peak is flattened, we can now increase the magnitude of V_{ref} above 100% of $V_{carrier}$. This will allow the logic high state time period to be increased which will increase the inverter's average output voltage level. In the example shown in figure 19, the coefficient of 1/6 is chosen for the third harmonic signal.

$$V_{ref} = |\hat{V}_{ref}| \sin(\omega_{V_{ref}} t + \varphi)$$

$$|\hat{V}_{3rd}| = \left(\frac{1}{6}\right) |\hat{V}_{ref}|$$

$$V_{3rd} = \left(\frac{1}{6}\right) \left| \hat{V}_{-ref} \right| \sin(3\omega_{V_ref}t + \varphi)$$

The combined signal is:

$$V_3 = \left(\frac{1}{6}\right) \left| \hat{V}_{-ref} \right| \sin(3\omega_{V_ref}t + \varphi) + \left| \hat{V}_{-ref} \right| \sin(\omega_{V_ref}t + \varphi)$$

With the chosen coefficient of 1/6, the fundamental amplitude ($\left| \hat{V}_{-ref} \right|$) can be increased by 15% [13]. This method is particularly appealing for 3 phase system applications. As can be seen from figure 19, the new combined reference voltage is no longer completely sinusoidal and therefore, the inverter output of a single phase is likewise changed. However, the wave shape effect of the third harmonic injection is eliminated in the line to line voltages of a balanced three phase inverter. This is because a 120° shift of the fundamental is a 360° shift of the third harmonic. The net result is simply that the inverter is now able to output a higher level of its dc link voltage.

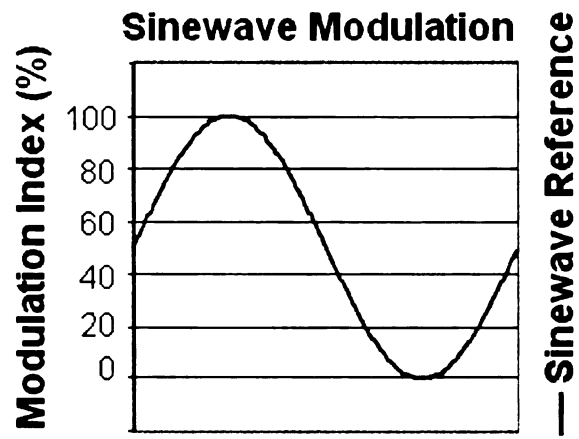


Figure 18 Standard sine wave reference signal at 100% modulation index [12]

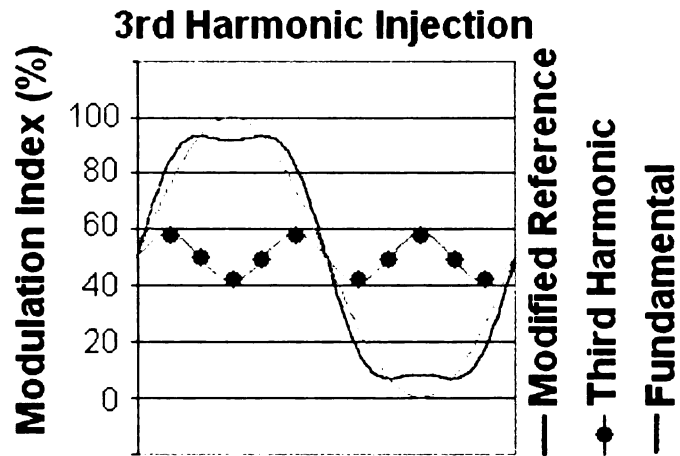


Figure 19 Reference signal modified with third harmonics, equivalent to standard sine wave reference signal at 100% modulation index [12]

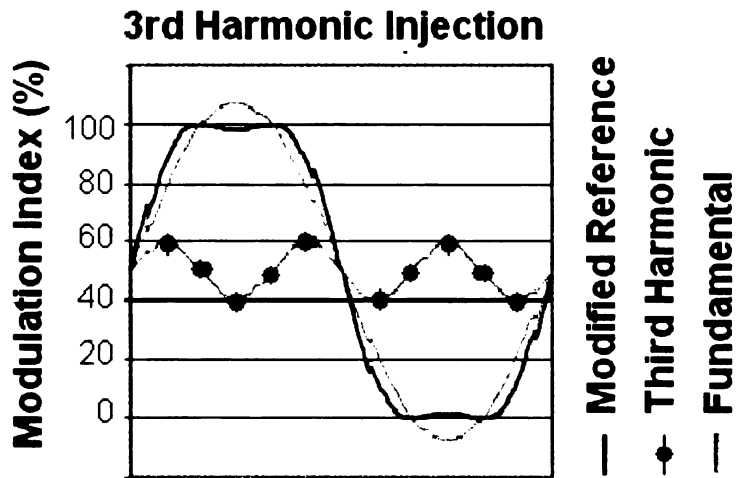


Figure 20 Reference signal modified with third harmonics at 100% modulation index [12]

2.2 Current Source Inverter

Figure 21. below shows the traditional current source inverter (CSI).

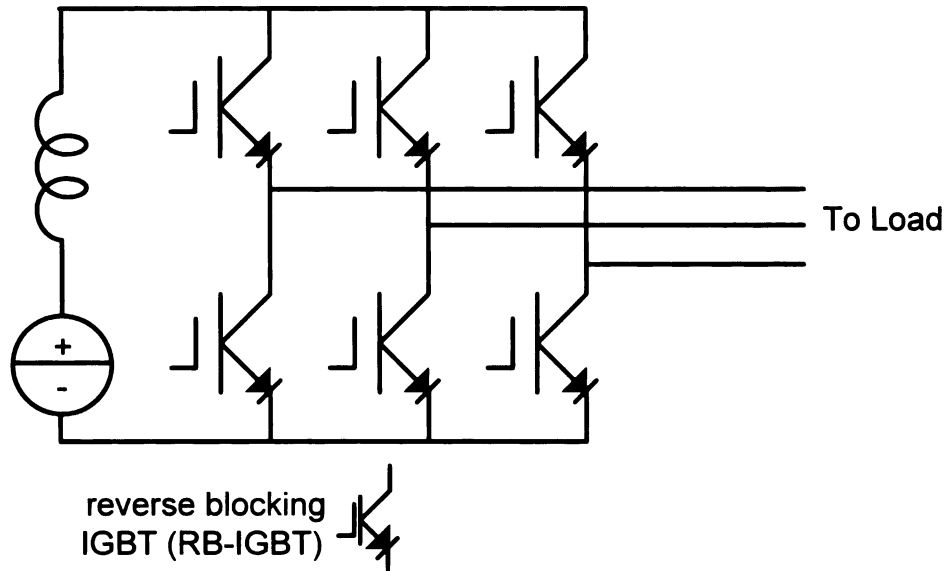


Figure 21 Traditional current source inverter

One exception may be that the reverse blocking IGBT (RB-IGBT) is a new device. In the past, the typical switching device of the current source inverter was either the thyristor, or the Gate Turn Off Thyristor in series with a power diode.

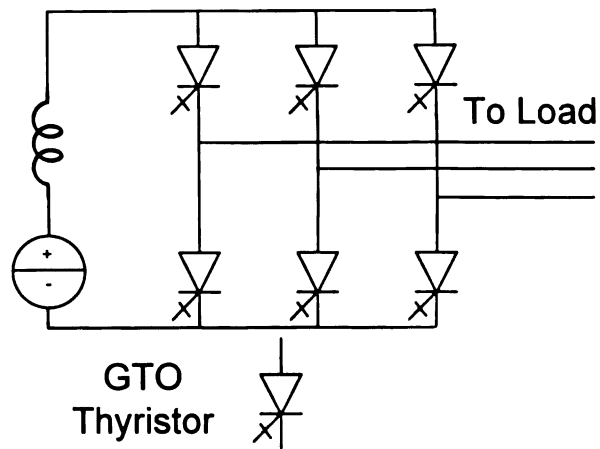


Figure 22 Current Source Inverter with Gate Turn Off Thyristors

In more recent years a RB-IGBT module has been used with the current source inverter. The main features of the CSI are the current source and the one directional current flow in the inverter. The current source is usually a voltage source in series with a large inductor. Since inductors cannot change their current magnitude instantaneously, the current source inverter provides a steady level of current. Current on the dc side is smoothed by an inductance, while the voltage on the dc side contains ac ripple [7]. A main advantage of the current source inverter is the smooth flow of current that they provide. A disadvantage, however, is that this type of inverter cannot withstand an open circuit condition in its inverter [9]. Such an un-allowed condition could exist when all top switches or all bottom switches remain open even for a very short period of time. In the event of an open circuit condition (which could result from miss-gating due to EMI, etc.) the current source will push current through the switching devices even though they are in their high resistance off state. This current produces destructively high temperatures in the devices. A safe guard against this condition is provided by providing overlap in the switching scheme. Each switch is caused to remain closed for an extended

period of time that overlaps with the time that the next device is turned on. This method is usually effective although it does cause some additional harmonics in the waveforms. Another problem that the current source inverter has is that it can only boost and cannot buck the output voltage levels. A solution to its inability to buck, is achieved by adding a DC-DC convert to the voltage source. This solution, however, comes at the cost of additional devices, added complexity, reduced reliability, and reduced efficiency.

2.3 Z-source Inverter

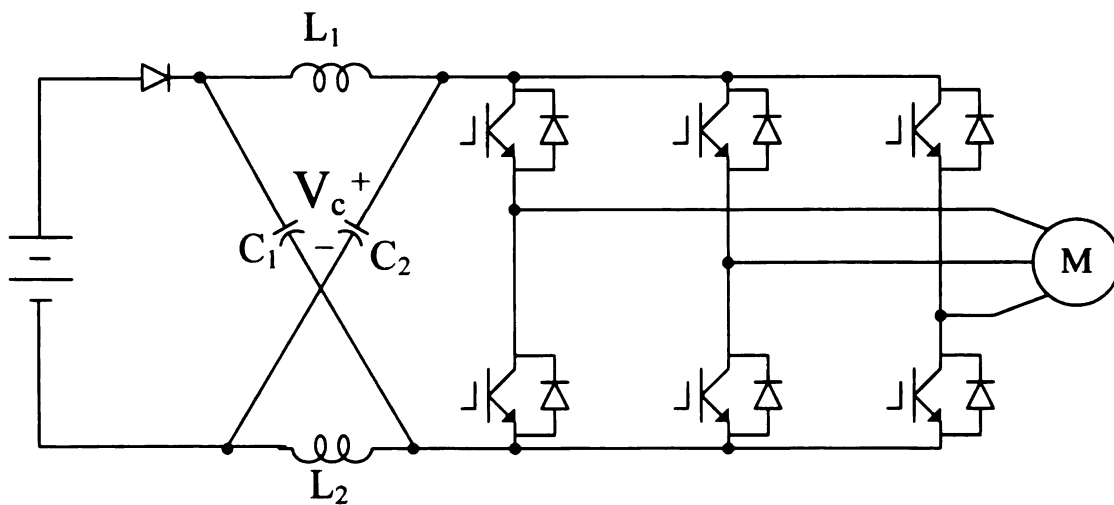


Figure 23 Z-source inverter

A typical Z-Source Inverter is shown in Figure 23. Notice that the Z-Source Inverter uses an impedance network on the DC Link where as the VSI used just a voltage source (such as a capacitor) and the CSI uses a current source (such as an inductor). This impedance network is composed of both inductors and capacitors. As such, it offers a unique combination of the ability to both buck and boost voltage levels to the output

unlike the VSI or the CSI. The Z-source inverter can be used for many applications, including dc-ac, ac-dc, ac-ac, dc-dc power conversions, with any ac or dc source and load. This work will discuss the Z-Source Inverter as it applies to the SHEV bus. Therefore, the focus will be on the dc-ac conversion.

Control of the ZSI differs from the traditional PWM for VSIs. Traditional PWM uses 8 different states (also called vectors). The first six vectors occur when the voltage of the DC link is impressed across the load. These are also called active vectors or states.

Some examples are:

State 100: top switch of the phase A leg is closed
 bottom switch of phase B leg is closed
 bottom switch of phase C leg is closed

State 100 implies that the top phase A switch (S_{ap}) is closed and that the top switches for phase B and C are open. This also implies that the corresponding bottom switches are of the opposite (or complimentary) state. See Figure 24 for a schematic example of the 100 state.

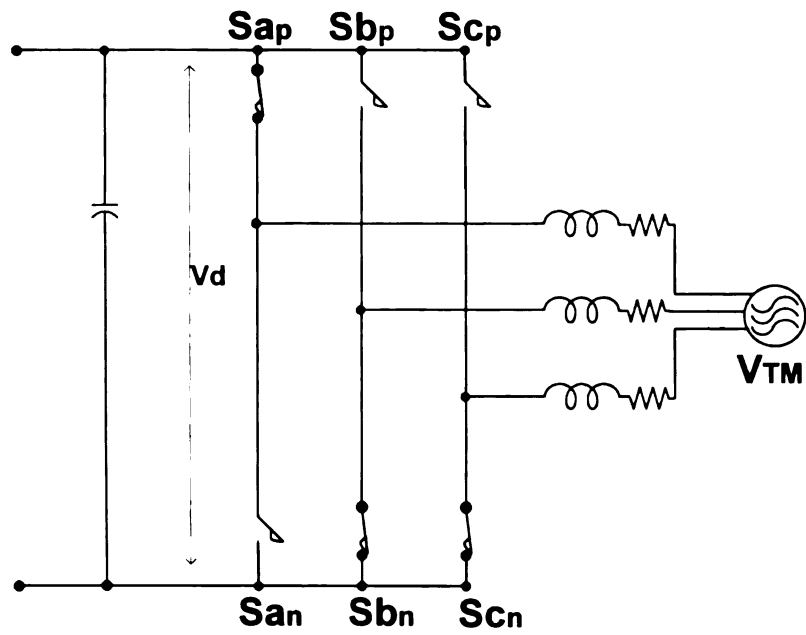


Figure 24 Illustration of the 100 switching vector

Figure 25 Shows the 011 vector.

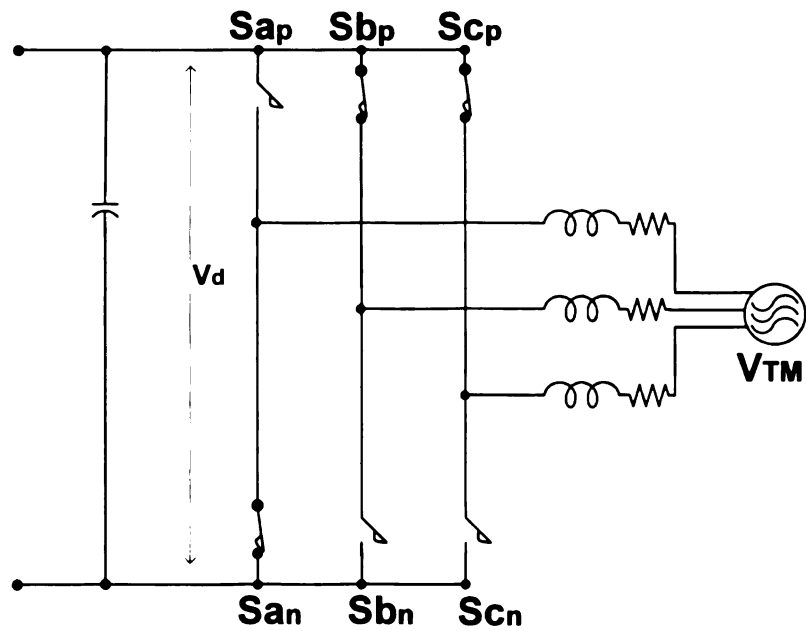


Figure 25 Illustration of the 011 switching vector

As mentioned above, there are a total of six active states:

- V_{001}
- V_{010}
- V_{011}
- V_{100}
- V_{101}
- V_{110}

The VSI also has two open circuit zero states in which the load terminals are shorted together through either the top dc rail or the bottom rail (vector V_{000} or V_{111}). See Figure 26.

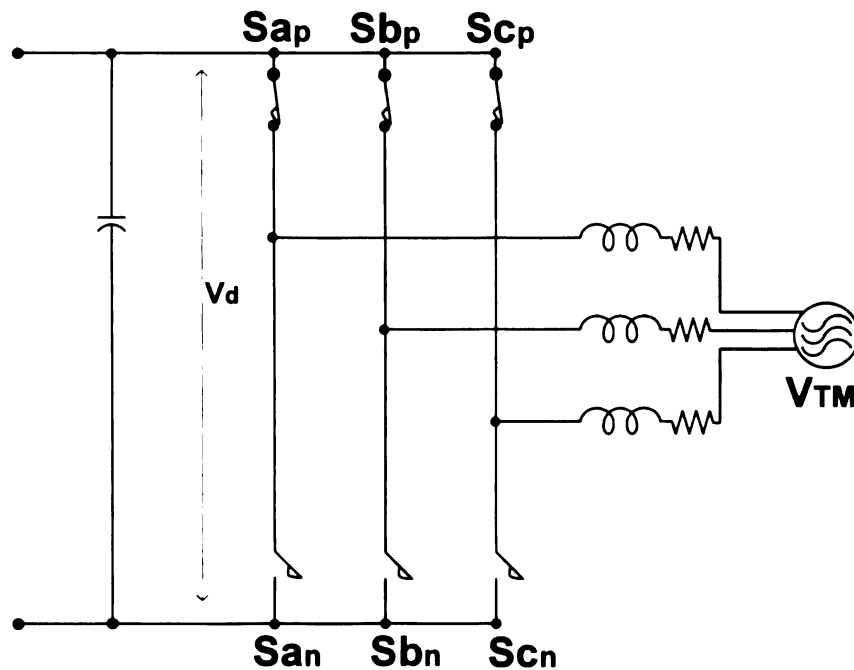


Figure 26 Illustration of the V_{111} switching vector

This is called the open circuit zero state because there is no complete circuit between the DC Link and the load (open circuit). Remember that the VSI does not allow the short

circuit zero state because this would cause a short circuit across the voltage source leading to extremely high currents through the switching devices resulting in their destruction. See figure 27 for a diagram of the traditional PWM wave forms.

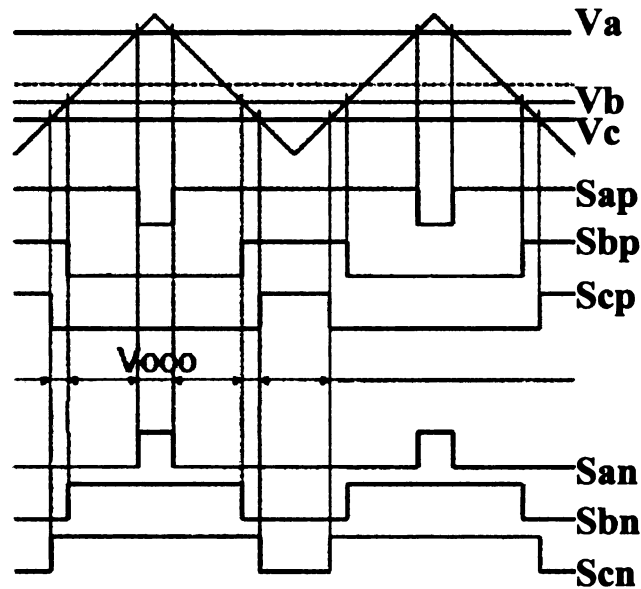


Figure 27 Traditional PWM Control Method

In this diagram, V_a^* , V_b^* , and V_c^* are the reference sinusoidal voltage signals. In this diagram, the frequency of V_a^* , V_b^* , and V_c^* are \ll the frequency of the triangle carrier wave and V_a^* , V_b^* , and V_c^* appear as straight lines during this short time period. The switching mechanism (modulator), as discussed in chapter one closes the related upper switch when its reference voltage signal is $>$ the carrier wave and opens the switch when the reference voltage signal is below the carrier wave. In the lower portion of this diagram, the switching signals are shown. Logic state high corresponds to closing the switch and logic state low corresponds to opening the switch. Also notice the open circuit zero state (e.g. V_{000}) switching signals.

2.3.1 ZSI Simple Control

The ZSI has all of the above 8 switching vectors plus three additional short circuit zero vectors. These short circuit zero vectors occur when both the upper and lower switch of a single phase leg are closed (e.g. S_{ap} and S_{an} are both closed, or both S_{bp} and S_{bn} , or both S_{cp} and S_{cn} are closed). In the case of the ZSI, this short circuit condition is acceptable due to the inductors of the impedance network which limit the current levels. To summarize, the ZSI allows all three types of states. It allows all six of the active states, both of the open circuit zero states, and all three of the short circuit zero states. Each of these state types has a specific purpose in the control of the ZSI and they will be discussed below.

2.3.1.1 Active States

During the 1,0,0 active state, the line to line voltage across phases AB of the load are equal to the DC Link voltage, also phase AC is equal to the same. The active states are used to apply a three phase balanced PWM sinusoidal wave form to the load.

2.3.1.2 Short Circuit Zero State

The short circuit zero state of the Z-Source also known as the shoot-through state [9] results in the following circuit. During this mode, the inductor current is directly

charging the capacitors thereby boosting their voltage $V_C = V_{C0} + \frac{1}{C} \int i_C dt$. Since the

inductor voltage on average is zero and since it is the series combination of the capacitor and the inductor that is in parallel with the inverter during the active state, this shoot-through state boosts the output voltage of the inverter. The amount of voltage boost from the ZSI is controlled by controlling the amount of time spent in this mode.

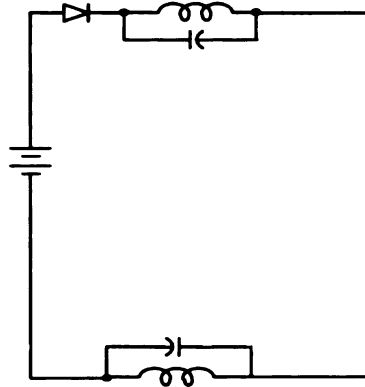


Figure 28 ZSI During SCZ State

See the wave forms in figure 29 to see the insertion of shoot-through states.

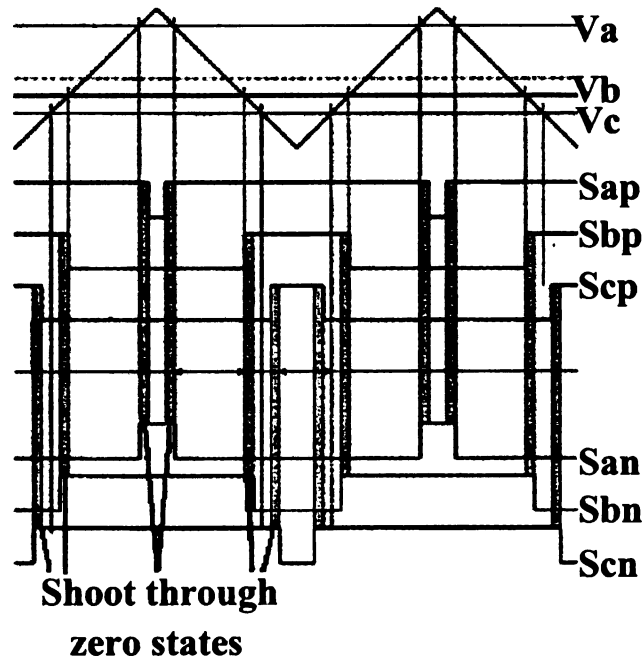


Figure 29 Modified PWM with shoot through zero states [16]

the sv

is gre

be les

100°

contr

obtai

volta

The

oper

gain

(the

thou

dow

wher

Shoot-through states must be inserted during periods of time when one or both of the switches on a phase leg are open. A switch being open occurs when the carrier wave is greater than the reference voltage wave. Therefore, the shoot-through duty ratio must be less than the active duty ratio meaning that the modulation index (M) must be less than 100% to use shoot-through. The maximum shoot-through duty ratio of the simple boost control is limited to (1-M) [17]. The thick curve in figure 30 shows the maximum obtainable voltage gain, MB (where B is the boost factor) versus M, which shows zero voltage boost and zero voltage gain at M=1.

$$B = \frac{T}{(T_1 - T_0)} \quad \text{Where } T_1 \text{ is the non-shoot-through time period}$$

T_0 is the shoot-through time period

T is the inverter switching period

The shaded area below and to the left of the bold curve is the possible regions of operation. Notice that as M approaches $\frac{1}{2}$, and as B is made to be large, that the possible gain (MB) grows very large. From the equation above, it can be seen that increasing T_0 (the shoot-through time period) will increase the boost factor B. It should be noted though, that the voltage stress across the devices increases as the modulation index goes down. Therefore, the best combination of M, B, and device ratings must be coordinated when developing the inverter design.

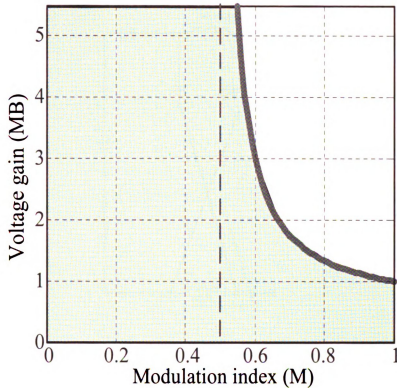


Figure 30 Voltage gain of the simple boost control [17]

2.3.1.3 Open Circuit Zero State

During this mode, the voltage across the inductors is much lower (approx. zero) than during the other modes. Current through the inductor flows into the capacitor increasing the voltage of the capacitor. As a result, the current through the inductor decreases

$$I_L = I_0 + \int V_L dt$$

and the output voltage to the load will also be decreased. The extent to which the output voltage is to be bucked is controlled by controlling the duration of the

time period of this mode.

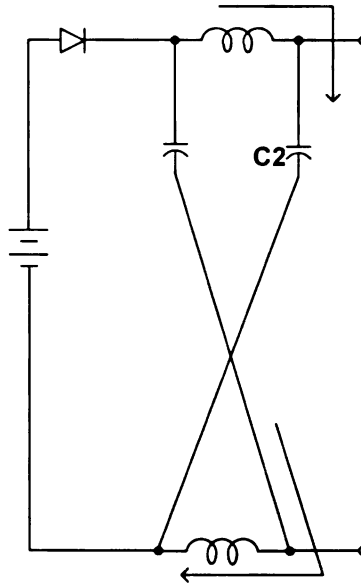


Figure 31 Z-Source Inverter in Open Circuit Zero Mode

The Z-source inverter advantageously utilizes the shoot-through states to boost the dc bus voltage by gating on both the upper and lower switches of a phase leg. Figure 29 shows the schematic of the Z-source network during the shoot-through state. Obviously the inductor current is boosted during this state. This is because the current ramps up through the inductors, whose currents are $I_L = I_0 + \int V_L dt$. During the open circuit zero state, none of the voltages (V_C or V_L) are impressed across the load. Therefore the average output voltage goes down as the open circuit Zero state increases. Therefore, the Z-source inverter can buck (by lowering the modulation index which increases the open circuit zero state) and boost voltage by increasing the shoot-through zero state (which increases B). The ZSI can buck, and boost voltage with one simple efficient structure. The inverter will not be damaged by either open circuit zero states or by short circuits zero (shoot-through) states and is therefore more reliable. During the

active states, the voltages are impressed across the load. Recall figures 24 & 25. With the ZSI, the switching period is broken down into three separate states:

Open circuit zero state

Shoot-through (short circuit zero state)

Active state

Their respective time periods are T_{1_open} , T_0 , and T_{1_active} . And as shown above, the buck or boost is controlled by controlling these time periods.

2.3.2 Maximum Boost Control

For a given modulation index, this method achieves the maximum voltage boost [17]. This method is very similar to the simple PWM control method. In this case however, all non-active states are shoot-through (boost) states. All six active states are unchanged. Thus the inverter's output will not be distorted. There are no open circuit zero states being used -- only active states and shoot-through zero states. As such, the boost factor B has changed as compared with the B from the simple PWM method. For

the maximum boost case, $B = \frac{1}{1 - 2\frac{T_0}{T}}$. The PWM waveforms of this method are

shown below in figure 32.

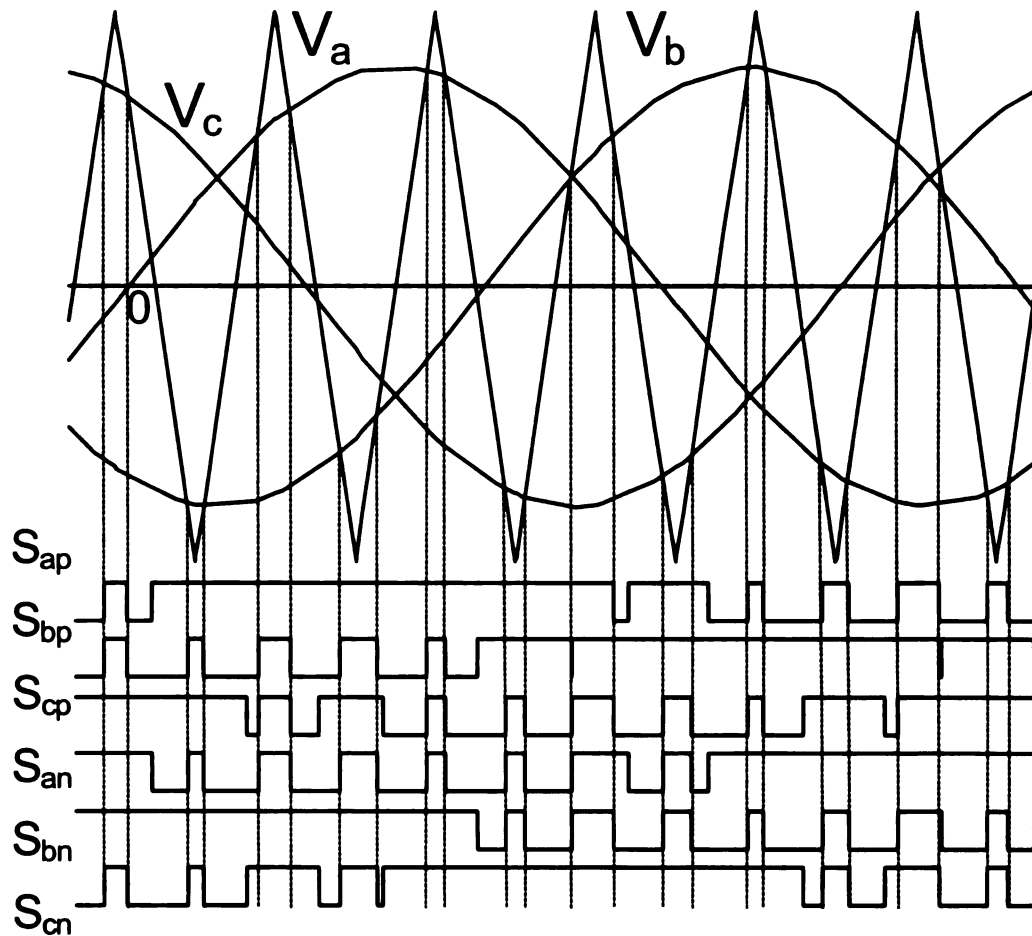


Figure 32 Maximum boost control strategy [17]

To achieve a given gain, the modulation index does not need to be reduced as much with this control method as it would with the simple PWM control method. Therefore, the voltage stress across the switching devices is less with this method. See figure 33. which shows the modulation index versus voltage gain for this method.

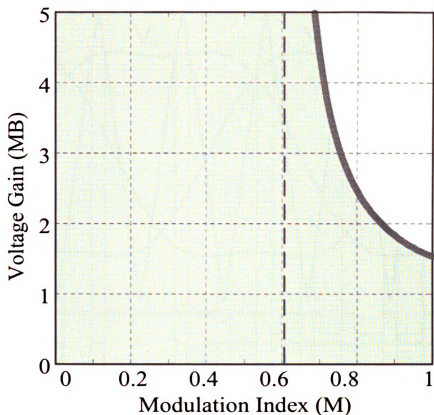


Figure 33 Voltage gain of the maximum boost control strategy [17]

Notice that a gain (MB) of five is achieved with a modulation index of approximately 0.7 where as a modulation index of .55 was required before.

This method may also utilize third harmonic injection to expand the allowed range of modulation indexes above 1. The related waveforms are shown in figure 34 below.

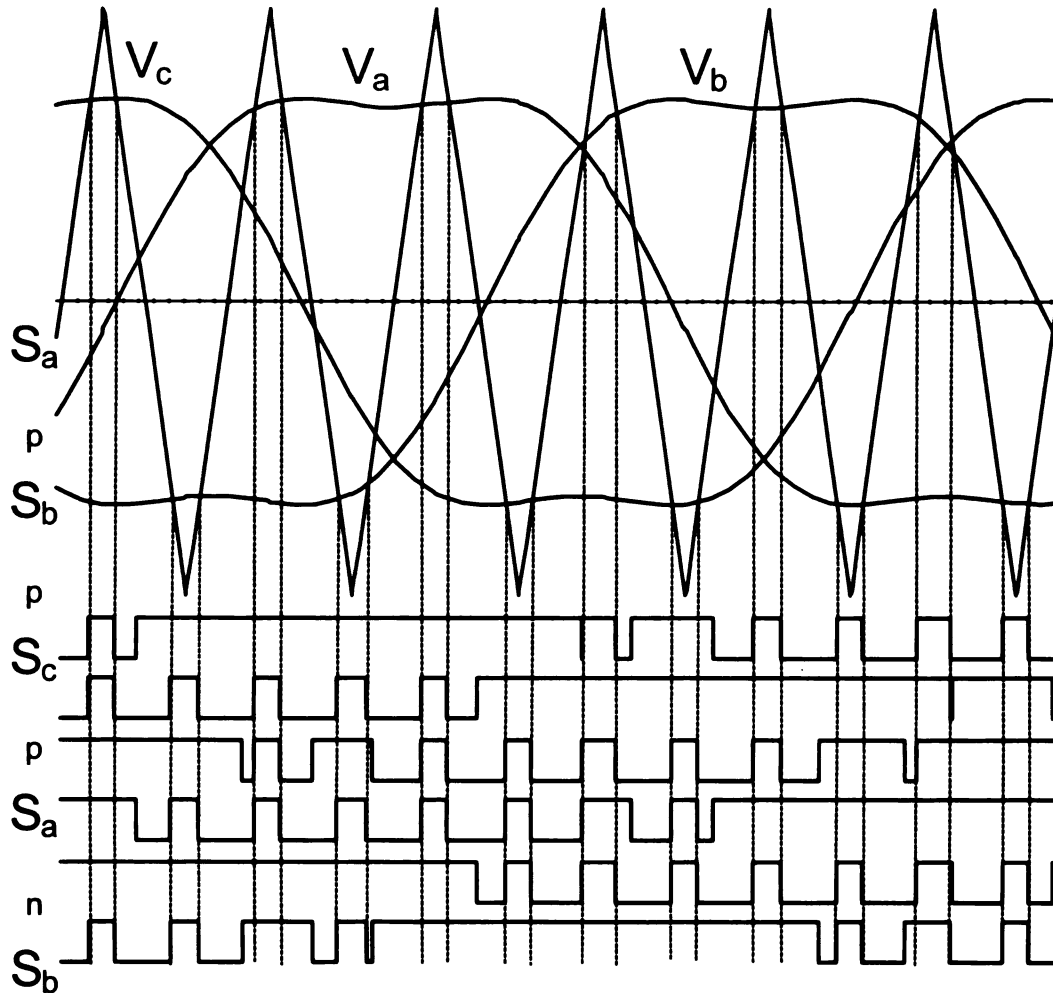


Figure 34 Maximum boost control with third harmonic injection strategy [17]

For the simple PWM method and for the Maximum boost PWM method, the maximum modulation index allowed is an index of one. In this control, the maximum modulation index $M = \frac{2}{\sqrt{3}}$ can be achieved at 1/6 third harmonic injection [17]. That is, the amplitude of the third harmonics injected is 1/6 of the amplitude of the reference signals (V_a , V_b , V_c). The voltage gain is identical to the previous control method for the same modulation index. That is, the slope of the voltage gain vs. modulation index curve

is not changed with the third harmonic injection. The only change is that the curve now extends further to the right showing that the modulation index now allowed is greater. See figure 35 below.

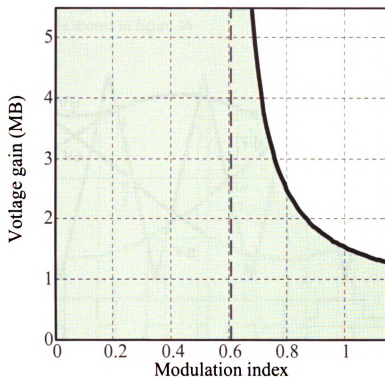


Figure 35 Voltage gain of the maximum boost control with third harmonic injection [17]

2.3.3 Maximum Constant Boost Control

From the Maximum Boost control method and as can be seen from figure 32, the shoot-through period varies throughout the reference voltage's cycle. This causes capacitor voltage ripple and inductor current ripple that is associated with the output frequency. The ripple is most predominant at low output frequencies. To mitigate this, the inductors

and capacitors of the ZSI's impedance network must be oversized. A method has been developed to achieve the same gain but with constant boost through out the output voltage cycle. This method known as "Maximum Constant Boost Control" [18] causes less voltage and current ripple and therefore requires smaller inductors and capacitors. The control scheme is shown in figure 36.

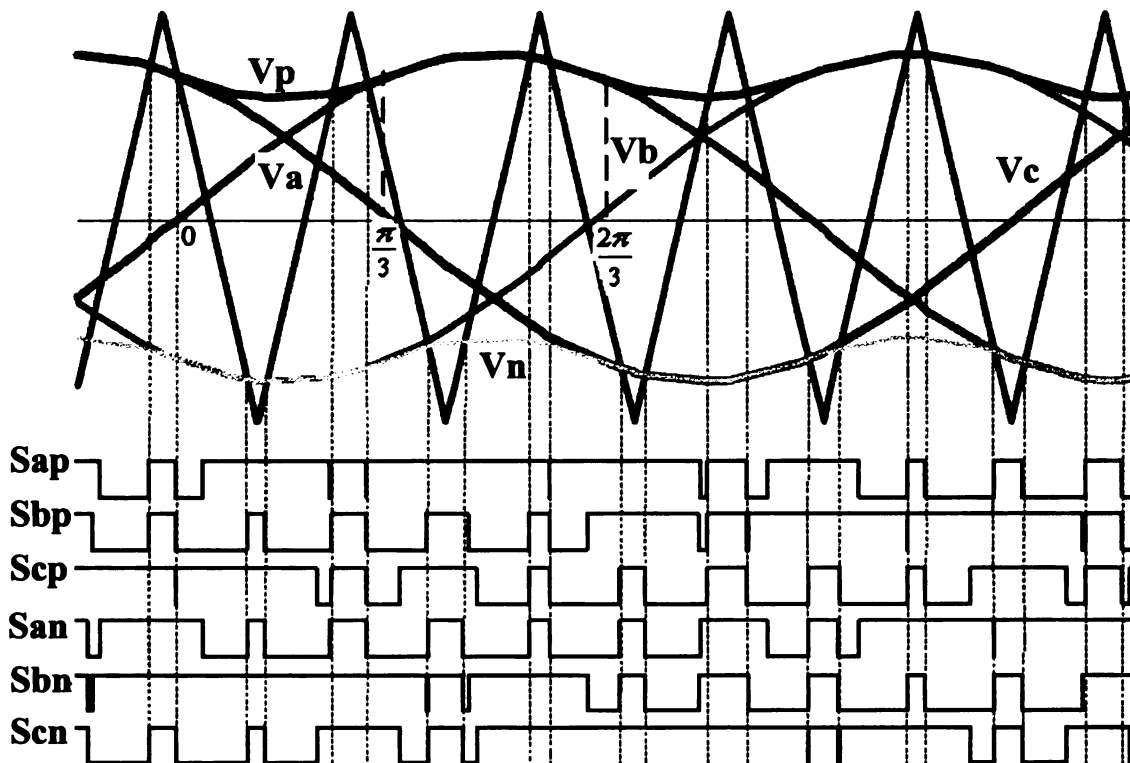


Figure 36 Maximum constant boost control strategy [18]

Notice that there are five reference voltage curves in the diagram above. There are the usual three sinusoids V_a^* , V_b^* , V_c^* separated by 120° which represent a three phase balanced system. In addition, there are two shoot-through envelope signals, V_p and V_n with a periodicity of three times the fundamental frequency (One in the positive portion of the graph and one in the negative portion). When the carrier signal is above the upper shoot-through envelope signal, shoot-through of the inverter switches will be triggered

and when the carrier signal is below the lower shoot-through envelope signal, a shoot-through will also occur. By looking at the graph of the five signals, it can be seen that the shoot-through periods are consistent unlike that of the maximum boost control method.

In the graph above, the distance between V_p and V_n is always $\sqrt{3}M$ and the shoot-

through duty ratio averages to $\frac{T_0}{T} = \frac{2 - \sqrt{3}M}{2} = 1 - \frac{\sqrt{3}M}{2}$ Where

T_0 is the shoot-through time period

T is the switching period

M is the modulation index

The duty ratio averaged over one switching period of the carrier signal is equal to that of all other switching periods of the carrier signal.

The goal of this method is to achieve maximum boost while remaining constant. See the graph of voltage gain (MB) vs. modulation index in figure 37. Gain approaches infinity

when M decreases to $\frac{\sqrt{3}}{3}$.

Figur

As se

$$\frac{T_0}{T} =$$

Observ

and tha

through

this thir

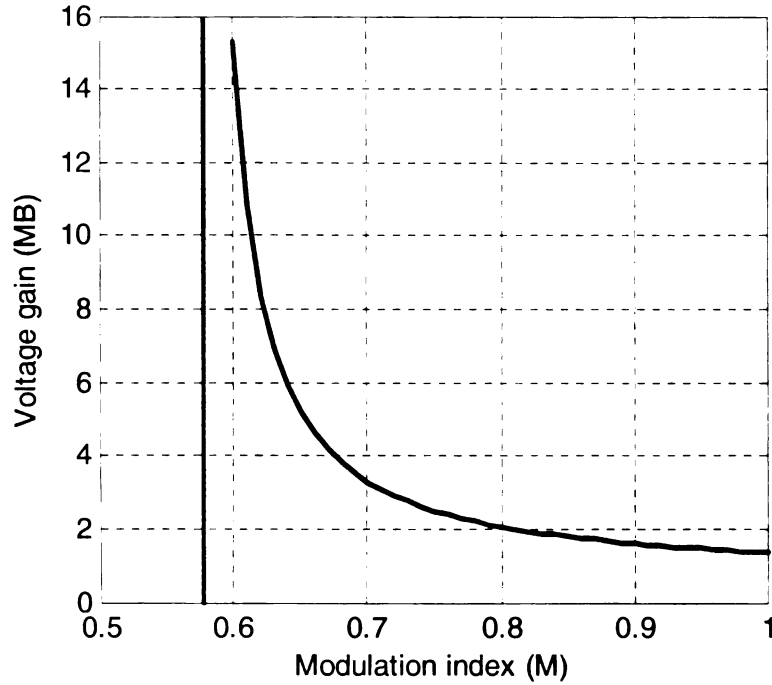


Figure 37 Voltage gain of the maximum constant boost control strategy [18]

As seen before with other PWM control methods, $B = \frac{1}{1 - 2\frac{T_0}{T}}$. and since

$$\frac{T_0}{T} = 1 - \frac{\sqrt{3}M}{2} , B \text{ can be expressed as } B = \frac{1}{\sqrt{3}M - 1} .$$

Observe that V_p and V_n are both third harmonics of the reference voltages V_a^* , V_b^* , V_c^* , and that V_p and V_n ride along the top and bottom of the reference voltages. Shoot-through switching is controlled by comparing V_p and V_n to the carrier signal. Suppose this third harmonic wave form were added directly to the reference voltages.

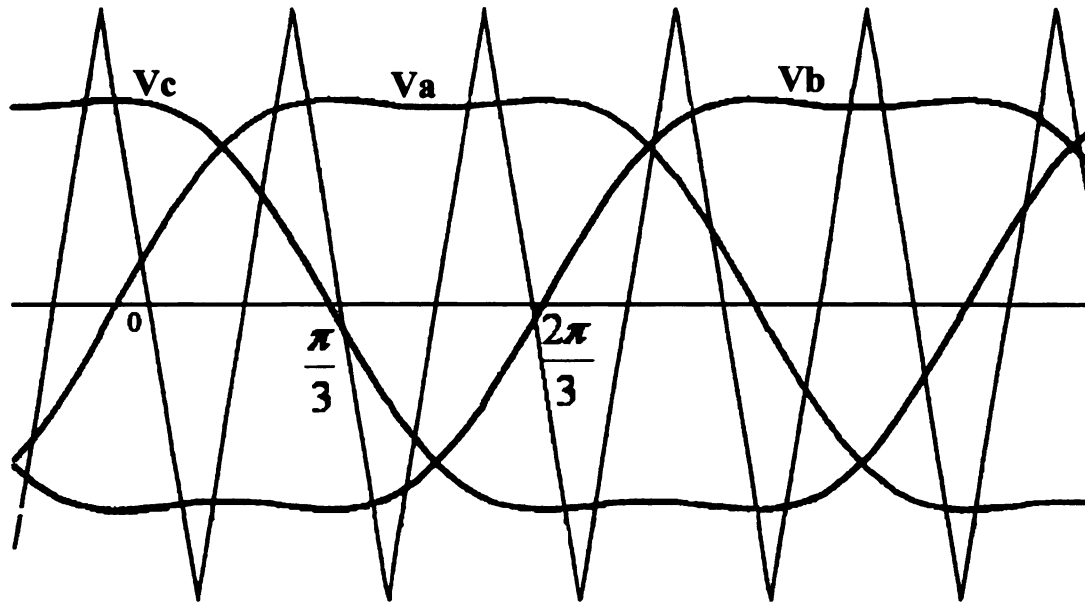


Figure 38 Third Harmonic Injection into Reference Signals

And then instead of the V_p and V_n envelope signals being sinusoids, we replace them with straight lines. What has been done is that the third harmonic component has been subtracted from the envelope signals and has been added to the reference signals (third harmonic injection). This leaves the reference signals shown above and now the envelope signals are straight lines as shown below.

Sap

Sbp

Scp

San

Sbn

Scn

Fig
The resu

duty rati

before \bar{V}

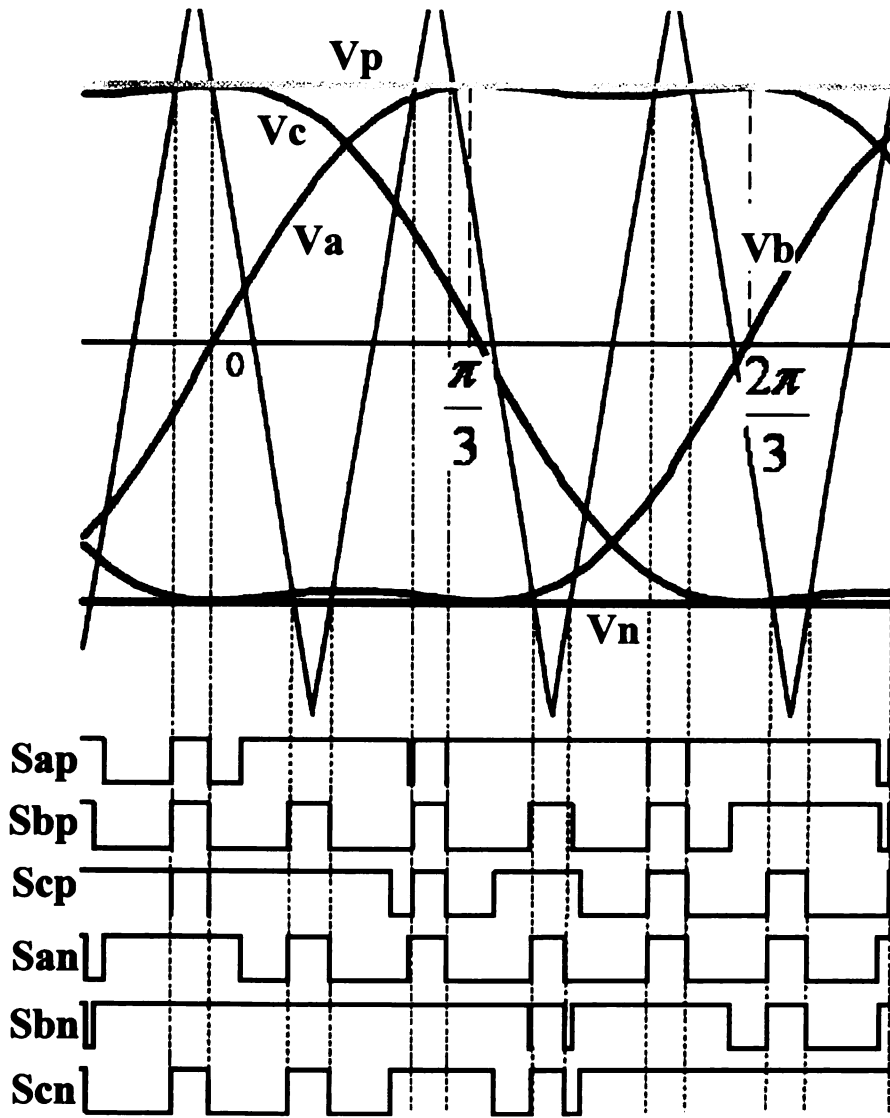


Figure 39 Third Harmonic Injection with Max. Constant Boost PWM [18]

The result is the same maximum constant boost PWM as before and the shoot-through

duty ratio is the same as before, $\frac{T_0}{T} = 1 - \frac{\sqrt{3}M}{2}$, and the gain equation is the same as

$$\text{before } \frac{\hat{v}_0}{V_{dc}/2} = MB = \frac{M}{\sqrt{3}M - 1} = G. \quad \text{Where:}$$

\hat{v}_0 is the output peak phase voltage

V_{dc} is the input dc voltage

G is the gain (MB)

The difference is that with this control method, the range of M is increased to $\frac{2}{3}\sqrt{3}$. The voltage gain vs. M is shown in Figure 40. The voltage gain can be varied from infinity to zero smoothly increasing M from $\frac{\sqrt{3}}{3}$ to $\frac{2}{\sqrt{3}}$ with shoot-through states (solid curve in Fig. 40) and then decreasing M to zero without shoot-through states (dotted curve in Fig. 40).

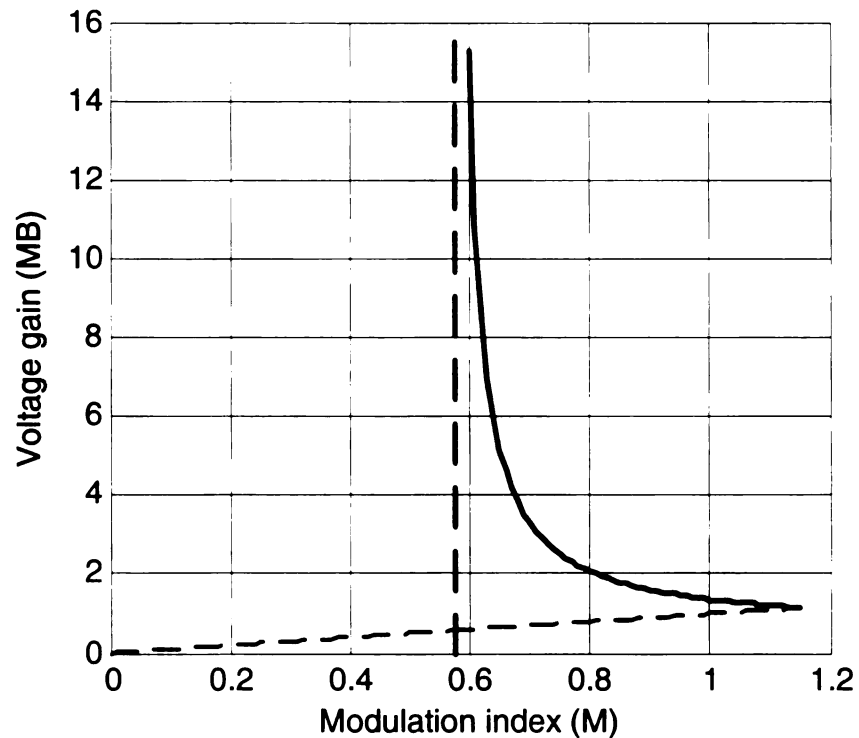


Figure 40 Voltage gain of the maximum constant boost control with third harmonic injection [18]

Voltage stress across the switching devices is $V_s = BV_{dc} = (\sqrt{3}G - 1)V_{dc}$. A graphical comparison of the voltage stresses of the control methods is shown in figure 41.

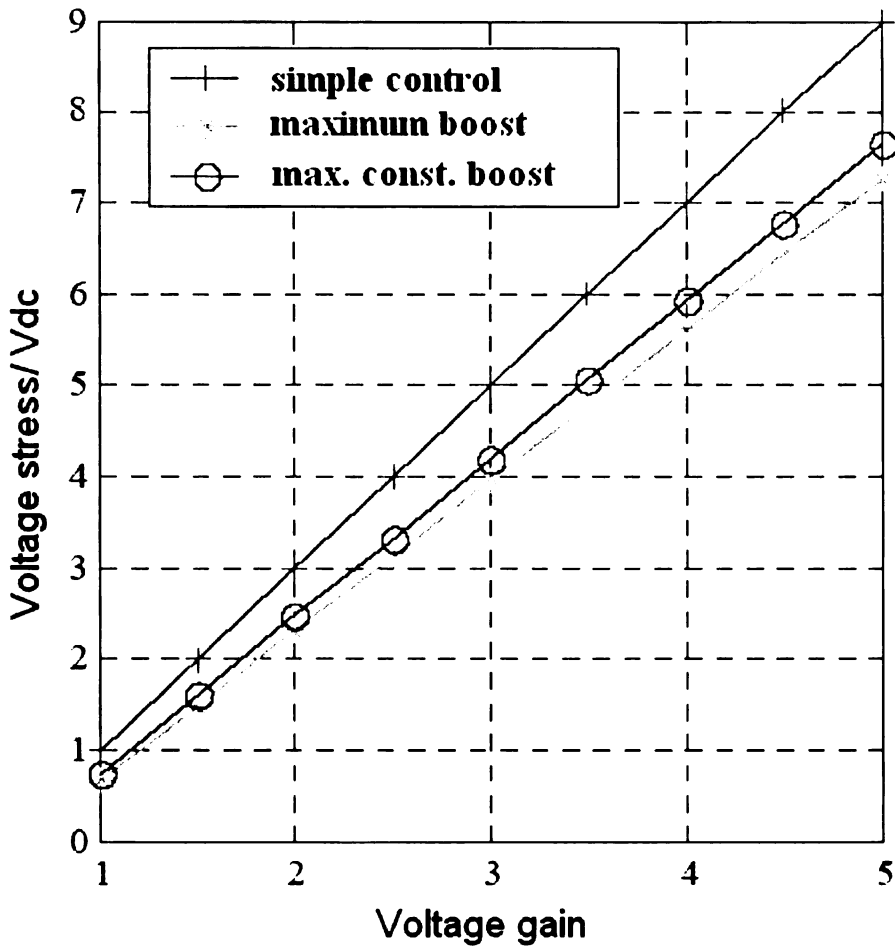


Figure 41 Voltage stress comparison of different control methods [18]

As can be seen, maximum constant boost causes higher voltage stress than maximum boost; however, maximum constant boost eliminates the output frequency ripple.

2.4 Input/Output Equations of the Z-source Inverter

The function of the Z-Source Inverter is to convert a DC input voltage into an ac

output voltage. Using V_0 as the DC input voltage and \hat{v}_i as the DC Link voltage across

the inverter, $\hat{v}_i = B * V_0$ [16]. From this it is seen that the DC Link voltage is

controlled by the boost factor B, where $B = \frac{1}{1 - 2 \frac{T_0}{T}} \geq 1$.

Where

T_0 is the shoot-through period

T is the switching period (period of the carrier signal)

The inverter switches deliver this DC voltage to the output using PWM to convert the DC to a sinusoidal ac voltage. The output of the inverter is

$$\hat{v}_{ac} = M * \frac{\hat{v}_i}{2} = M * B * \frac{V_0}{2}$$

Where

\hat{v}_{ac} is the peak ac output phase voltage

M is the modulation index.

This equation shows that the output can be bucked or boosted by choosing the correct buck/boost factor B_B where $B_B = M * B = (0 \sim \infty)$.

Where M is the modulation index. This equation shows that the output voltage can be stepped up and down by choosing an appropriate buck–boost factor, B_B .

$$B_B = M * B = (0 \sim \infty).$$

3. INTRODUCTION TO POWER ELECTRONICS TOPOLOGIES AND THEIR OPERATING PRINCIPLES

The purpose of this thesis is to investigate traction drive systems for a series hybrid electric bus. The purpose of the power electronics is to control the flow of power from or to the ICE's generator, to or from the batteries, and to or from the traction motor. The voltage must be managed in terms of ac frequency and magnitude. The amount of power flow to or from the system batteries must be managed to control the state of charge of the batteries. Power flow to or from the traction motor must be controlled to provide the desired acceleration/deceleration and speed of the bus. In this process, of controlling the power flow for the battery, traction motor, and generator, all must be managed so that optimal efficiency is achieved. Several circuit topologies have been chosen for further investigation. Below is a summary of the topologies which will be discussed in more detail.

- Traditional Input Rectifier/VSI to Output VSI
- Input Rectifier/VSI to Output CSI with Z-Source impedance network
(battery in parallel with Z's capacitor)
- Input Rectifier/CSI to Output VSI with Z-Source impedance network
(battery in parallel with Z's capacitor)
- Input Rectifier/VSI to Output CSI with Z-Source impedance network
(battery in parallel with Input Converter)

Each topology and its operating principles will be discussed. The traditional Input Rectifier/VSI to Output VSI will be discussed first due to its historical familiarity. This topology will be used to discuss the general function of the power electronics to deliver and control power. Chapter two discussed the specific methods used to control the inverters. This chapter discusses not how it is controlled (SPWM, etc.), but what it is being controlled to do. Where power is to come from and where it is to be delivered to. The hybrid bus has the flexibility of choosing where power is to come from and where it is to be delivered to. The goal is to make choices that optimize efficiency. In general, this means that the ICE and generator are to be operated at only one or two power and angular velocity settings to supply average power required. The batteries are to provide the “dynamic” load. That is the power above and below the average power needed. In a typical bus route, the bus must accelerate and decelerate many times. The total energy expended by the bus on its bus route divided by the amount of time it takes, gives us the average power. In this example, while the bus is accelerating, the traction motors typically requires more power that this average power level. This additional momentary power variance is to be provided by the batteries. With this method, the ICE power vs. angular velocity is chosen to be its most efficient operating point. Operation at the most efficient point is not possible with the conventional bus since the ICE alone must provide all of the range of angular velocity and of power that the bus’s wheels require. Also, the hybrid bus is capable of recapturing deceleration energy which is wasted by conventional busses. To move power consistent with these goals, several operation modes are encountered. These modes are listed here:

Hybrid Operational Modes:

1. Battery and Traction Motor mode

The traction motor is lightly loaded, the battery is supplying power to the traction motor, and the generator is off.

2. Battery, Starter Motor and Traction Motor mode

The battery is supplying power to the traction motor and simultaneously providing power to the generator. The generator is momentarily being used as a motor to start the internal combustion engine (ICE).

3. Generator, Battery Discharge and Traction Motor mode

The traction motor is medium to heavily loaded. The generator and the battery are both supplying power.

4. Generator, Battery Charging and Traction Motor mode

During this mode, the Traction Motor load has decreased and the battery transitions from discharging to charging.

5. Regenerative Braking and Battery Charging mode

During this mode, the load at the traction motor becomes negative and the traction motor functions as a regenerative brake (generator). The battery is charging.

In order to be considered for use on the hybrid bus, a specific power electronics circuit topology must be able to function in each mode. There are four topologies to be discussed. The first is the traditional Input Rectifier/VSI to Output VSI shown below.

This circuit architecture uses a capacitor in the center to provide constant voltage and varying current. Because of the constant voltage provided to the inverters, and the bidirectional current flow in the inverters, these inverters are called voltage source inverters (VSI).

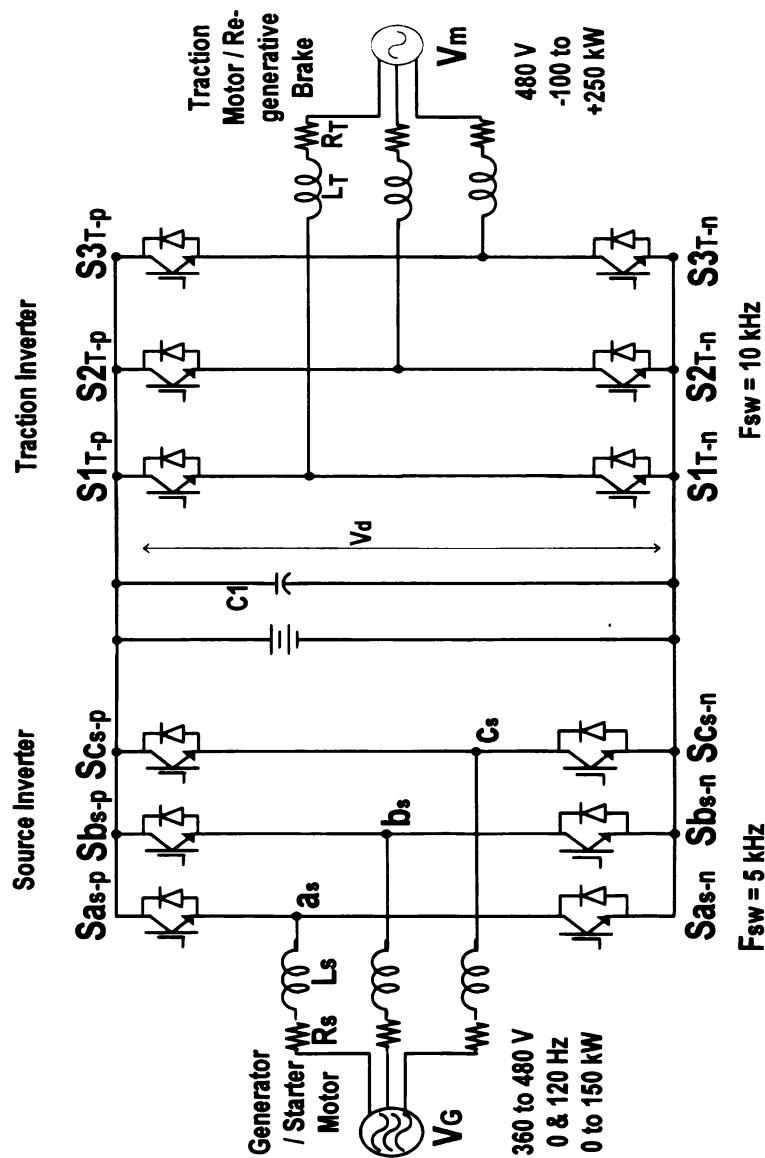


Figure 42 Traditional Input Rectifier/VSI to Output VSI. The left end of the schematic shows the generator which is connected to the ICE. This end is considered the power flow input. The term rectifier is also used since the input converter may be used as a passive rectifier. Voltage sources in the center and a VSI at the output

The second circuit architecture is the Input Rectifier/VSI to Output CSI with Z-Source impedance network (battery in parallel with Z's capacitor). Because of the bidirectional current flow allowed by the input converter (on the left of the schematic), the input converter is called a VSI. Notice that the output converter (right side) only allows one directional current flow but bidirectional voltage blocking. As such, it is called a CSI. The network in the center is made up of the unique combination of capacitors and inductors and is called the Z-Source (Impedance-Source).

The third circuit architecture is the Input Rectifier/CSI to Output VSI with Z-Source impedance network (battery in parallel with Z's capacitor). This topology is the same as directly above except that the converters are swapped end for end. In this case, the input converter is the CSI which allows only one directional current flow and bi-directional voltage blocking while the output converter is the VSI converter. Its schematic is now shown below.

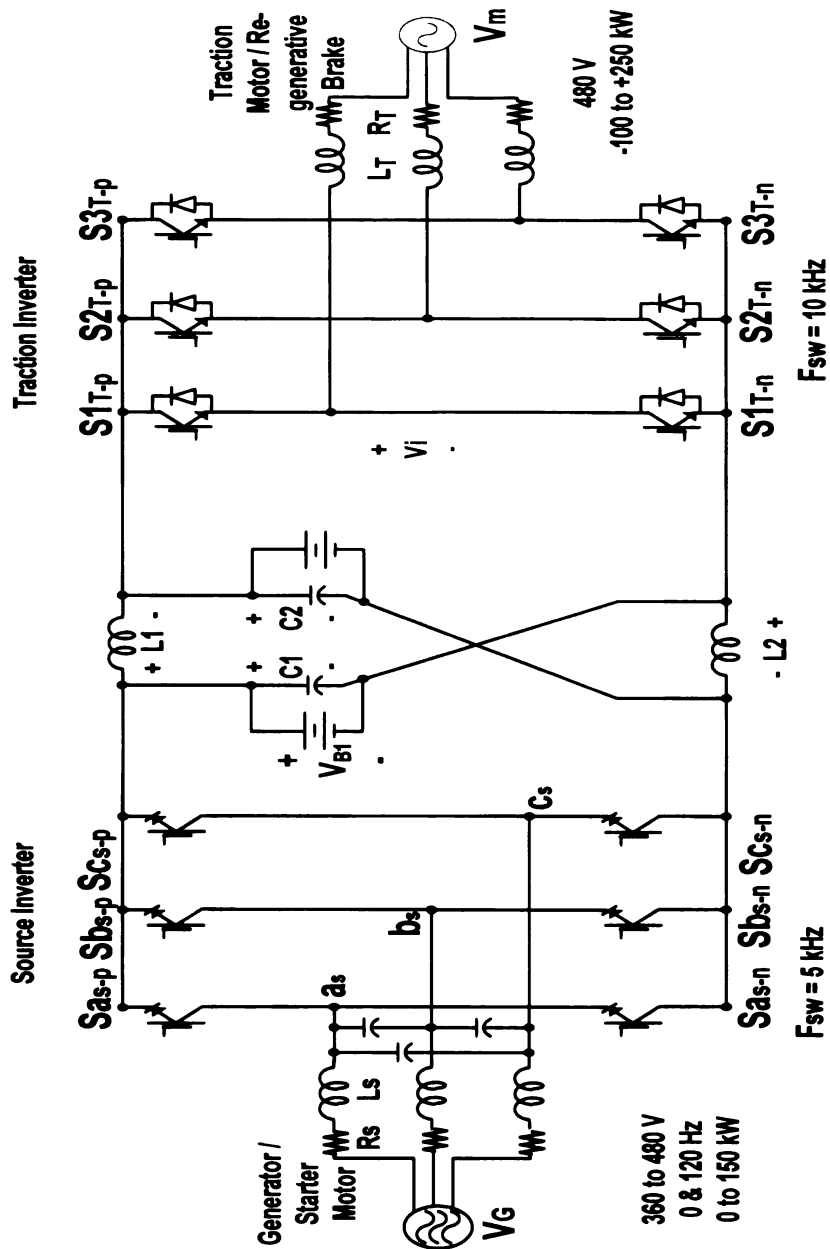


Figure 44 Input Rectifier/CSI to Output VSI with Z-Source impedance network (battery in parallel with Z's capacitor). The left end of the schematic shows the generator which is connected to the ICE. This end is considered the power flow input. The term rectifier is also used since the input converter may be used as a passive rectifier. Z-Source network in the center and a VSI at the output

The fourth circuit architecture is the Input Rectifier/VSI to Output CSI with Z-Source impedance network (battery in parallel with Input Converter). This is like the second circuit shown above except that the battery position is different. The schematic is shown below.

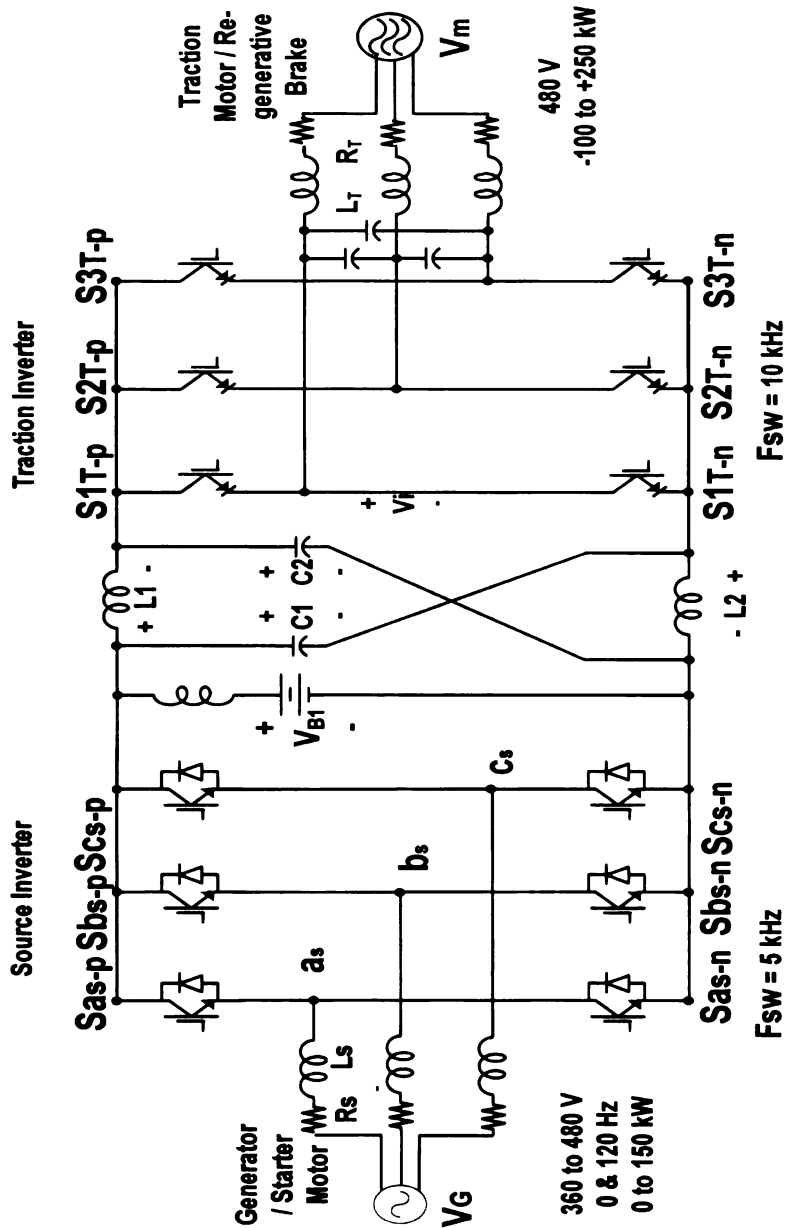


Figure 45 Input Rectifier/VSI to Output CSI with Z-Source impedance network (battery in parallel with Input Converter). The left end of the schematic shows the generator which is connected to the ICE. This end is considered the power flow input. The term rectifier is also used since the input converter may be used as a passive rectifier. Z-Source network in the center and a CSI at the output

Sections 3.1 to 3.4 discuss the operational principles of these four circuits. Because of its historical familiarity, the traditional VSI – VSI topology example (section 3.1) will be used to explain the operational modes in detail. Also, a discussion regarding the pros and cons of using a high voltage battery vs. a low voltage battery is included in this section (section 3.1.3).

3.1. Traditional Input Rectifier/VSI to Output VSI

The schematic of this topology is shown above in Fig. 42 Recall from chapter 2, that the VSI must have a voltage source that is greater than the desired output voltage level.

$$V_{LL} = \frac{\sqrt{3}}{\sqrt{2}} \frac{V_{dc}}{2} M$$

Where: V_{LL} is the line to line RMS output voltage

V_{dc} is the dc input voltage

M is the modulation index [$0 \leq M \leq 1.0$]

Therefore, the VSI is considered a buck converter. If V_{dc} cannot be as high as we would like, a DC/DC converter can be added to the circuit architecture to achieve the required input voltage. First, this circuit's functionality in each of the five modes will be discussed. Following that, the use of a high voltage battery will be discussed and then the use of a low voltage battery with DC/DC converter will be discussed.

3.1.1 Battery & Traction Motor Mode

In the first operation mode, (Battery and Traction Motor) the entire load is being

supplied with battery power through the traction motor. This mode assumes that the state of charge (SOC) of the batteries has reached the maximum allowed for longevity. Therefore, the ICE and generator will be off and all switches of the input VSI will be open. Current from the battery will flow to the traction motor through the output VSI. The output VSI will control the switching functions to provide the required voltage level and frequency. This mode is typically encountered when the bus is sitting still and the bus driver has depressed the accelerator pedal so that the bus will begin to move. In this particular state, a low voltage and low frequency output is required from the output VSI. The low voltage is controlled by using a small modulation index “M” and the low frequency is controlled by a motor controller that is designed for permanent magnet alternating current motors (PMAC). The motor control algorithm controls the voltage phase to provide “d” and “q” axis currents such that the stator field is 90^0 out of phase with the rotor field, i.e. the “d” axis current = 0. This efficiently accelerates the bus with the maximum torque that is available at the chosen current level.

3.1.2 Battery, Starter Motor, Traction Motor Mode

The second mode is the “Battery, Starter Motor and Traction Motor mode.” Typically, this mode follows the first mode discussed. For example, when the amount of power to the traction motor that is requested by the bus driver exceeds the average power level, or the SOC of the battery is below the desired level, the ICE should be started. In this state, the battery is providing power to the traction motor and to the generator. The generator is now being used as a starting motor for the ICE. The switching of the input VSI is now being operated to provide the desired starter motor speed (output voltage frequency) and

voltage level to produce the needed starter motor torque. As mentioned before, the voltage phase is controlled to provide the best torque angle. Once the ICE is started, the input VSI will begin active rectifier mode. It is at this moment that the generator stops functioning as a motor and begins functioning as a generator. The modulation index and VSI phase angle vs. generator phase angle are controlled to pull the average power from the generator. It is the input VSI that controls the power of the ICE. The ICE is governed to maintain the specified angular velocity. The following example helps to explain this power flow control.

Power flow from the generator to the DC link can be modeled as follows.

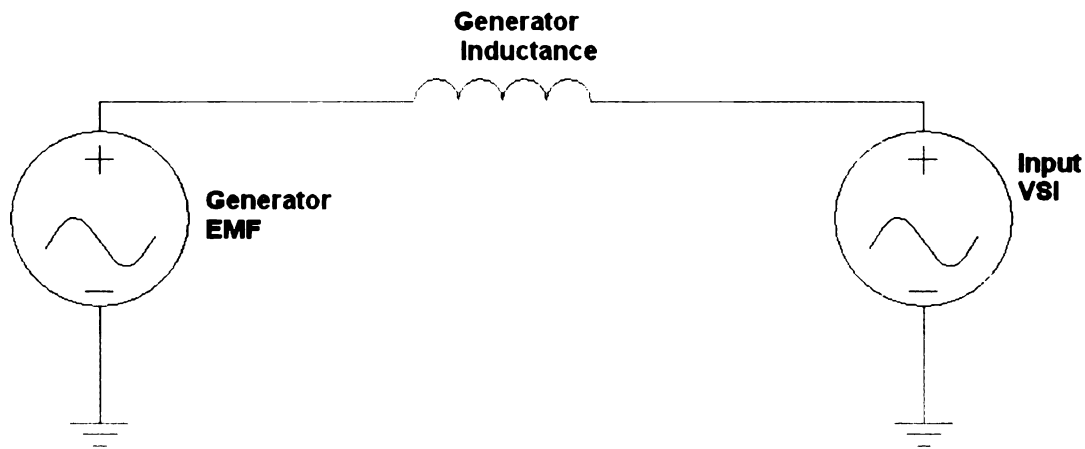


Figure 46 A single phase model of the Voltage Source Inverter and the Generator

In this model, the sinusoidal voltage source on the right represents the voltage of the VSI and the sinusoidal source on the left represents the EMF voltage of the generator. Between these two sources is the generator's inductance and negligible resistance. Power

flow through this inductance can be seen to be

$$P_{1\phi} = \frac{V_{VSI} \sin(\theta_{VSI}) - V_{GEN} \sin(\theta_{GEN})}{Z}$$

Shifting the phase of both sources by 90° does not change the power. We then have:

$$P_{1\phi} = \frac{V_{VSI} \cos(\theta_{VSI}) - V_{GEN} \cos(\theta_{GEN})}{Z} \quad \text{If we let } V_{GEN} \text{ be the}$$

reference voltage and treat the angle as 0 we arrive at the following.

$$P_{1\phi} = \frac{V_{VSI} \cos(\theta_{VSI}) - V_{GEN}}{Z} \quad \text{In this equation it can be seen that the variables}$$

that are controlled by the VSI are the voltage magnitude and angle of the inverter. V_{GEN} is determined by the angular velocity of the generator which is determined by the angular velocity of the ICE, Z is a constant of the generator. Accordingly, power flow (positive or negative) can be controlled by controlling the V_{VSI} and θ_{VSI} relative to the voltage magnitude and angle of the generator.

3.1.3 Generator, Battery Discharge, Traction Motor Mode

The third mode is the “Generator, Battery Discharge and Traction Motor mode.” In this mode, the input VSI operates as an active rectifier. The voltage and phase angle of the generator is monitored. The modulation index and VSI phase angle vs. the generator phase angle are controlled by the VSI to pull the specified power from the generator. Generator voltage polarity matches that of the DC link, current flows through the rectifier, and power is thereby transferred to the DC link. In this mode, the power requested by the bus driver exceeds the average power which the ICE and generator are

now providing, and the excess power is provided by the battery.

3.1.4 Generator, Battery Charging, Traction Motor Mode

The next mode is the “Generator, Battery Charging and Traction Motor.” Very similar to the mode discussed just above. In this mode, however, the battery is now receiving charge rather than providing power. This mode is typically entered when traction motor power drops below the average power level. When the bus driver raises the accelerator pedal, the output VSI reduces modulation index (thereby voltage) and or phase angle to decrease the amount of power being pushed to the traction motor. If this amount of power is below the average power being supplied by the ICE, generator and input VSI, the excess power flows into the battery.

3.1.5 Regenerative Braking and Battery Charging Mode

The “Regenerative Braking and Battery Charging mode” occurs when the traction motor becomes a generator. If the bus is moving and the bus driver allows the accelerator pedal to return to the full up position, the output VSI will enter the regenerative brake mode. This is accomplished by control of the Traction Motor VSI phase angle and modulation index. By causing the output VSI phase angle to lag that of the traction motor, the traction motor pushes power to the DC link through the output inverter thus functioning as a generator (regenerative brake). See Figure 47 below. The negative torque slows the bus and generates power that will be stored in the battery. In this mode, the ICE may be stopped or may continuing running depending upon the needs of the battery SOC and

the allowed max rate of change. When power flow is controlled via inverter phase angle vs. phase angle of an ac machine, voltage magnitude is also controlled via modulation index. With these two controls, power factor can be maintained near unity.

Control of the transition from motoring mode to braking mode can be shown with the following graphs. While in motoring mode, the phase angle of the output VSI is controlled to lead that of the traction motor. See Figure 47 below.

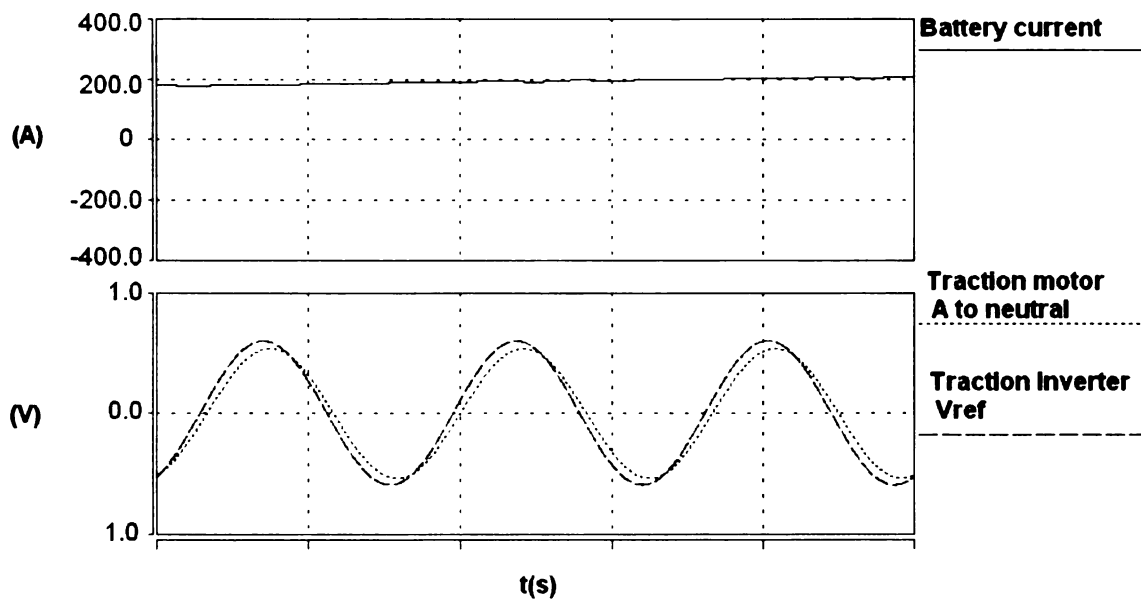


Figure 47 Voltage Phase Angle Control

As can be seen, the battery current is positive showing that the battery is discharging (providing power to the traction motor). The transaction to the regenerative mode is effected by retarding the phase angle of the VSI with respect to the angle of the traction motor (brake).

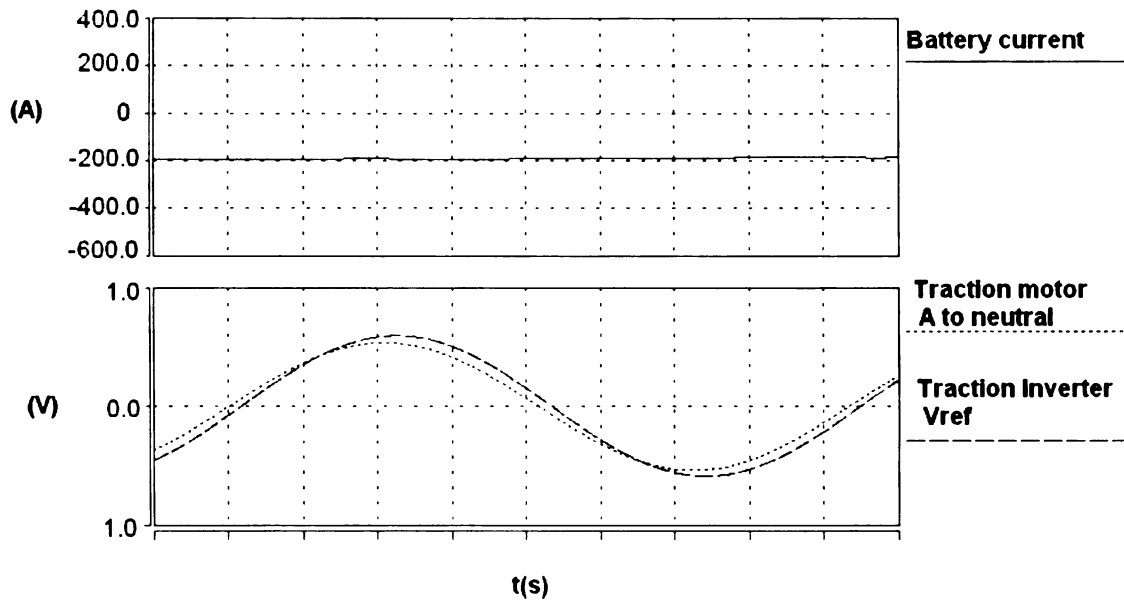


Figure 48 Voltage Phase Angle Control

The above graphs shows the case where the ICE & generator are off, and the traction motor voltage leads the inverter voltage thus pushing power from the traction motor (now in regenerative mode) to the DC link through the output VSI. the negative battery current in the top graph shows that the battery is being charged by the regenerative process. The VSI's reference control voltage is shown in the graph above since it more clearly illustrates the principle than the actual discrete voltage pulses of the PWM waveform. Voltage magnitudes are normalized.

3.1.6 High voltage battery

Figure 42 above shows the high voltage battery option where the battery is in parallel with the capacitor. In this case, the battery will need to be at least

$$V_{dc} = \frac{2\sqrt{2}}{\sqrt{3}} \frac{480}{M} = 784Vdc$$

In order to achieve a sinusoidal voltage of 480 V_{RMS} line to line. This calls for a series combination of at least 62 batteries if we use the 12.8V lithium ion battery as an example.

3.1.7 Low voltage battery with DC/DC converter

For the low voltage (LV) battery case, the battery will require a DC/DC converter between the LV battery and the DC link. If a 205 V battery is used, this would be 16 12.8 V batteries in series. The DC/DC converter must be able to boost voltage when delivering power from the batteries to the DC link and it must be able to buck voltage when delivering power from the DC link to the batteries. In this case also, a minimum voltage of 784V at the DC Link must be achieved which requires a boost gain of 3.8. Below is a schematic of a typical DC/DC converter.

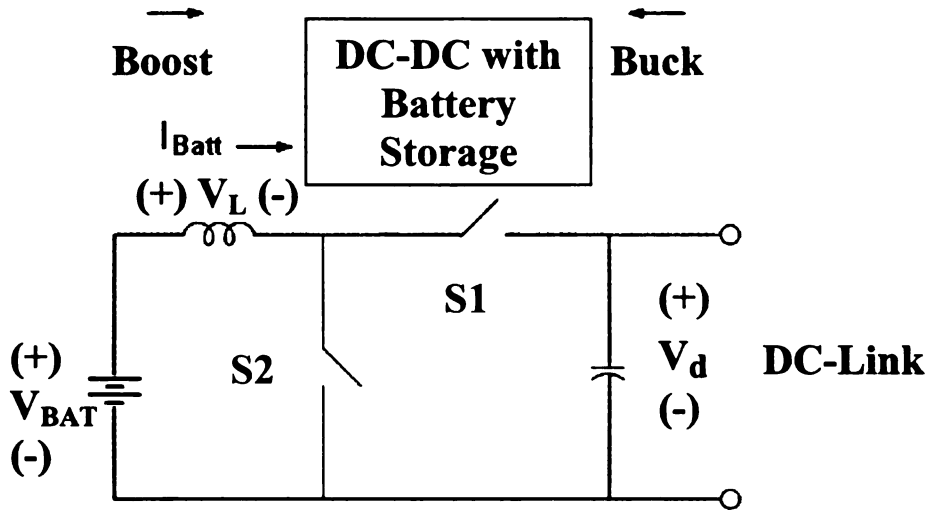


Figure 49 DC/DC Converter

The typical DC/DC converter for such an application has the following gain equation:

The switch function is denoted by the switching period T where $T = T_{ON} + T_{OFF}$. For the inductor, the average voltage across the inductor during steady state is zero. This gives:

$$\bar{V}_L = \frac{(V_{IN} * T_{ON} + (V_{DC} - V_{IN})T_{OFF})}{T} = 0$$

$$V_{IN} * T_{ON} = (V_{DC} - V_{IN})T_{OFF}$$

$$V_{IN} * T_{ON} + V_{IN} * T_{OFF} = V_{DC} * T_{OFF}$$

$$V_{IN} (T_{ON} + T_{OFF}) = V_{DC} * T_{OFF}$$

$$\frac{V_{DC}}{V_{IN}} = \frac{T}{T_{OFF}}$$

$$\frac{V_{DC}}{V_{IN}} = \frac{T}{T - T_{ON}}$$

Section 3.1.8 below gives a comparison of the high voltage battery versus low voltage

and discusses the pros and cons. The comparison is discussed here in the back to back VSI section, but the principles apply to the other topologies as well.

3.1.8 Comparison of the high voltage battery vs. the low voltage battery

High Voltage Battery Option

The high voltage battery has the advantage of being able to connect directly to the DC-Link without the use of a DC-DC converter. This option is simple in design and uses fewer electronic components. It does, however, require a greater number of batteries to be stacked in series. There is also a fundamental problem with connecting batteries in series. If the Lithium Ion battery is used as an example, due to its lighter weight and relatively fast charging rate, e.g. Valence Technologies U27-FN130, it can receive a maximum charge current of 100A. A series connection of 51 batteries is needed to achieve a total voltage of 654 volts. With such a series connection, a failure of any one of the 51 batteries will cause a serious degradation of performance. The reliability equation for series-parallel arrays of electronic components is as follows.

$$R(t) = [1 - p^n F^n(t)]^m - [1 - (1 - qF^n(t))]^m$$

Where:

- R(t) is the reliability,
- p is the conditional probability of a short,
- q is the conditional probability of an open,

- m is the number of parallel paths,
- n is the number of components in series,
- $F(t)$ is the cumulative distribution function of time to failure of series components [19]

In this particular case, the short circuit failure rate is quite low for batteries. Typically, battery failures occur from an increase in resistance and or a decrease in voltage. As a result, reliability decrease is much more likely to occur from series connections than from parallel connections.

If it is necessary to receive a charge at greater than 100 A, additional parallel combinations of 51 series batteries will be needed. As can be seen, the number of batteries required can add up quickly. Also, with series connections, each battery is slightly different than the other batteries that it is connected to (different internal resistance, different voltage level, etc.) As a result, some of the series batteries are putting out more power than others. Under high current levels, a poorly functioning battery may actually be dissipating more power than it is providing. The net result is a compromised performance of the whole stack.

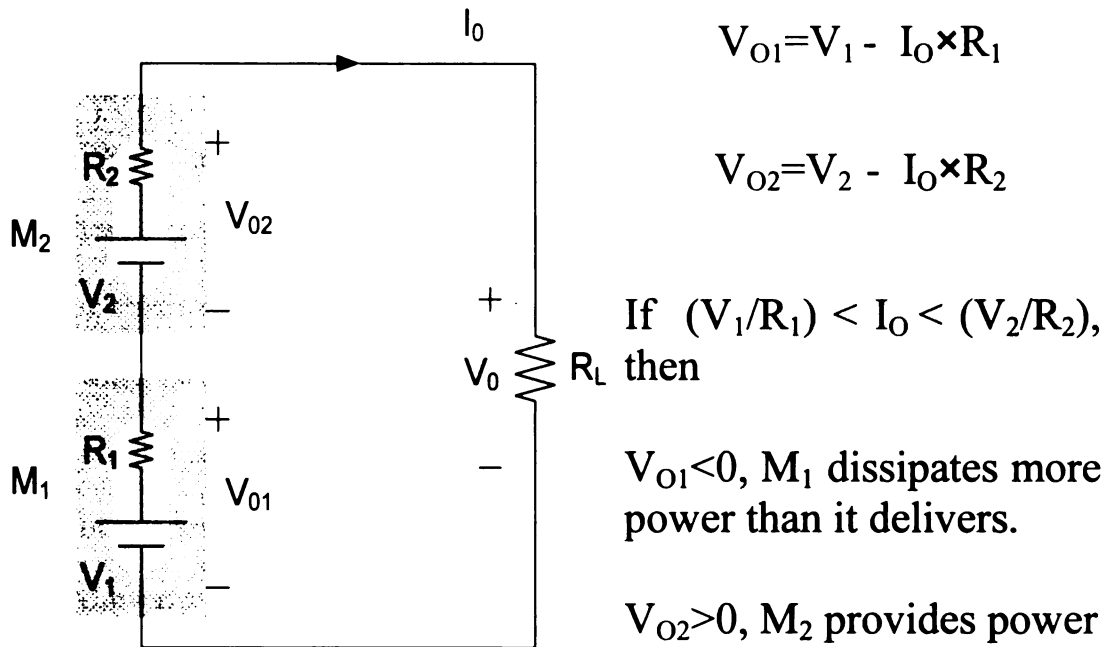


Figure 50 Series Combination of Battery Cells; See Note ⁱ

As the age of the batteries increase, these conditions worsen. Due to these factors, the high voltage battery has a lower reliability than the DC-DC boost and low voltage battery combination. Battery management electronics can be added to monitor individual battery condition and allow for by-passing weak cells, but this adds to the complication and cost.

Typically, a high voltage series stack is more costly than a low voltage stack of the same Amp hour rating as it is easier for the manufacturer to assemble large battery cells than two smaller cells in series. Also with the high voltage battery stack comes the additional safety concerns for service personnel, rescue workers, etc.

ⁱ Used with permission from Chen, Lihua 04-04-07

Low Voltage Battery with DC-DC buck/boost converter

With a low voltage stack, a DC-DC buck/boost converter is required. Since the low voltage stack voltage level is less than that of the DC Link, a boost converter is required between the DC Link and the batteries. This boost function is required when the batteries are delivering power to the DC Link. When the DC Link is delivering power to the batteries, a buck function is required. The disadvantage of this low voltage arrangement is that this additional circuit (DC-DC buck/boost converter) is needed. Along with the additional circuitry, come additional cost and complexity and lowering of reliability due to the additional components. The advantages of this design however, is that the total number of batteries in series will decrease, and this will increase system reliability for the reasons discussed above.

The use of a DC-DC converter adds an extra level of control for the battery SOC by controlling the DC output voltage level. Although this level of control is not needed to control battery SOC since coordinated control of the generator inverter/rectifier and traction motor inverter/converter also achieve SOC control. Still, the DC-DC converter can provide this as well as an added level of battery health monitoring and control. The low voltage option also reduces voltage levels present when the vehicle is not running which can reduce risk factors to passengers and emergency personnel in the case of a collision involving the bus. The low voltage option reduces the energy losses during low power operation by

reducing the DC rail voltage and thereby the voltage across the IGBT modules. THD is reduced during lower power operation by reducing the DC rail voltage to lower output voltage and thereby keeping the modulation index of the inverters higher which reduces THD.

Summary of High Voltage Battery Option vs. Low Voltage Battery Option

High Voltage Option

Pros:

- Battery Voltage = DC Link Voltage and a DC-DC converter is not Required

Cons:

- Greater number of Batteries in series and a related decrease in reliability of the battery stack

Low Voltage Option

Pros:

- Lower number of batteries in series and a related increase in reliability of the battery stack.
- Extra level of control for battery SOC
- Reduced non-operating voltage levels
- Reduced energy loss during low power operation
- Reduced THD during low power operation

Cons:

- A DC-DC converter is required
- Decreased reliability due to additional components.

3.2 Input Rectifier/VSI to Output CSI with Z-Source impedance network

(battery in parallel with Z's capacitor)

The schematic for this architecture is re-displayed here for convenience.

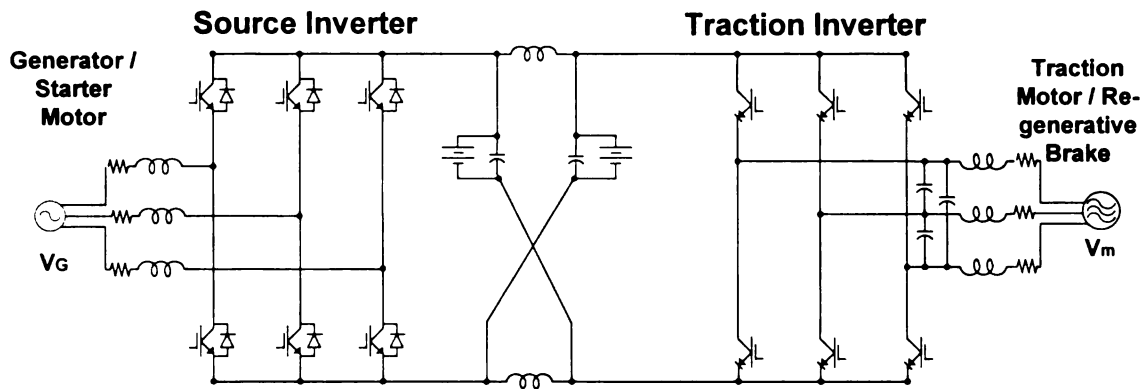


**Figure 51 Back to Back VSI, CSI with Z-Source Network
Re-displayed for convenient reference**

The meaning of the different hybrid operational modes has been well covered in the previous section. However, some discussion is needed regarding regenerative braking. In the case of the back to back VSI discussed in section 3.1, the regenerative power flow is easy to visualize since its current flow can simply reverse directions on the Dc link.

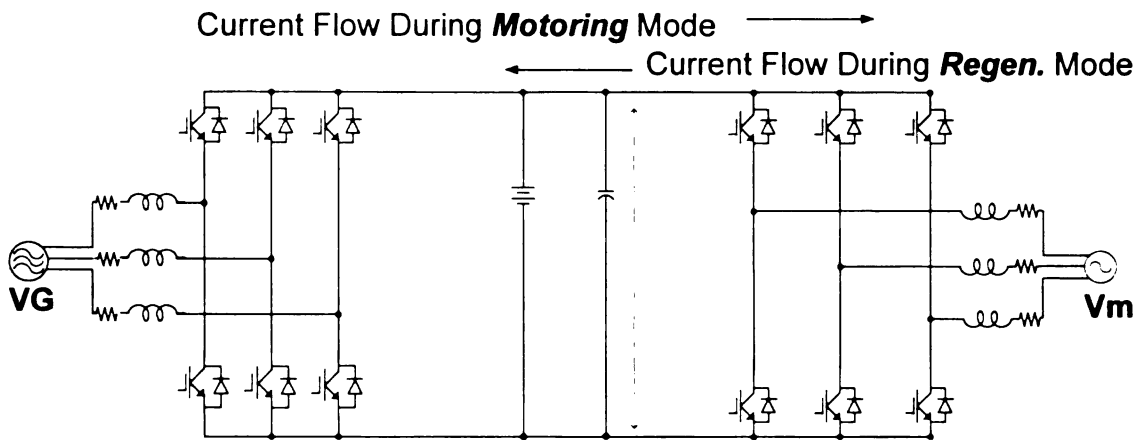
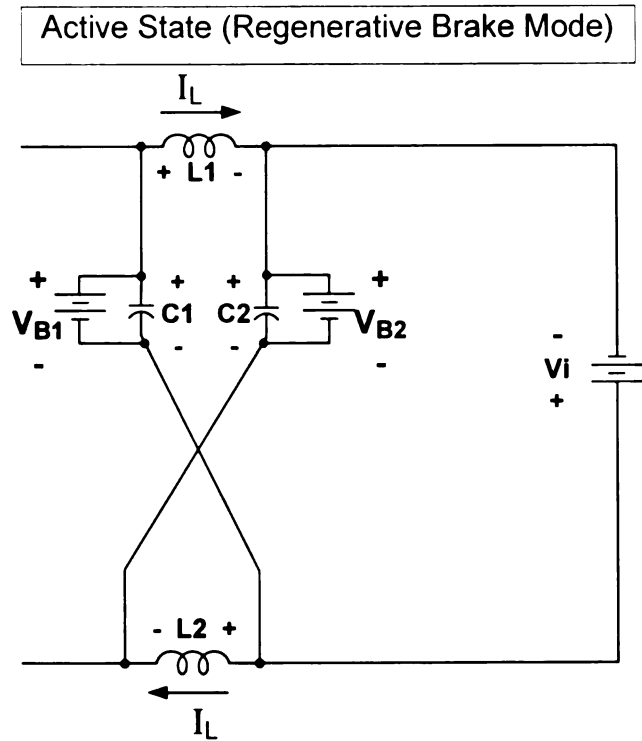


Figure 52 Back to Back VSI topology

Showing the direction of current flow for regenerative braking and for motoring modes

In the case of the VSI-Z-CSI shown in Fig. 51 above, the Traction Motor/Regenerative Brake is driven by a CSI. The CSI uses reverse blocking IGBT modules which only allow current flow in one direction. Therefore, it is somewhat less obvious how the regenerative power flow occurs. To go into regenerative braking, the CSI shifts its phase so that the polarity of the traction motor inverts. The voltage across the stator windings is phase shifted such that the stator field is now resisting the rotation of the rotor. The traction motor is now a generator with its positive terminal on the bottom rail of the DC link. See Figure 53.



**Figure 53 Back to Back VSI, CSI Z-Source Topology
Modeling the active state of the regenerative mode**

During the active state of regeneration, the output inverter functions as an active rectifier and can be modeled as a DC source. During this active state, the regenerative energy is being stored in the Z-Source inductors. The voltage across each inductor is $V_L = V_i + V_C$ where V_C is the capacitor voltage. This voltage level is greater than that of the previous state and therefore the inductor magnetic field is building. The next state is the open circuit zero state for the CSI and active state or short circuit zero state of the VSI. The short circuit zero state of the VSI is shown below.

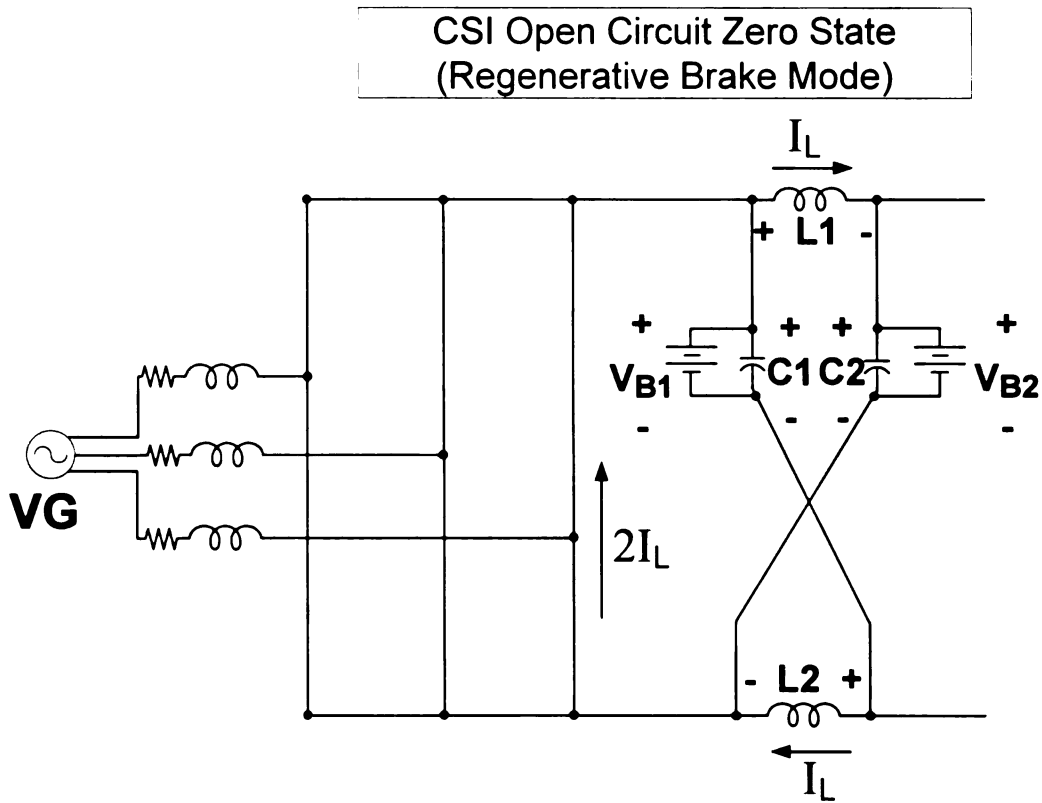


Figure 54 VSI-Z-CSI Regenerative Mode with VSI in SCZ

It is during this state that regenerative braking energy is transferred to the Z-Source capacitors and batteries thereby raising their voltage and SOC.

3.2.1 High voltage battery

The high voltage battery option is shown in the schematic above. The Z-Source topology has the ability to both buck and boost voltage levels. Therefore, the high voltage battery does not need to be as high as in the back to back VSI topology. This mitigates some of the concerns associated with the high voltage case.

3.2.2 Low voltage battery with DC/DC converter

The low voltage option is still applicable. With a DC/DC converter connected in parallel across the Z-Source capacitor, all of the hybrid modes still function in the same manner as with the high voltage battery. With a DC/DC converter controlling the voltage on the DC link, an extra degree of control has been added to the overall design. It is necessary that this now be coordinated with the modulation index of the inverters which adds some complexity to the controls.

3.3 Input Rectifier/CSI to Output VSI with Z-Source impedance network (battery in parallel with Z's capacitor)

The schematic is re-displayed here for convenience.

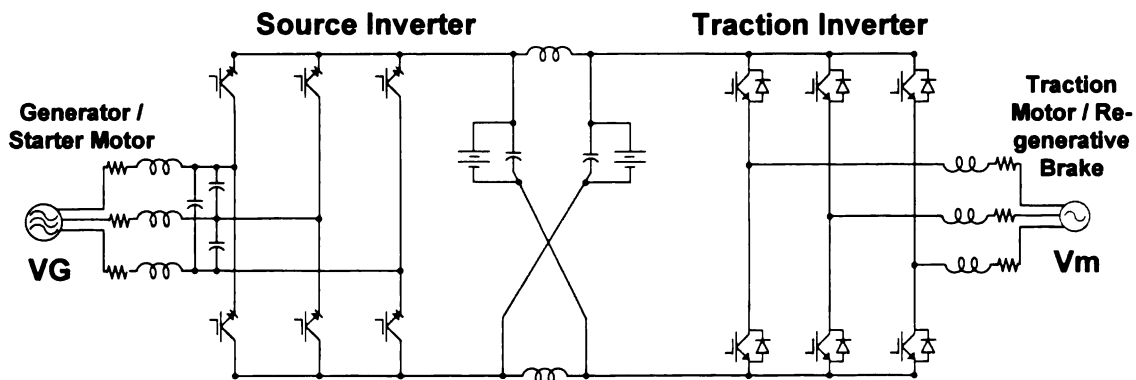


Figure 55 CSI-Z-VSI Topology

In this case, the regenerative braking is again apparent since current direction on the DC link is allowed to change directions as was the case with the back to back VSI. The hybrid mode that should be explained here is the ICE starting mode. While the generator is operating in generation mode, power is transferred from the generator to the DC link. That is, positive current is delivered to the positive voltage DC link. However, to use the generator as a starter motor, power needs to be delivered in the opposite direction. The power direction cannot be changed by simply changing the current direction. The CSI uses reverse blocking IGBT modules.

$$\langle V_{CSI} \rangle = V_B \quad \text{and}$$

$$\langle V_{CSI} \rangle = 2V_B D_{ST} + \langle V_{CSI_AO} \rangle (1 - D_{ST})$$

Where:

$\langle V_{CSI_AO} \rangle$ is average CSI inverter voltage during the VSI's active and open circuit states

T_a is VSI active time period

T_o is VSI open circuit time period

T_{ST} is VSI shoot-through period

$$T = T_a + T_o + T_{ST}$$

D_{ST} is T_{ST}/T

$$\langle V_{CSI_AO} \rangle = \frac{V_B - 2V_B D_{ST}}{(1 - D_{ST})}$$

For the starting operation, the Z-source network will need to be operated with a VSI short circuit (shoot through) duty cycle large enough to cause voltage inversion. When the shoot-through state is over on the VSI end and the VSI goes to the open-circuit mode, the voltage on the inductors L1 and L2 will invert. The magnitude of this inversion must

be $>V_B$ so that V_{CSI} becomes negative. During this VSI open circuit state, the CSI switches will be operated to deliver power to the generator so that it is used as a motor.

Simulation of Reverse Power Flow to Generator

MATLAB CODE

```
VB=1; %Battery Voltage normalized
T=1; %switching period normalized
Dst_1=0;
Dst_end=.9;
Dst=Dst_1:(Dst_1+Dst_end)/100:Dst_end; %shoot-through duty cycle
for i=1:length(Dst)
V1act(i)= (VB*(1-2*Dst(i)))/(1/T-Dst(i));
end
plot(V1act,Dst)
xlabel('DC Voltage across Inverter')
ylabel('Shoot-Through Duty Cycle')
title('Plot of DC Voltage vs. Shoot-Through Duty Cycle')
grid on
```

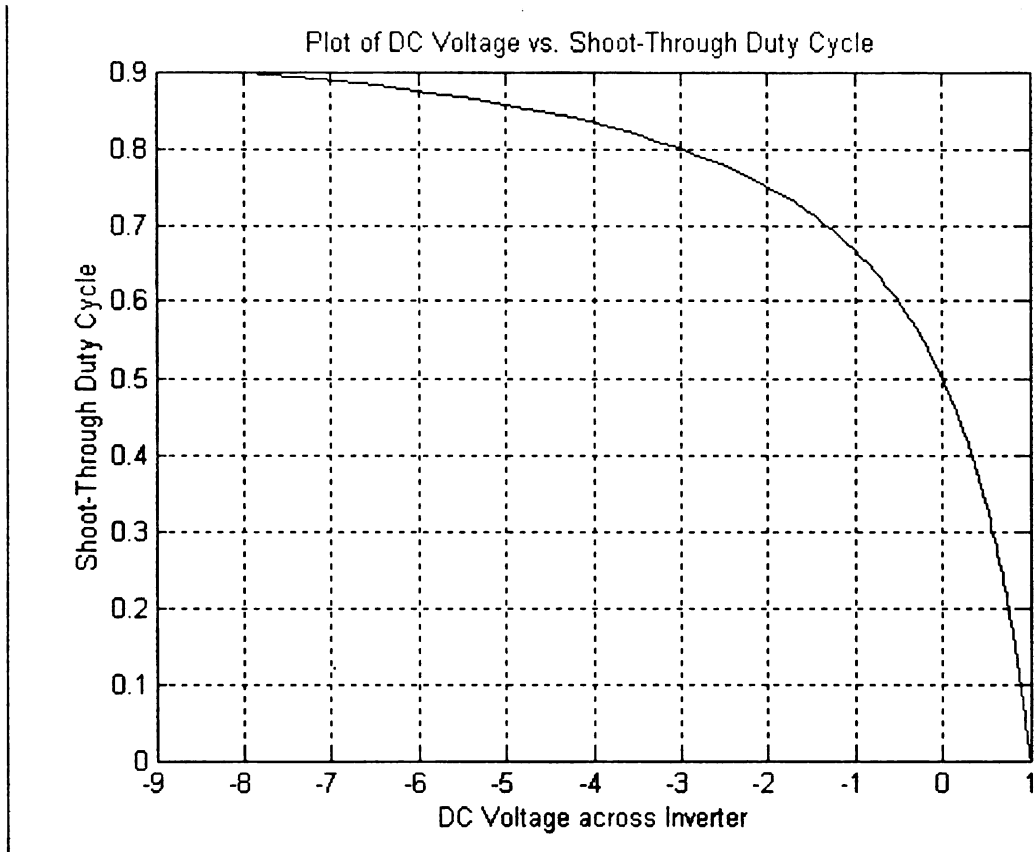


Figure 56 Shoot-Through Duty Cycle vs. DC Voltage Across Inverter

3.3.1 High voltage & Low voltage battery options.

As in section 3.2, both high voltage and low voltage battery options will work with this topology. The low voltage option will require a DC/DC converter.

3.4 Input Rectifier/VSI to Output CSI with Z-Source impedance network (battery in parallel with Input Converter)

This circuit architecture is re-shown here for convenience.

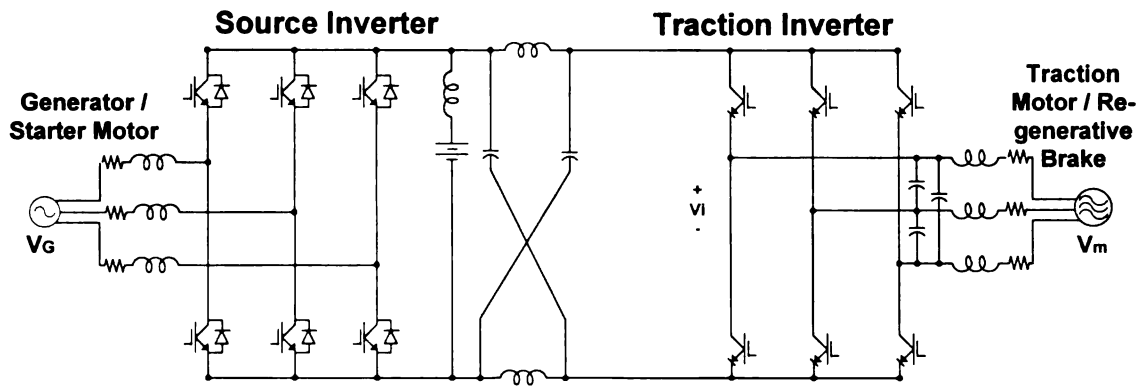


**Figure 57 Input VSI/Rectifier to Output CSI topology
Battery is parallel to the Input VSI**

This topology is similar to the topology of section 3.2 with a few exceptions. In this case, the battery is parallel to the input inverter rather than parallel to the Z-source capacitors. The “Battery and Traction Motor mode” functions very much like that of section 3.2. Also, the “Battery, Starter Motor and Traction Motor mode”, “Generator, Battery Discharge and Traction Motor mode”, and “Generator, Battery Charging and Traction Motor mode” each function very much like section 3.2. It is the “Regenerative Braking and Battery Charging mode” that is different. During re-generative braking mode, as before, the output inverter is controlled such that the stator field now resists the rotation of the rotor and the voltage polarity across the traction inverter is now reversed (positive terminal is down). The current in inductors L1 and L2 remains constant, and the re-generative braking current flows through the Z-source capacitors and to the battery. This occurs during the Active State of the Re-Generative Braking Mode. Following this state, are the Open-Circuit Zero state and the Short-Circuit Zero state. The duration of each state is controlled to achieve the desired level of braking resistance and or the rate of battery charge. Desired braking resistance in excess of that available

via regenerative braking must be accomplished with the traditional mechanical friction brakes. The mechanical friction brakes must be made an integral part of the hybrid (friction & electro-mechanical) braking control system. A schematic of each of the three regenerative braking states are shown below in Fig.58, 59, & 60.

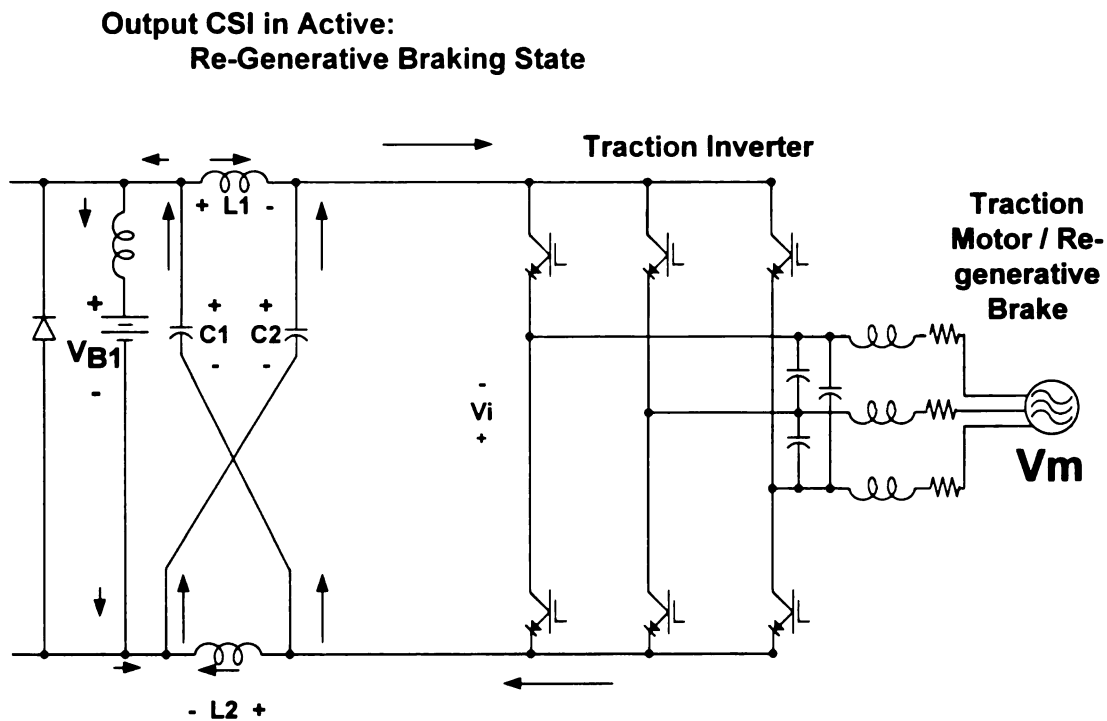


Figure 58 Regenerative Braking with VSI-Z-CSI and Battery Parallel to VSI Active State

**Output CSI in Open-Circuit Zero:
Re-Generative Braking State**

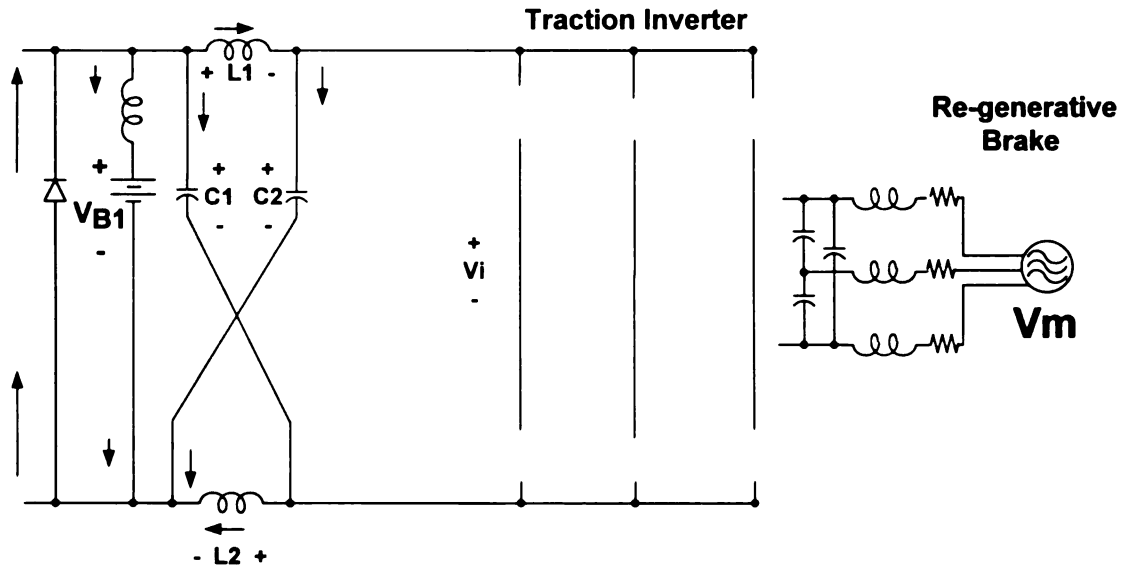


Figure 59 Regenerative Braking with VSI-Z-CSI and Battery Parallel to VSI Open Circuit Zero State

**Output CSI in Short Circuit Zero:
Re-Generative Braking State**

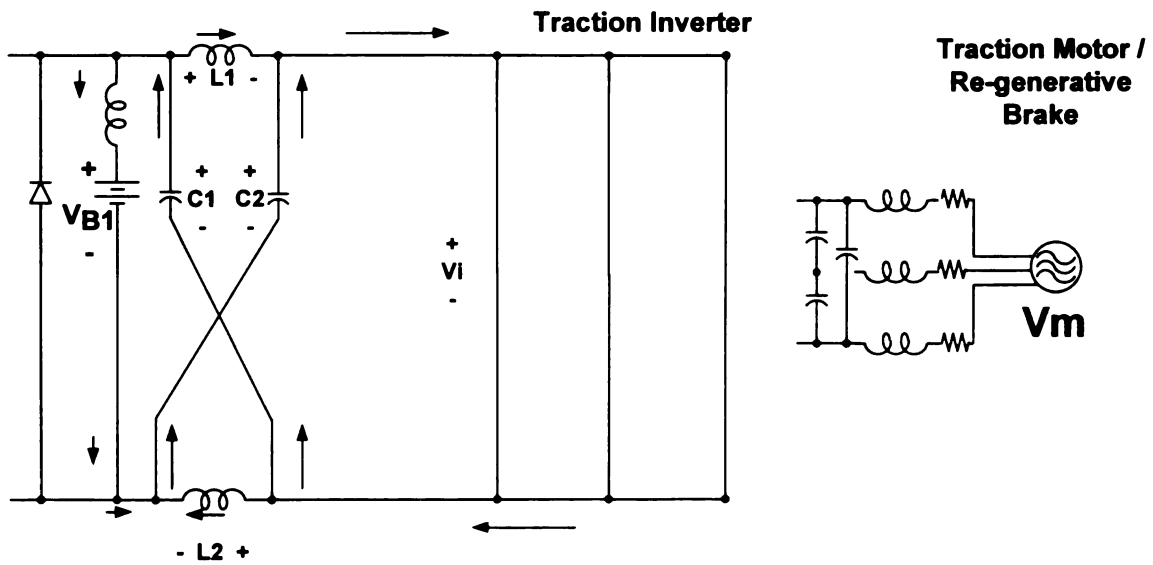


Figure 60 Regenerative Braking with VSI-Z-CSI and Battery Parallel to VSI, Short Circuit Zero State

3.4.1 High voltage

The high voltage battery option will also work well with this topology. The battery, as is shown in the schematics above, is protected with a series inductor. This allows the magnitude of currents through the battery to be controlled, and it maintains the current flow to the battery during the non-active states of regenerative braking.

3.4.2 Low voltage battery with DC/DC converter

The battery's DC/DC buck boost converter would be connected parallel to the input inverter just as the high voltage battery would be. An example schematic is shown in Fig. 61 below.

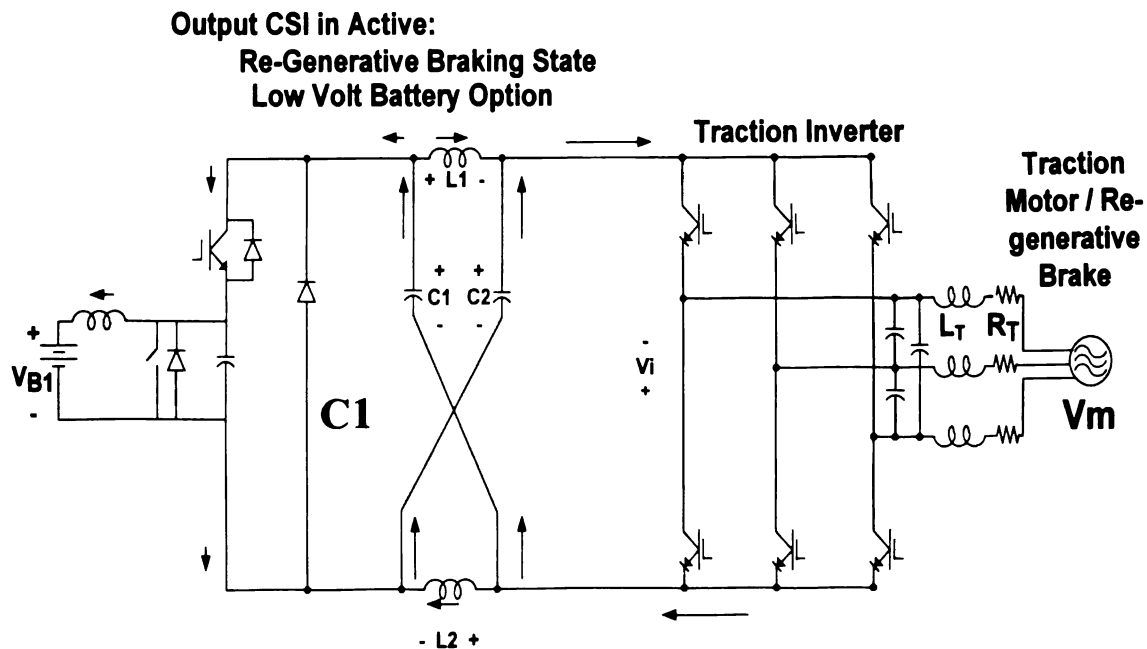


**Figure 61 Input VSI to Output CSI with Z-Source DC Link
Low Voltage Battery Option with DC/DC converter**

3.5 Summary

Each of the circuits show:

- 1.) Traditional Input Rectifier/VSI to Output VSI (VSI-VSI)
- 2.) Input Rectifier/VSI to Output CSI with Z-Source impedance network (VSI-Z-CSI) (battery in parallel with Z's capacitor)
- 3.) Input Rectifier/CSI to Output VSI with Z-Source impedance network (CSI-Z-VSI) (battery in parallel with Z's capacitor)
- 4.) Input Rectifier/VSI to Output CSI with Z-Source impedance network (VSI-Z-CSI) (battery in parallel with Input Converter)

Have unique features which have been discussed. Circuit 1.) has the limitation of only being able to buck voltage levels when providing power from the DC Link to the traction motor. Circuit 2.) has the ability to both buck and boost voltage levels and with its CSI output, it provides a smooth voltage wave to the traction motor. Circuit 3.) also has the ability to buck and boost voltage levels. Its input CSI will have smooth voltage wave forms for the input generator. However, since the traction motor must handle a larger amount of power, the smooth voltages provided by a CSI would be of greater advantage at the output. On the other hand, an output inverter must be sized for larger shoot-through currents and a CSI must be sized for all of the shoot-through current to go through one phase leg of the inverter. The shoot-through currents of a VSI are shared by all three phase legs. The specifics of topology designs are presented in chapter 4.

4. COMPARISON OF POWER ELECTRONICS TOPOLOGIES

4.1 Methodology for Comparison

Various methods are available for comparing one circuit topology to another. A comparison method that lends itself well to power electronics circuits is the determination of the Switching Device Power of each different circuit. This is the method that will be used in this analysis and it is discussed below.

4.2 Description of Switching Device Power Comparison

Switching Device Power (SDP) is a calculated value. The SDP rating of a circuit is related to the cost of a design which will be explained in a moment. The SDP of a single switching device is the product of the Voltage across a device during its open state and the Current through the device during its closed state.

$$SDP = V_{OPEN} * I_{CLOSED}$$

Notice that this is not the power dissipated by the device, nor the power flow. The SDP is a relative bench mark. Both current capacity of a device and voltage blocking ability contribute to the size and cost of the device. As such, SDP can be used as a type of cost comparison bench mark. The SDP rating of a circuit takes the SDP of each switching device and aggregates them to arrive at the total for the whole circuit. The total SDP of a circuit can then be compared to the total SDP rating of the other circuits.

To summarize:

Several factors contribute to the total SDP rating of a circuit.

Voltage stress on a switching device.

Current stress on a switching device

The total number of switching devices in the circuit

More on the Voltage Rating of a Switching Device

A semiconductor switching device has a voltage breakdown rating which is the maximum voltage that a device can withstand while continuing to block the flow of current. When the device is in its intended open state (gate voltage is below V_{g-on} and the p-n junction remains reverse biased) only a negligible reverse saturation current is allowed to flow. But when the voltage across the device becomes too large, the device will begin to allow current due to thermal instability, tunneling, or avalanche multiplication which is not desirable and will destroy IGBTs or any semiconductor device which is not designed for this specific type of current. The designed voltage rating of a switching device is directly related to its size and cost. Hence, a circuit that can do the same job as another circuit at lower switch size and cost is a preferable circuit design. This is one of the reasons why the voltage stress that a particular circuit imposes across a switching device is determined. This value is included in the SDP rating of a circuit design.

As shown above, the current stress is also a part of the SDP rating. The current that a semiconductor can conduct in the closed switch state is also related to the cost and size. Therefore, we also include a circuit's required current flow in the SDP calculation.

More on the Current Rating of a Switching Device

The amount of current that can flow through a bipolar junction type device (such as that used in an IGBT) is directly related to the available number of charge carriers in its PN junctions, its diffusion coefficient, junction area, and base width. It is inversely related to the diffusion length in the base region. As such, the material used in the PN junction and its size affect the current capacity of the device and are directly related to cost and size.

Finally, the total number of switching devices that a circuit requires is included. Therefore, a circuit that can do the same job with fewer switching devices receives a more favorable impact on its SDP rating. The next sections derive the SDP equations for the four sub-circuits included in this study.

DC/DC – Boost - Buck Converter

Traditional VSI Inverter

Traditional ZSI Inverter

Current Fed ZSI Inverter

4.3 DC/DC Boost – Buck Converter

For the low voltage battery option, a boost-buck converter is required. This converter typically connects a 360 V_{DC} battery to the 780V DC Link. To transfer power from the batteries to the DC Link, the battery voltage must be boosted to the level of the DC Link. To transfer power from the DC Link to the Batteries, the DC Link voltage must be bucked.

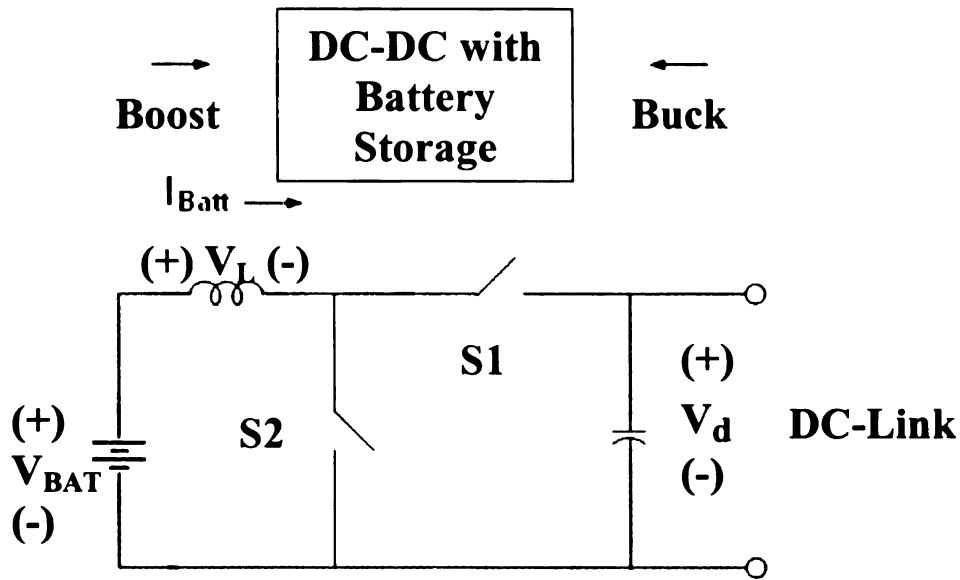


Figure 62 DC/DC Boost-Buck Converter

The voltage stress on each of the two Boost-Buck converter switches is V_{DC} the DC Link voltage. Average current through the switching devices is derived as follows.

First note that

$$P_{out} = P_{in}$$

$$V_{DC} I_o = V_{BAT} \cdot I_{BAT}$$

$$I_{BAT} = \frac{P_o}{V_{BAT}}$$

The two switches S_1 and S_2 are operated in a complimentary manner (When S_1 is open, S_2 is closed and vice versa).

\bar{I}_{S2} is average current through switch S_2 , and

t_{2_on} is the amount of time that S_2 is closed during a switching period T_s ,

Because of the large inductor in this circuit it can be assumed that I_{BAT} is the same during

each switch state (S_1 closed or S_2 closed).

$$\bar{I}_{S2} = \frac{I_{BAT} \cdot t_{2_on}}{T_S}$$

$$\bar{I}_{S1} = \frac{I_{BAT}(T_S - t_{2_on})}{T_S}$$

This gives the following

$$SDP_{AV} = \bar{I}_{S2} \cdot V_{DC} + \bar{I}_{S1} \cdot V_{DC}$$

$$= \frac{I_{BAT} \cdot t_{2_on} \cdot V_{DC}}{T_S} + \frac{I_{BAT}(T_S - t_{2_on})V_{DC}}{T_S}$$

$$= \frac{I_{BAT} \cdot t_{2_on} \cdot V_{DC} + I_{BAT} \cdot T_S \cdot V_{DC} - I_{BAT} \cdot t_{2_on} \cdot V_{DC}}{T_S}$$

$$= I_{BAT} \cdot V_{DC}$$

$$SDP_{AV} = \frac{P_o}{V_{BAT}} V_{DC}$$

4.4 Traditional VSI with PWM

To derive the SDP equation for the traditional VSI inverter, we will refer to the circuit below.

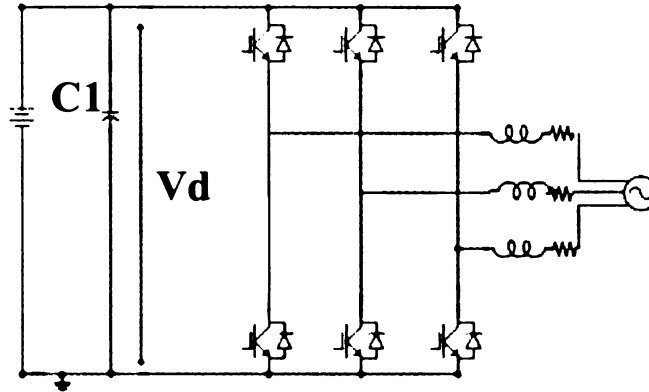


Figure 63 Traditional VSI

The voltage across an inverter switch is the DC link voltage. For the circuit topologies in this study, the required voltage at the traction motor and at the generator are both 480V line to line, RMS. Therefore:

$$V_{DC} = \frac{2\sqrt{2} \cdot V_{LL}}{\sqrt{3}M}$$

Where: V_{LL} is the RMS line to line voltage at the motor
 M is the modulation index of the inverter (Simple PWM)
 V_{DC} is the DC Link voltage

The PWM of the inverter is operated in such a way that the constant V_{DC} is impressed

across the load in pulses that average out to a sinusoidal wave form. Because of this and the inductance of the load, the output current is simply:

$$I_{Line} = \frac{P_{3\phi}}{\sqrt{3} \cdot \cos(\phi) \cdot V_{LL}}$$

Where: $P_{3\phi}$ is the 3 phase power delivered to the Motor

I_{Line} is the Motor's RMS line current that flows through the IGBT

Note that I_{Line} is an RMS value. To get the average current that the IGBT conducts, we integrate the current sinusoid over one half cycle and divide by this period.

$$I_{av} = \frac{\int_0^{\pi} \hat{I}_{Line} \sin(\omega t) d\omega t}{\pi} = \frac{2}{\pi} \hat{I}_{Line}$$

Where \hat{I}_{Line} is the peak line current

$$I_{av} = \frac{2\sqrt{2}P_{3\phi}}{\sqrt{3} \cdot \cos(\phi) \cdot V_{DC} \sqrt{3} \cdot M} \sqrt{2} \frac{2}{\pi} = \frac{8P_{3\phi}}{3\pi \cdot \cos(\phi) \cdot V_{DC} \cdot M}$$

The average SDP of the traction inverter is

$$(SDP)_{av} = 6 \cdot V_{DC} \cdot I_{av} = \frac{16P_{3\phi}}{\pi \cdot \cos(\phi) \cdot M}$$

Where 6 is the number of switches used in the inverter

**4.5 Traditional Z-Source Inverter [the Voltage Fed Z-Source Inverter (VF-ZSI)]
with PWM**

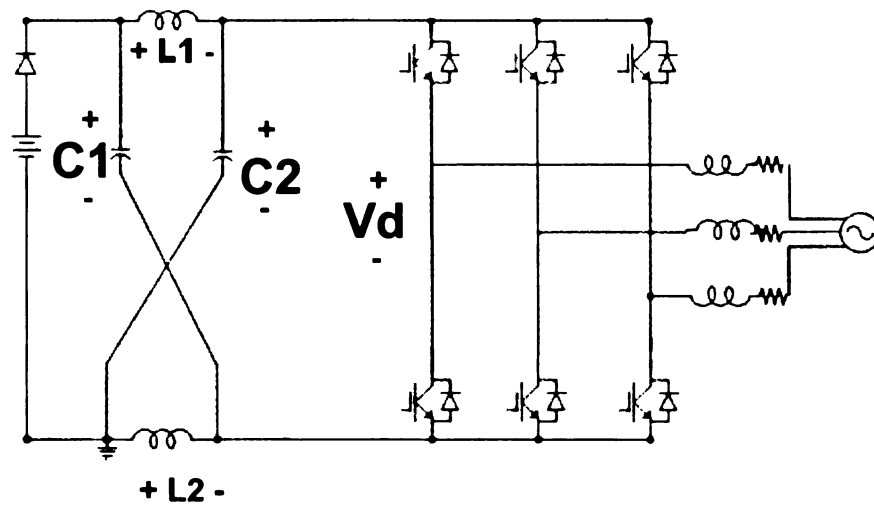


Figure 64 Traditional Z-Source Inverter

SDP_{AV} for the ZSI is based upon average current through the switching devices times the voltage across the switching devices when they are open. This is the same as with the traditional VSI topology. However, the ZSI has a few differences. First the ZSI has all of the traditional switching states as the VSI, and it also has a short circuit zero switching state. During this short circuit zero (SCZ) state, the current through the switching device is $2I_{LZ}$. During this SCZ switching state, all six switching devices are gated on so that the current will be shared by all three phase legs of the inverter. As such,

the current in a switching device is $\frac{1}{3}(2I_{LZ})$ and the average time period of this state is

T_{SCZ}/T_S .

Where: T_S is the switching period.
 T_{SCZ} is the SCZ period.

Therefore the average switching device current contributed by the SCZ state is

$\frac{2}{3}I_{LZ} \frac{T_{SCZ}}{T_S}$. The other switch states of the Z-source inverter are the same as the

traditional VSI (open circuit and active states). The current of these two states follow the same equation as that of the VSI except that this current is averaged over a smaller

portion of time which is the switching period minus the SCZ period $\left(\frac{T_S - T_{SCZ}}{T_S}\right)$.

The average current is the sum of the current during these two time periods (SCZ time period T_{SCZ} , and active + open time period $(T_S - T_{SCZ})$).

$$I_{AV} = \frac{2}{3}I_{LZ} \frac{T_{SCZ}}{T_S} + \frac{4P_{3\phi}}{3V_{DC}M\pi \cos(\theta)} \left(\frac{T_S - T_{SCZ}}{T_S}\right)$$

Where $P_{3\phi}$ is the power of the motor
 M is the modulation index of the inverter (V_{ref}/V_{tri})
 I_{AV} is average current
 I_{LZ} is inductor current
 T_{SCZ} is short circuit zero time period
 T_S is switching period
 V_{DC} is the DC link voltage

Due to the boost capability of the Z-source topology, the voltage across the switches is not the DC input voltage. In this case the switch voltage is the boost factor times the input DC Voltage

$$V_{DC} = B \cdot V_{IN}$$

Where:

V_{DC} is the DC link voltage (the voltage across the inverter)

B is the boost factor, and

V_{IN} is the input DC voltage

$$B = \frac{T_S}{T_S - 2T_{SCZ}} \quad [16] \text{ Therefore,}$$

$$V_{DC} = \frac{T_S}{T_S - 2T_{SCZ}} V_{IN}.$$

Where:

V_{DC} is the voltage across the inverter.

Therefore, the average SDP of the Traction Motor Inverter of the Z-source topology is

$$SDP_{AV} = 6 \left[\frac{2}{3} I_{LZ} \frac{T_{SCZ}}{T_S} + \frac{4P_{3\phi}}{3V_{DC} M \pi \cos(\theta)} \left(\frac{T_S - T_{SCZ}}{T_S} \right) \right] \left(\frac{T_S}{T_S - 2T_{SCZ}} V_{IN} \right)$$

4.6 Current Fed Z-Source Inverter (CF-ZSI).

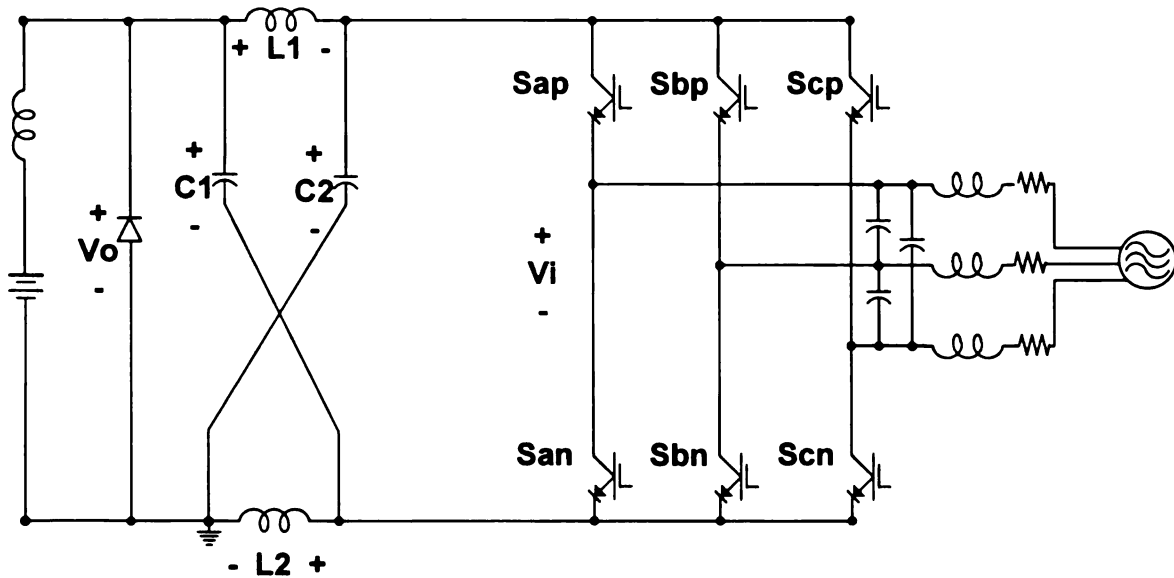


Figure 65 Current Fed ZSI

This topology is very similar to the traditional ZSI. The difference is that the switching devices of the CF-ZSI block reverse current flow. The traditional VSI-ZSI allows reverse current flow due to the anti-parallel diode.

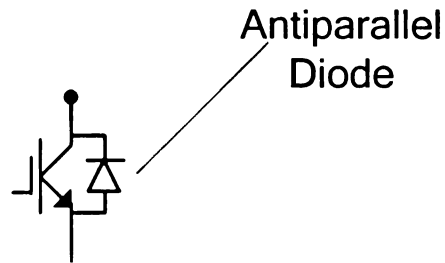


Figure 66 IGBT Module Schematic

The switching device of the current fed ZSI does not allow reverse current flow and can be modeled as shown in figure 67. This device is also called a non-punch through IGBT (NPT-IGBT). [22]

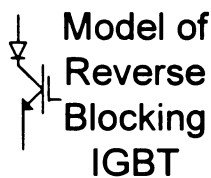


Figure 67 Reverse Blocking IGBT Module Schematic (RB-IGBT)

For this thesis, the following schematic symbol, as shown in figure 68, will be used to represent this device.



Figure 68 RB-IGBT Symbol

Given a current source input, an inverter constructed of the reverse blocking IGBTs, will function like a current source inverter. The CF-ZSI however, has the ability to both buck and boost current (boost and buck voltage, respectively) where as the traditional CSI can

only buck current (boost voltage). For this discussion, the switching methodology for the CSI is based upon a duality of the traditional Simple PWM switching for voltage source inverters. The following duality will be used:

The list below shows traditional switching states of a VSI on the left and the corresponding (dual) switch state used for the CSI on the right. Figure 69 shows an example of the 011, 100 switching state.

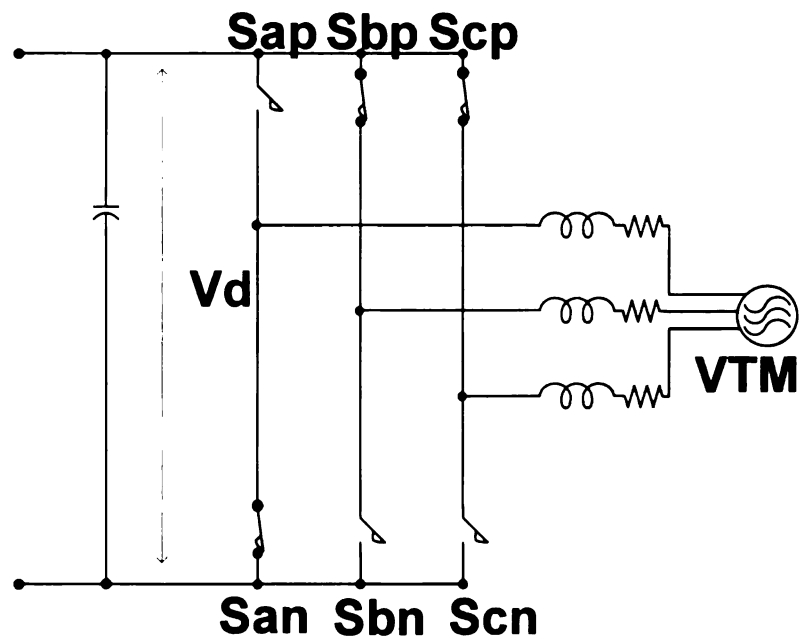


Figure 69 Illustration of the 011,100 switching vector

<u>VSI</u>		<u>CSI</u>
OCZ states:		SCZ states:
000, 111 or 111, 000	⇒	100, 100 or 010, 010 or 001, 001
Active states:		
100, 011	⇒	100, 001
110, 001	⇒	010, 001
010, 101	⇒	010, 100
011, 100	⇒	001, 100
001, 110	⇒	001, 010
101, 010	⇒	100, 010

Although the switching device and switch control methodologies are very similar to the traditional IGBT, and traditional PWM used in VSIs and VF-ZSIs; the equation for current through the switch device is significantly different than that of the VF-ZSI. The shoot-through mode (short circuit zero state (SCZ)) of the previously discussed VF-ZSI occurs during the open circuit zero (OCZ) states of operation. But the SCZ of the CF-ZSI occurs during its active states. First the OCZ states and SCZ states of the VF-ZSI are explained.

OPEN CIRCUIT ZERO, & SHORT CIRCUIT ZERO STATES OF THE VF-ZSI

These OCZ states occur when the positive half of the reference voltages (V_{a_ref} , V_{b_ref} , and V_{c_ref}) are less than the triangular carrier wave and when the negative half of the reference voltages are greater than the triangular carrier wave. The SCZ states occur

when the PWM carrier wave is greater than the positive DC reference voltage and when the PWM carrier wave is less than the negative DC reference voltage. See figure 69

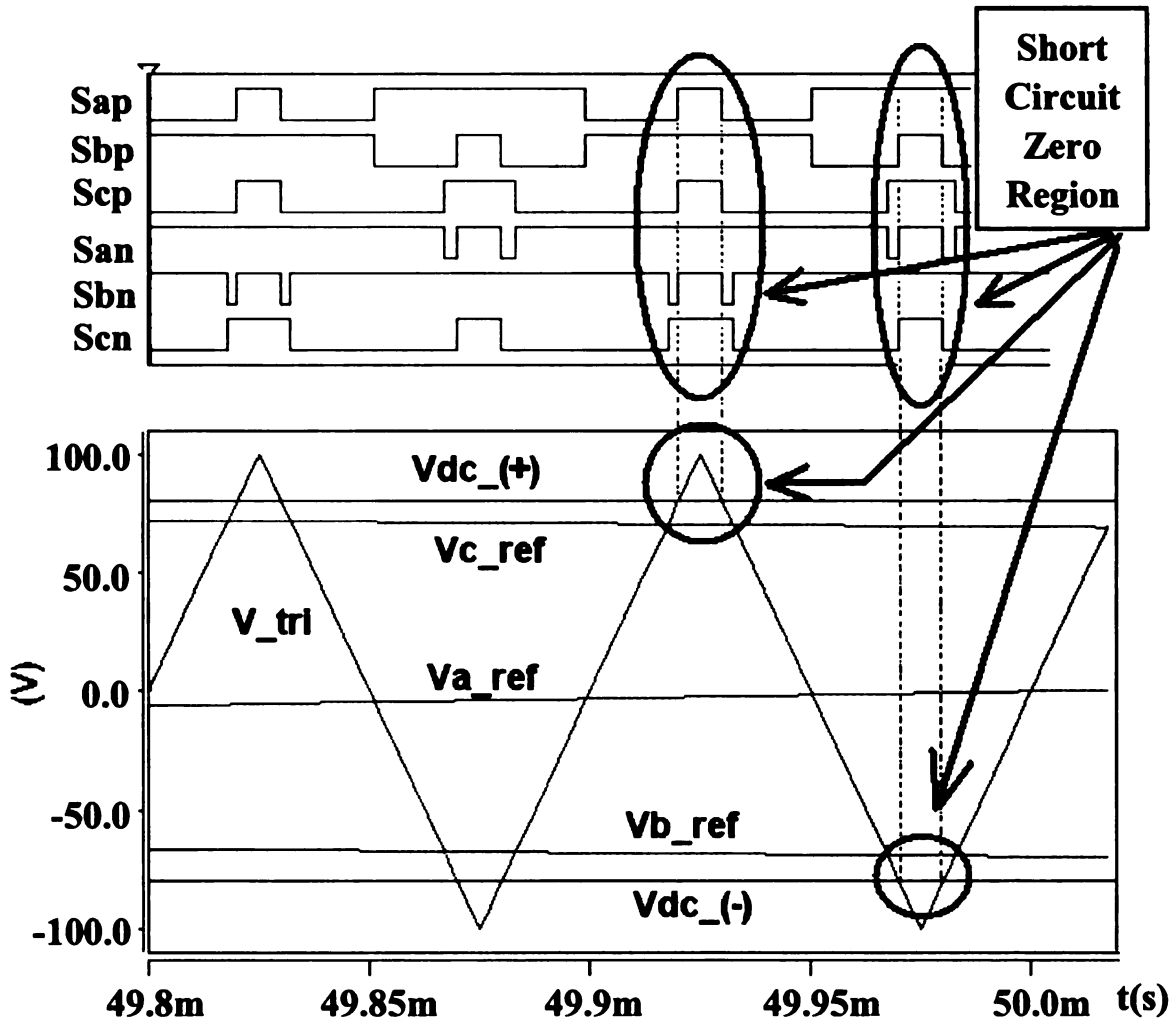


Figure 70 SCZ Switch States of VF-ZSI

Sap through Scn represent the switch states of the inverter. See fig (69)

V_{tri} is the triangular reference voltage (PWM carrier wave)

V_{a_ref}, V_{b_ref}, V_{c_ref} are sinusoidal switch state control reference voltages

V_{dc_+} and V_{dc_-} are DC reference voltages that control the SCZ switch states

Secondly, the SCZ states of the CF-ZSI are explained.

SHORT CIRCUIT ZERO STATES OF THE CF-ZSI

The CF-ZSI however has a different SCZ state. The SCZ of the CF-ZSI occurs during the other wise active states. As before, the active states occur when the positive reference voltages are greater than the triangular carrier wave and when the negative reference voltages are less than the PWM carrier wave. However, the OCZ state now occurs when Vdc_(+) reference voltage passes below the carrier wave and when Vdc_(-) passes above the carrier wave. This is where the SCZ state had existed for the VF-ZSI inverter. Further, the period of the SCZ varies during the cycle of the reference voltage. Also, all of the SCZ current is conducted by each of the three phase legs of the inverter in turn, rather than by all phase legs at the same time. First, phase “A” leg conducts the SCZ current during the 30° to 90° portion of its reference voltage cycle, then the phase “B” leg carries it during the 30° to 90° portion of its cycle, then in a similar manner, the phase “C” leg will conduct. (With the VF-ZSI, all three phase legs conduct 1/3 of the SCZ current during each carrier wave cycle). In the diagram below, it is the phase “A” leg that is conducting the SCZ currents. As the phase “A” reference voltage moves through its cycle from 30° to 90° the SCZ period is controlled by the moment that Vdc_+ and Va_ref intersect with the positive portion of the carrier wave, and when Vb_ref and Vdc_(-)

intersect the negative part of the carrier wave. As $V_{a_ref} \left[\hat{V}_a \sin(\omega t) \right]$ and as $V_{b_ref} \left[\hat{V}_b \sin(\omega t - 120^\circ) \right]$ move through their cycles, the period of the SCZ pulse changes.

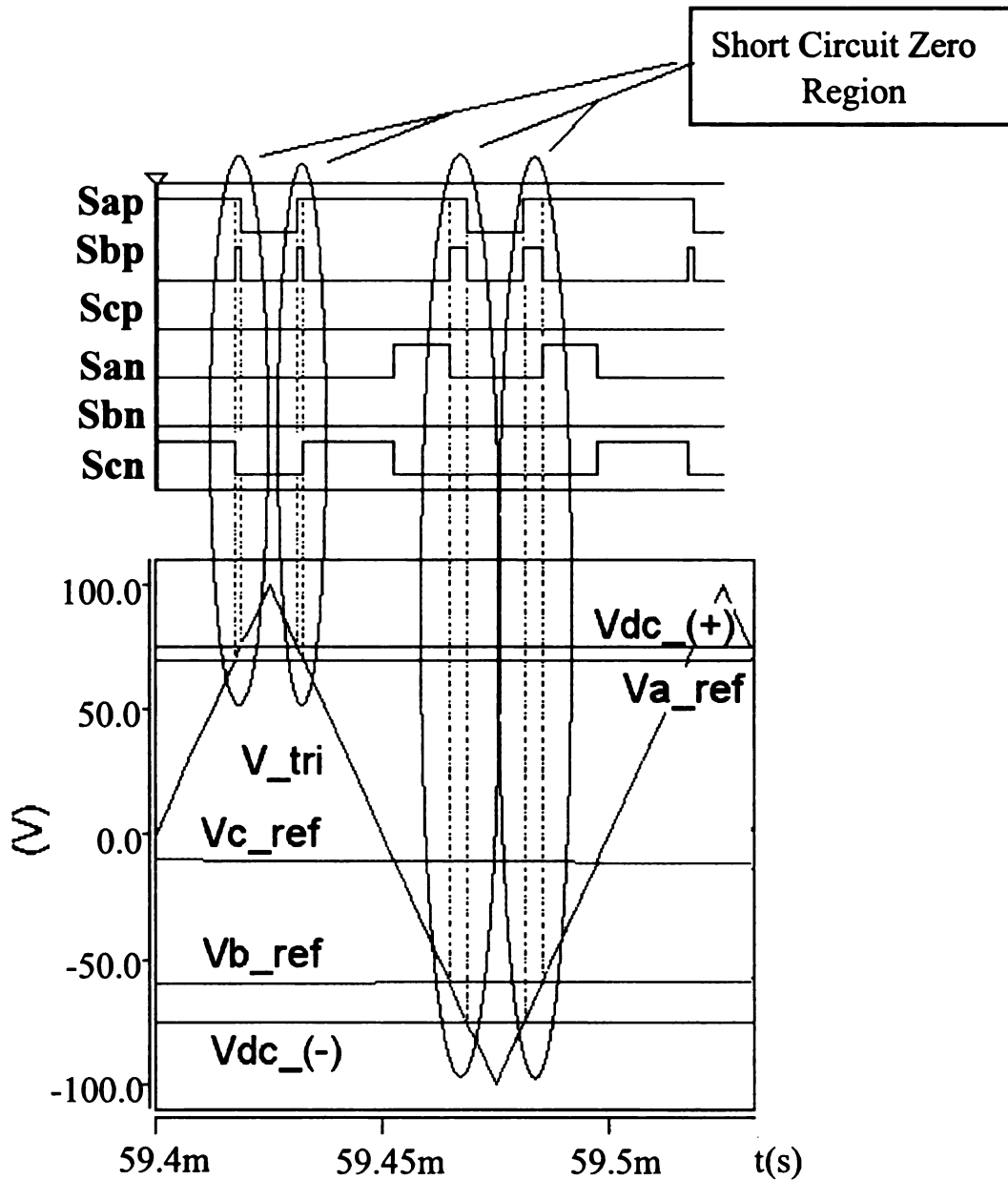


Figure 71 SCZ Regions of the CF-ZSI

Sap through Scn represent the switch states of the inverter. See fig (70)

V_{tri} is the triangular reference voltage (PWM carrier wave)

V_{a_ref}, V_{b_ref}, V_{c_ref} are sinusoidal switch state control reference voltages

V_{dc_+} and V_{dc_-} are DC reference voltages that control the SCZ switch states

In order to calculate the average current during SCZ, the total SCZ time summed over the

reference voltage period must first be determined and then divided by the period of the reference voltage. This gives us the portion of the reference voltage wave form that is used for the SCZ state. Since the SCZ current of the ZSI is twice the inductor current, the

average SCZ current is as follows: $I_{SCZ_Ave} = 2 * I_{LZ} * T_{SCZ_AVG}$

Where

$$T_{SCZ} = 6 \left[\sum_{k=0}^{k_{final}} \left[2 \left(\frac{T_{SW}}{4} \right) * \left(\frac{I_{dc_ref} - \hat{I}_{ref} \sin\left(k(T_{sw} \omega_{motor}) + \frac{\pi}{6}\right)}{I_t} \right) + 2 \left(\frac{T_{SW}}{4} \right) \left(\frac{I_{dc_ref} + \hat{I}_{ref} \sin\left(k(T_{sw} \omega_{motor}) + \frac{\pi}{6} - \frac{2\pi}{3}\right)}{I_t} \right) \right] \right]$$

$$T_{SCZ_AVG} = \left(\frac{\omega_{motor}}{2\pi} \right) * T_{SCZ}$$

and

$$k = 0, 1, 2, \dots, k_{final}$$

$$k_{final} = \frac{\left(\frac{\pi}{2} - \frac{\pi}{6}\right)}{\left(T_{sw} \omega_{motor}\right)}$$

Example:

$$\text{If } \omega_{motor} = 1000rpm = 104.72 \text{ rad/s}$$

$$\text{And } Ts = 0.0001$$

$$\text{Then: } k_{final}=100$$

I_{LZ} = the impedance network inductor current

ω_{motor} = electrical angular velocity of the traction motor or generator

f_{PWM} = frequency of the carrier wave

T_{SCZ} = total short circuit zero time period during one cycle of the traction motors voltage or current sine wave.

T_s = is the switching time period also know as the period of the PWM carrier wave.

T_{SCZ_AVG} = the proportion of time spent in the SCZ state.

$T_{SCZ_AVG} * T_s$ = the average amount of SCZ time during one PWM switching cycle.

V_{DC} = the DC link voltage

\hat{V}_{ref} = the peak voltage level of the PWM reference voltage which is compared to the carrier wave to determine the required switch state.

Notice

step of

T_{SCZ}

increm

$\frac{1}{2}$
 $\frac{1}{2}$

V_t = the peak voltage level of the PWM carrier wave.

Notice that two SCZ states occur for each half cycle of the carrier wave, and that each step of k adds the time period of another one of these SCZ states.

T_{SCZ} is a summation of each SCZ state from $\pi/6$ to $\pi/2$ in $\frac{1}{2}T_{sw}\omega_{motor}$ sized increments. Notice in fig. 71 that the period of time from point (1.) to point (2.) is $\frac{1}{2}T_{sw}\omega_{motor}$.

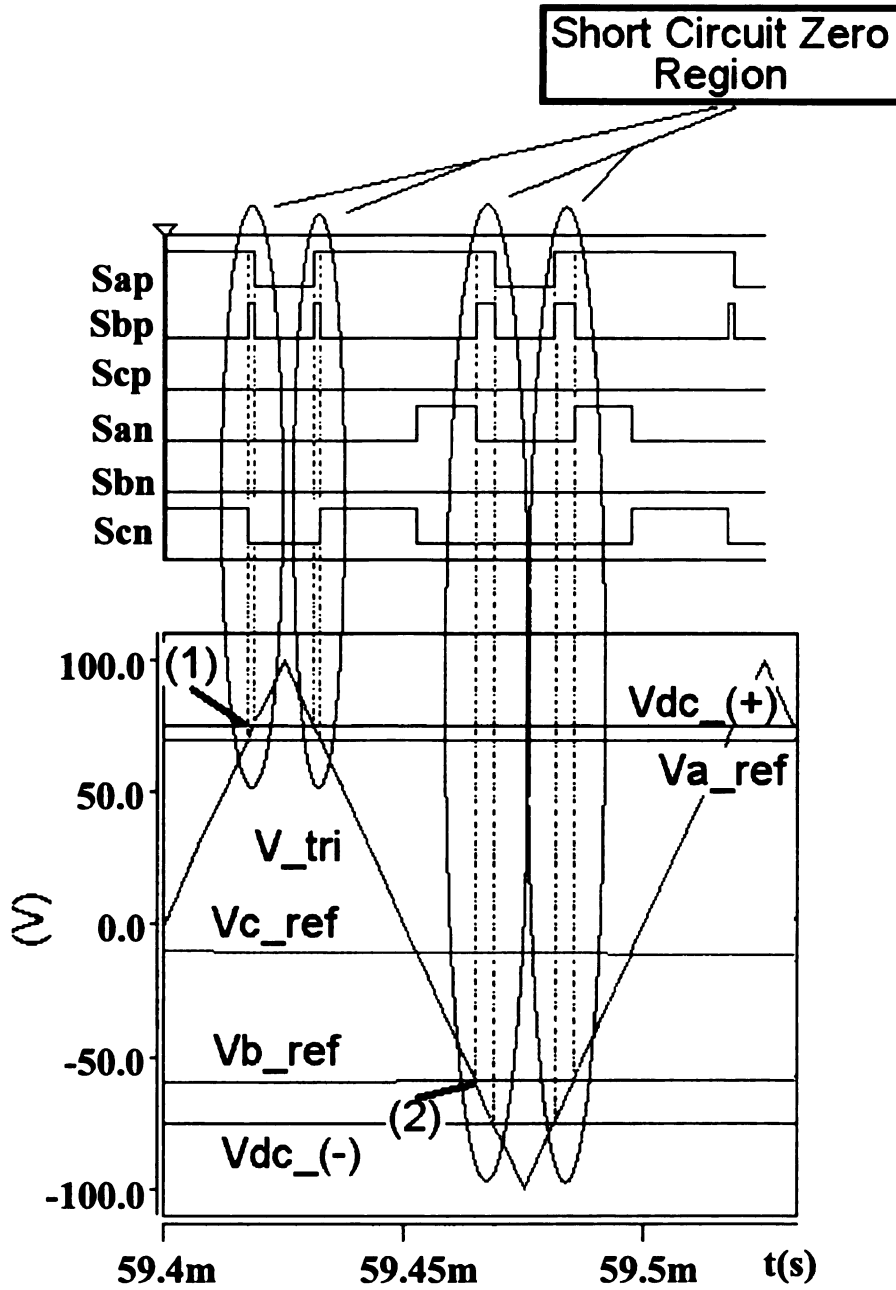


Figure 72 SCZ Switch States of CF-ZSI detail

$$I_{Active_Ave} = \frac{8P_{3\phi}}{3V_{DC}M\pi \cos(\theta)} \left(\frac{T_S - T_{SCZ_AVG}T_S}{T_S} \right) =$$

$$\frac{8P_{3\phi}}{3V_{DC}M\pi \cos(\theta)} (1 - T_{SCZ_AVG})$$

And the total average current through the switching devices is the weighted sum of the (1)active and open state currents with (2)the SCZ currents.

$$I_{ave_SCZ} = 2I_{LZ}T_{SCZ_AVG}$$

$$I_{Ave} = 2I_{LZ}T_{SCZ_AVG} + \frac{8P_{3\phi}}{3V_{DC}M\pi \cos(\theta)} (1 - T_{SCZ_AVG})$$

Where $V_{DC} = \bar{V}_c$

$\bar{V}_c =$ The average voltage across the Z network capacitor.

The equation for voltage across the switching devices is similar to that of the Voltage Fed ZSI. T_{SCZ} of the VSI ZSI is replaced by $T_{SCZ_AVG} * T_S$

$$V_{DC} = \frac{T_S}{T_S - 2T_{SCZ}} V_{IN} = \frac{T_S}{T_S - 2T_{SCZ_AVG} * T_S} V_{IN}$$

Where: V_{IN} is the input voltage

$V_S = V_{DC}$ is the voltage across the switching devices.

As a result, the SDP of the Current Fed ZSI which has 6 switches is

$$SDP_{CF-ZSI} = 6 * V_S * I_{AVE}$$

$$SDP_{CF-ZSI} = 6 \left(\frac{V_{IN}}{1 - 2T_{SCZ_AVG}} \right) \left(\frac{2}{3} I_{LZ} T_{SCZ_AVG} + \frac{8P_{3\phi}}{3V_{DC}M\pi \cos(\theta)} (1 - T_{SCZ_AVG}) \right)$$

4.7 Application of Equations to the Back to Back Topologies

Maximum voltage and average currents have been calculated for the various sub-circuits included in this study. These can now be combined to form the SDP equations of the complete back-to-back inverter circuits.

4.7.1 Back to Back VSI-to-VSI Network Topology

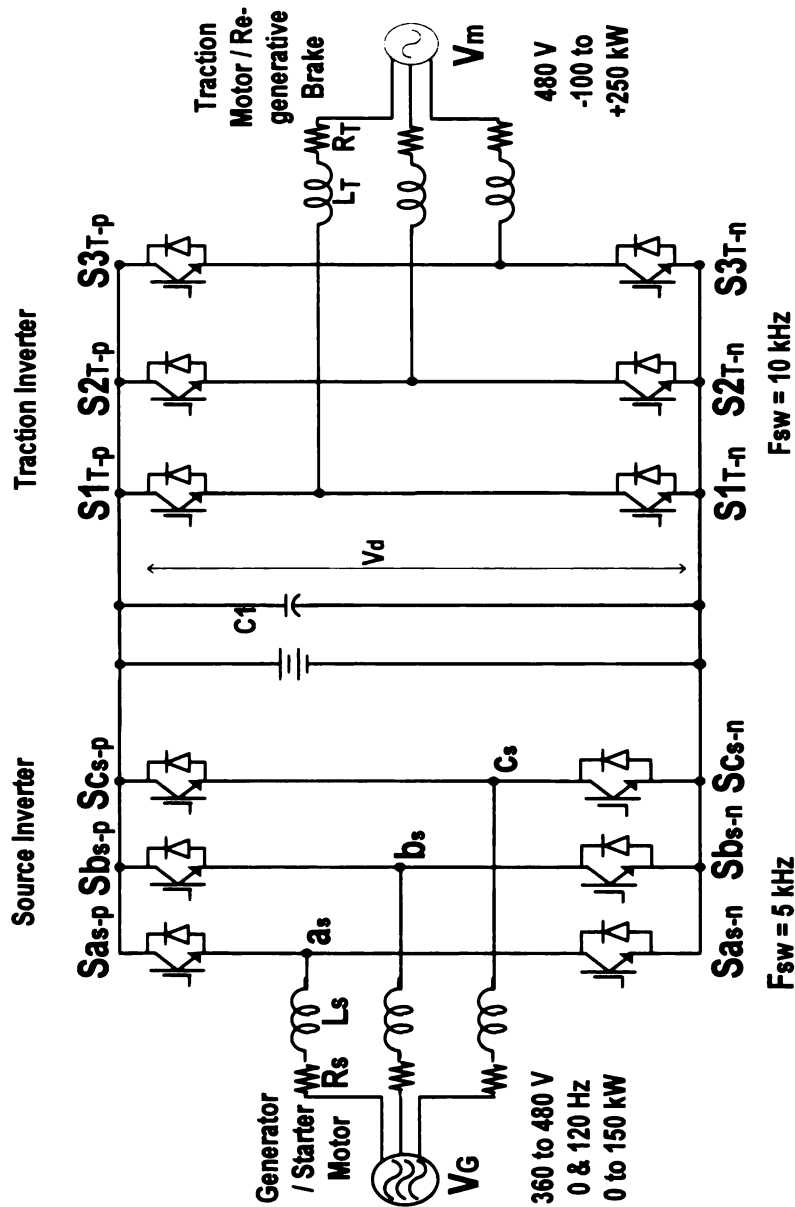


Figure 73 Back to Back VSI-to-VSI Network Topology

The Back

generator

inverters

Since the

in the eq

motor gen

motor gen

variables

The Back to Back VSI-to-VSI Network Topology shown above uses a VSI inverter at the generator end and at the traction motor end of the circuit. Each of these traditional VSI inverters function in the same way and the SDP is calculated in the same way for both. Since the power levels are different from one end to the other, different variables are used in the equations. For the following discussion, it will be assumed that the 3 phase motor/generator at the left end is the generator connected to the diesel engine and the motor/generator (motor/brake) at the right end is the traction motor. The following variables are hereby added or clarified:

M_G is the modulation index of the generator inverter

M_{TM} is the modulation index of the traction motor inverter

$P_{3\phi-G}$ is the maximum 3 phase power delivered by the
Generator

$P_{3\phi-TM}$ is the maximum 3 phase power delivered to
the Traction Motor

I_{L-G} is the RMS Generator line current that flows through
the generator inverter IGBTs

I_{L-TM} is the RMS Traction Motor line current that flows
through the traction motor inverter IGBTs.

I_{AV-G} is the average current through the switching devices of
the generator inverter

I_{AV-TM} is the average current through the switching devices
of the traction motor

$(SDP)_{AV-G}$ Is the SDP rating of the generator inverter

$(SDP)_{AV-TM}$ Is the SDP rating of the traction motor inverter

$(SDP)_{av-DC/DC}$ Is the SDP rating of the DC/DC converter

Therefore,

$$(SDP)_{av-G} = 6 \cdot V_{DC} \cdot I_{av-G} = \frac{16P_{3\phi-G}}{\pi \cdot \cos(\phi) \cdot M_G}$$

The combination of a VSI at both ends of the voltage source DC link is just a matter of summing the individual equations as follows (traction motor inverter, generator inverter, and DC/DC converter).

$$\begin{aligned} SDP_{AV-VSI-VSI} &= \\ (SDP)_{av-TM} + (SDP)_{av-G} + (SDP)_{av-DC/DC} &= \\ \frac{16P_{0-TM}}{\pi \cdot \cos(\phi) \cdot M_{TM}} + \frac{16P_{3\phi-G}}{\pi \cdot \cos(\phi) \cdot M_G} + \frac{P_{o-BAT}}{V_{BAT}} V_{DC} &= \end{aligned}$$

4.7.2 Back to Back VSI-to-CSI Z-Network Topology (VSI-Z-CSI)

In the following topology, a traditional VSI inverter, which uses the standard free wheeling diode anti-paralleled with an IGBT, is used at the generator end of the circuit. A reverse blocking IGBT is used in the inverter at the traction motor end of the circuit. The impedance network (L1, C1, L2, C2) is between the traditional inverter and the reverse blocking inverter. We will interchangeably call this the “Back to Back VSI-to-CSI Z Network Topology” or “VSI-Z-CSI”.

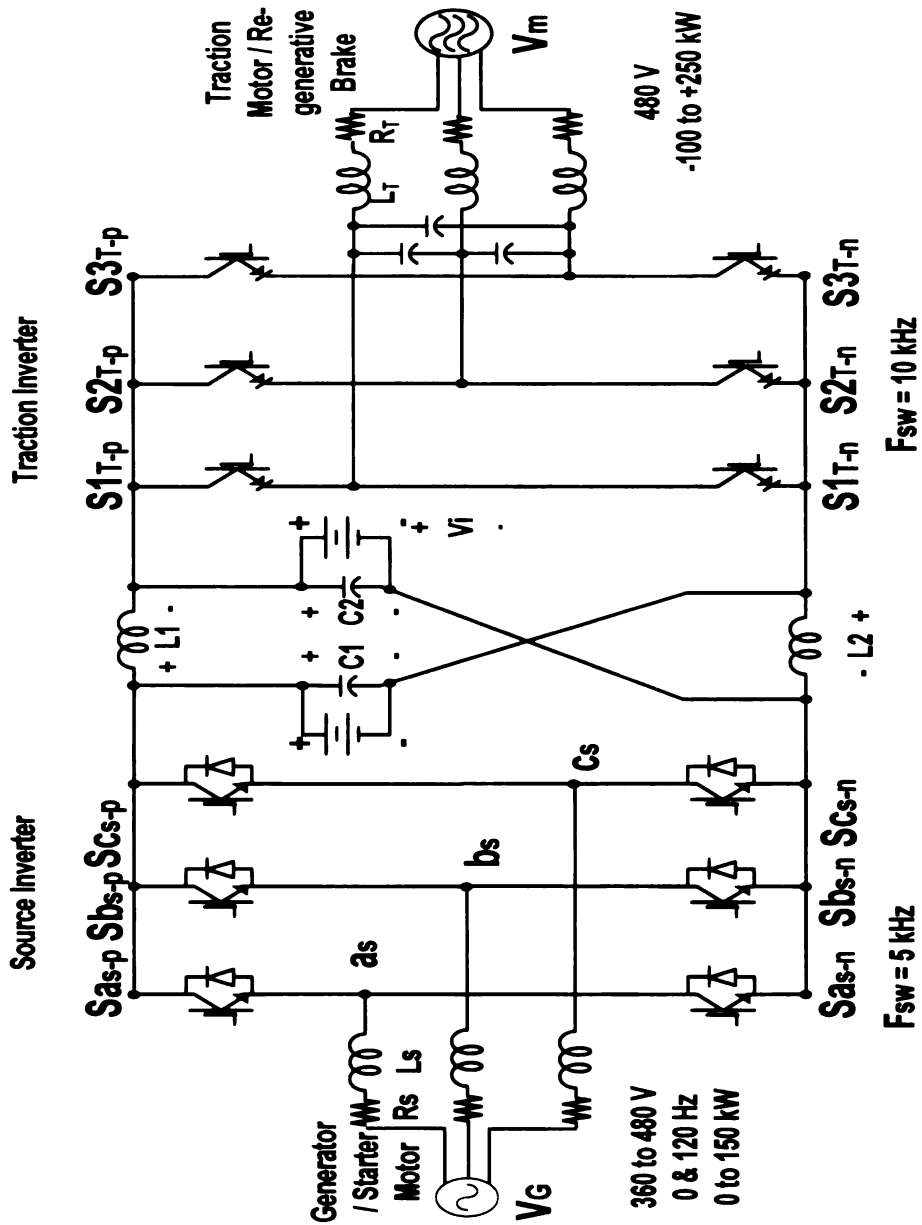


Figure 74 VSI-Z-CSI

The traditional inverter connected to the generator is primarily operated as a controlled rectifier which delivers the generator's power to the rest of the circuit. This controlled rectifier's switching states must be coordinated with those of the traction motor inverter, however. When the traction motor inverter goes into its open circuit state, $2I_L$ will flow

through the freewheeling diodes of the generator inverter.

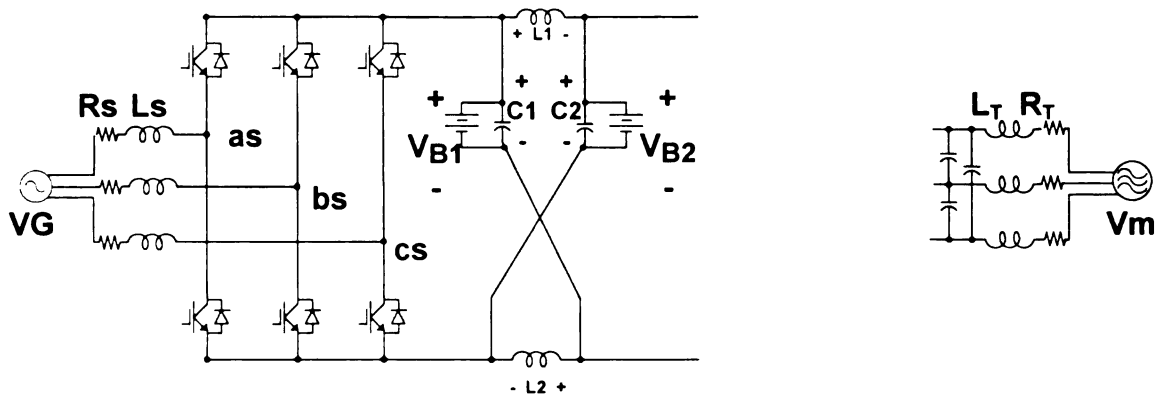


Figure 75 VSI-Z-CSI; CSI in OCZ State

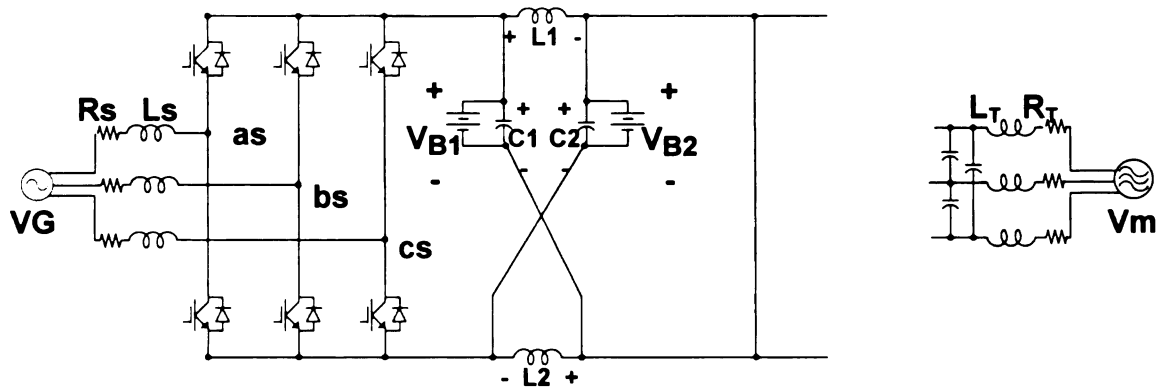


Figure 76 VSI-Z-CSI; CSI in SCZ State

$$I_{AV-G} = \frac{2}{3} I_{LZ} \frac{T_{OCZ-TM}}{T_S} + \frac{8P_{3\phi-G}}{3V_{DC-G}M_G\pi \cos(\theta)} \left(\frac{T_S - T_{OCZ-TM}}{T_S} \right)$$

Where:

I_{AV} is average current through the switching devices

I_{LZ} is inductor current of the Z network

T_{OCZ-TM} is open circuit zero time period of the traction motor inverter which is also the SCZ time period of the generator inverter.

T_S is switching period which is the same for both inverters

$P_{3\phi-G}$ is the three phase power being generated by the generator

M_G is the modulation index of the generator inverter

V_{DC-G} is the DC voltage across the generator inverter

And in this case,
$$V_{DC-G} = \frac{V_{LL-G} 2\sqrt{2}}{\sqrt{3}M_G}$$
 Therefore,

$$I_{AV-G} = \frac{2}{3} I_{LZ} \frac{T_{OCZ-TM}}{T_S} + \frac{2\sqrt{6}P_{3\phi-G}}{3\pi \cos(\theta)V_{LL-G}} \left(\frac{T_S - T_{OCZ-TM}}{T_S} \right)$$

The Traction Motor Voltage is:

$$\bar{V}_{DC-TM} = \bar{V}_C = B \cdot V_{DC-G} = \frac{T_S}{T_S - 2T_{SCZ-TM}} V_{DC-G}$$

Where

T_{SCZ-TM} = SCZ time period of the traction motor inverter.

$$B = \frac{T_S}{T_S - 2T_{SCZ-TM}} \text{ and as shown above,}$$

$$V_{DC-G} = \frac{V_{LL-G} 2\sqrt{2}}{\sqrt{3}M_G} .$$

SDP of the generator inverter is

$$SDP_{av-G} = 6 \left[\frac{2}{3} I_{LZ} \frac{T_{OCZ-TM}}{T_S} + \frac{2\sqrt{6}P_{3\phi-G}}{3\pi \cos(\theta)V_{LL-G}} \left(\frac{T_S - T_{OCZ-TM}}{T_S} \right) \right] * \left[\frac{T_S}{T_S - 2T_{SCZ-TM}} \frac{V_{LL-G} 2\sqrt{2}}{\sqrt{3}M_G} \right]$$

And the SDP for the current fed ZSI has already been discussed and is shown here with the appropriate variables for the VSI-Z-CSI Network circuit topology.

$$SDP_{AV-TM} = 6 * V_{SW} * I_{AVE} = 6V_{d-TM} * \left(\frac{2}{3} I_{LZ} \frac{T_{SCZ-TM}}{T_S} + \left(\frac{8P_{3\phi-TM}}{3V_{DC-TM}M_{TM}\pi \cos(\theta)} \right) \left(1 - \frac{T_{SCZ-TM}}{T_S} \right) \right)$$

For the case where one DC/DC converter is used and it is in parallel with just one of the Z network capacitors, the SDP of the DC/DC converter was also shown before and is

$$SDP_{AV-DC/DC} = \frac{P_{o-BAT}}{V_{BAT}} V_c = \frac{P_{o-BAT}}{V_{BAT}} B \cdot V_{DC-G}$$

$$SDP_{AV-DC/DC} = \frac{P_{o-BAT}}{V_{BAT}} \left(\frac{T_S}{T_S - 2T_{SCZ-TM}} \right) \frac{V_{LL-G} 2\sqrt{2}}{\sqrt{3}M_G}$$

The SDP of the combined topology is

$$SDP_{AV-VSI-Z-CSI} = SDP_{AV-G} + SDP_{AV-TM} + SDP_{AV-DC/DC}$$

$$SDP_{AV-VSI-Z-CSI} =$$

$$6 \left[\frac{2}{3} I_{LZ} \frac{T_{OCZ-TM}}{T_S} + \frac{2\sqrt{6}P_{3\phi-G}}{3\pi \cos(\theta)V_{LL-G}} \left(\frac{T_S - T_{OCZ-TM}}{T_S} \right) \right] \left[\frac{2\sqrt{2}V_{LL-G}}{\sqrt{3}M_G} \right] +$$

$$6 \left[\left(\frac{2\sqrt{2}V_{LL-G}}{\sqrt{3}M_G} \right) \left(\frac{T_S}{T_S - 2T_{SCZ}} \right) \right]^*$$

$$\left[\left(\frac{2}{3} I_{LZ} \frac{T_{SCZ-TM}}{T_S} + \left(\frac{8P_{3\phi-TM}}{3V_{DC-TM}M_{TM}\pi \cos(\theta)} \right) \left(1 - \frac{T_{SCZ-TM}}{T_S} \right) \right) \right] +$$

$$\frac{P_{o-BAT}}{V_{BAT}} \left(\frac{T_S}{T_S - 2T_{SCZ}} \right) \frac{V_{LL-G} 2\sqrt{2}}{\sqrt{3}M_G}$$

4.7.3 Back to Back CSI-to-VSI Z-Network Topology

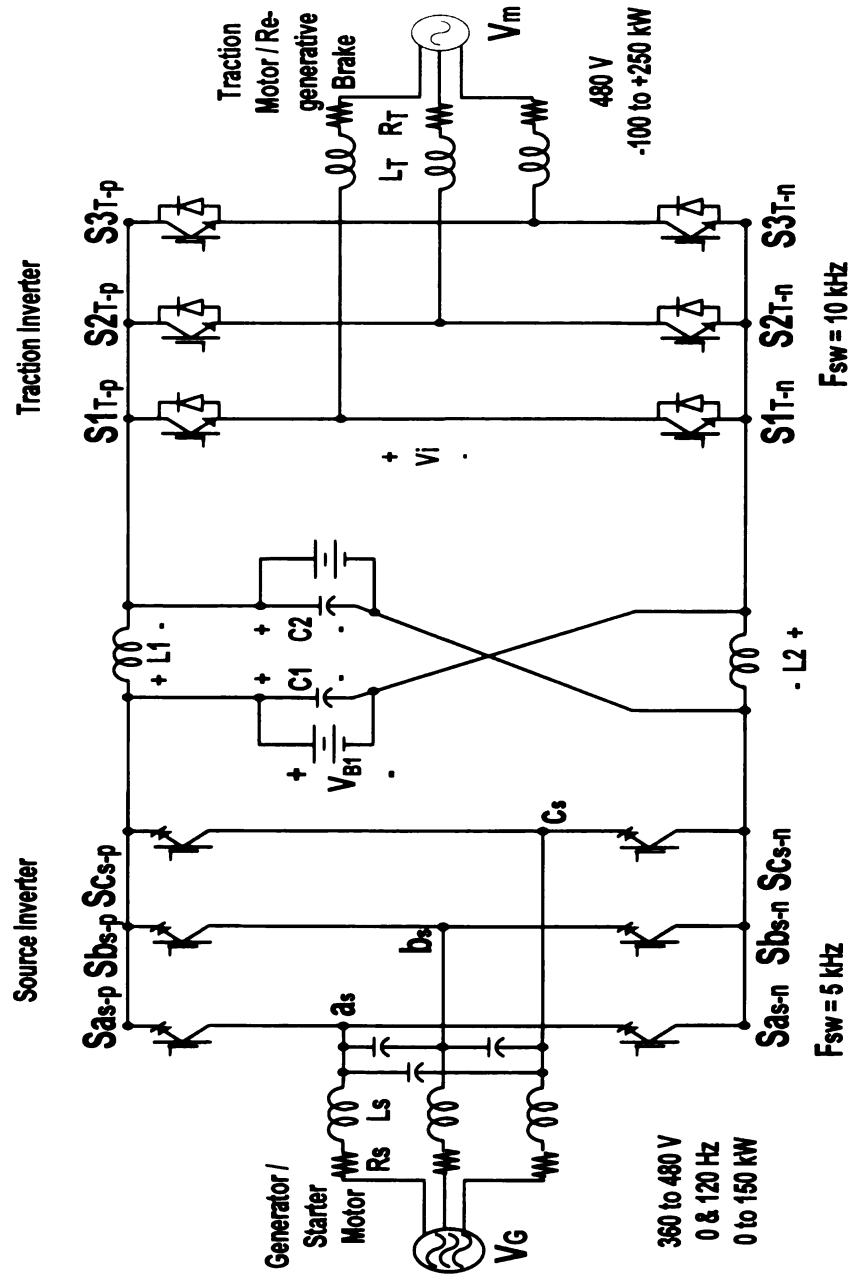


Figure 77 CSI-Z-VSI

This arrangement places the inverter with the reverse blocking IGBTs (CSI) at the generator end of the circuit. Therefore, the CSI functions primarily as a controlled rectifier. As before, the generators controlled rectifier must be operated in a way that

coordinates switching states with the VSI at the traction motor end of the circuit. During the traction motors open circuit zero states, the generator's inverter must be in a SCZ state or an active state. It is during this state that the generator CSI switching devices conduct $2I_{LZ}$. Unlike the traditional VSI type of inverter with switching modules that do not block reverse current, only one phase leg can be operated in the SCZ state at a time. Therefore one phase leg must handle the entire $2I_{LZ}$ current. However, the phase leg that is used for this is rotated from one SCZ state to the next. As a result, the average SCZ current that a phase leg must conduct is still $1/3$ of the $2I_{LZ}$. Also recall that the SCZ current flowing through the generator's switching devices flow only during the traction motor's open circuit zero state (T_{OCZ-TM}).

$$I_{AV-SCZ-G} = \frac{2}{3} I_{LZ} \frac{T_{OCZ-TM}}{T_S}$$

Where I_{AV} is average current through the switching devices

I_{LZ} is inductor current of the Z network

T_{OCZ-TM} is open circuit zero time period of the traction motor inverter which causes $2I_{LZ}$ to flow through the generator switch devices

T_S is switching period which is the same for both inverters

The active state switching device current of the generator's CSI is

$$I_{AV-Active-G} = \frac{4P_{3\phi-G}}{3V_{d-G}M_G\pi\cos(\theta)} \left(\frac{T_S - T_{OCZ-TM}}{T_S} \right)$$

Where: V_{d-G} is the DC voltage across the generator inverter.

$$V_{d-G} = \frac{V_{LL-G} 2\sqrt{2}}{\sqrt{3}M_G}$$

$$I_{AV-Active-G} = \frac{4\sqrt{3}M_G P_{3\phi-G}}{3 \cdot 2\sqrt{2} \cdot V_{LL-G} M_G \pi \cos(\theta)} \left(\frac{T_S - T_{OCZ-TM}}{T_S} \right)$$

$$I_{AV-Active-G} = \frac{\sqrt{6}P_{3\phi-G}}{3V_{LL-G}\pi \cos(\theta)} \left(\frac{T_S - T_{OCZ-TM}}{T_S} \right)$$

Therefore, the average current for active and SCZ states are:

$$I_{AV-G} = \left[\frac{2}{3} I_{LZ} \frac{T_{1-TM}}{T_S} + \frac{2\sqrt{6}P_{3\phi-G}}{3V_{LL-G}\pi \cos(\theta)} \left(\frac{T_S - T_{OCZ-TM}}{T_S} \right) \right]$$

The average current for the traction motor VSI and for the DC/DC converter have been derived before and the voltage across the generator inverter switches is

$$\frac{2\sqrt{2}V_{LL-G}}{\sqrt{3}M_G} 2V_C.$$

These are:

$$I_{AV-TM} = \frac{2}{3} I_L \frac{T_{SCZ-TM}}{T_S} + \frac{8P_{3\phi-TM}}{3V_{dc}M_{TM}\pi \cos(\theta)} \left(\frac{T_S - T_{0-TM}}{T_S} \right)$$

$$\text{Where: } V_{dc-TM} = \bar{V}_c = V_{dc-G} \left(\frac{T_S}{T_S - 2T_{SCZ-TM}} \right)$$

$$I_{AV-DC/DC} = \left[\frac{P_{O-BAT}}{V_{BAT}} \right]$$

$$V_{dc-TM} = \frac{2\sqrt{2} \cdot V_{LL-G}}{\sqrt{3}M_G} \left(\frac{T_S}{T_S - 2T_{SCZ-TM}} \right)$$

Therefore, the SDP of the back to back CSI-Z-VSI topology is

$$SDP_{AV-CSI-Z-VSI} = SDP_{av-G} + SDP_{av-TM} + SDP_{AV-DC/DC}$$

$$SDP_{AV-CSI-Z-VSI} =$$

$$6 \left[\frac{2}{3} I_{LZ} \frac{T_{OCZ-TM}}{T_S} + \frac{2\sqrt{6}P_{3\phi-G}}{3V_{LL-G}\pi \cos(\theta)} \left(\frac{T_S - T_{OCZ-TM}}{T_S} \right) \right]^*$$

$$\left[\frac{2\sqrt{2}V_{LL-G}}{\sqrt{3}M_G} \right]^+$$

$$6 \left[\frac{2}{3} I_{LZ} \frac{T_{SCZ-TM}}{T_S} + \frac{8P_{3\phi-TM}}{3V_{dc-TM}M_{TM}\pi \cos(\theta)} \left(\frac{T_S - T_{SCZ-TM}}{T_S} \right) \right]^*$$

$$\left[\frac{T_S}{T_S - 2T_{SCZ}} \frac{2\sqrt{2}V_{LL-G}}{\sqrt{3}M_G} \right]^+$$

$$\left[\frac{P_{O-BAT}}{V_{BAT}} \frac{2\sqrt{2}V_{LL-G}}{\sqrt{3}M_G} \left(\frac{T_S}{T_S - 2T_{SCZ}} \right) \right]$$

4.7.4 Comparison of Circuit Topologies

To help facilitate a comparison, the SDP of each topology is restated here.

Back to Back VSI-to-VSI Network Topology

$$(SDP)_{av-TM} + (SDP)_{av-G} + (SDP)_{av-DC/DC} =$$

$$\frac{16P_{3\phi-TM}}{\pi \cdot \cos(\phi) \cdot M_{TM}} + \frac{16P_{3\phi-G}}{\pi \cdot \cos(\phi) \cdot M_G} + \frac{P_{O-DC/DC}}{V_{BAT}} V_{DC}$$

Back to Back VSI-to-CSI Z-Network Topology

$$SDP_{AV-VSI-Z-CSI} =$$

$$6 \left[\frac{2}{3} I_{LZ} \frac{T_{OCZ-TM}}{T_S} + \frac{2\sqrt{6}P_{3\phi-G}}{3\pi \cos(\theta)V_{LL-G}} \left(\frac{T_S - T_{OCZ-TM}}{T_S} \right) \right] \left[\frac{2\sqrt{2}V_{LL-G}}{\sqrt{3}M_G} \right] +$$

$$6 \left[\left(\frac{2\sqrt{2}V_{LL-G}}{\sqrt{3}M_G} \right) \left(\frac{T_S}{T_S - 2T_{SCZ-TM}} \right) \right]^*$$

$$\left[\left(\frac{2}{3} I_{LZ} \frac{T_{SCZ-TM}}{T_S} + \left(\frac{8P_{3\phi-TM}}{3V_{DC-TM}M_{TM}\pi \cos(\theta)} \right) \left(1 - \frac{T_{SCZ-TM}}{T_S} \right) \right) \right] +$$

$$\frac{P_{O-BAT}}{V_{BAT}} \left(\frac{T_S}{T_S - 2T_{SCZ-TM}} \right) \frac{V_{LL-G} 2\sqrt{2}}{\sqrt{3}M_G}$$

Back to Back CSI-to-VSI Z-Network Topology

$$SDP_{AV-CSI-Z-VSI} =$$

$$\begin{aligned} & 6 \left[\frac{2}{3} I_{LZ} \frac{T_{OCZ-TM}}{T_S} + \frac{2\sqrt{6}P_{3\phi-G}}{3V_{LL-G}\pi \cos(\theta)} \left(\frac{T_S - T_{OCZ-TM}}{T_S} \right) \right] \left[\frac{2\sqrt{2}V_{LL-G}}{\sqrt{3}M_G} \right] + \\ & 6 \left[\frac{2}{3} I_{LZ} \frac{T_{SCZ-TM}}{T_S} + \frac{8P_{3\phi-TM}}{3V_{dc-TM}M_{TM}\pi \cos(\theta)} \left(\frac{T_S - T_{SCZ-TM}}{T_S} \right) \right] \\ & \left[\frac{T_S}{T_S - 2T_{SCZ-TM}} \frac{2\sqrt{2}V_{LL-G}}{\sqrt{3}M_G} \right] + \\ & \left[\frac{P_{O-BAT}}{V_{BAT}} \frac{2\sqrt{2}V_{LL-G}}{\sqrt{3}M_G} \left(\frac{T_S}{T_S - 2T_{SCZ-TM}} \right) \right] \end{aligned}$$

Comparison

It is now desired to compare each of these SDP equations. To do so, a basic operating scenario is considered. A typical set of operating parameters is the following:

If we ignore the traction motor inverter losses, than power entering this inverter is equal to the power leaving the inverter. Therefore,

$$P_{DC} = P_{3\phi-TM}$$

$$V_{DC-TM} \bar{I}_{DC} = P_{3\phi-TM}$$

$$\bar{I}_{DC} = \frac{P_{3\phi-TM}}{V_{DC-TM}}$$

Where \bar{I}_{DC} is the average DC current entering the traction motor inverter.

In steady state, the average Z network capacitor current is equal to zero. Since the positive rail of the inverter is connected to the Z network inductor, capacitor junction, the average current there is the sum of the average inductor current plus the average capacitor current.

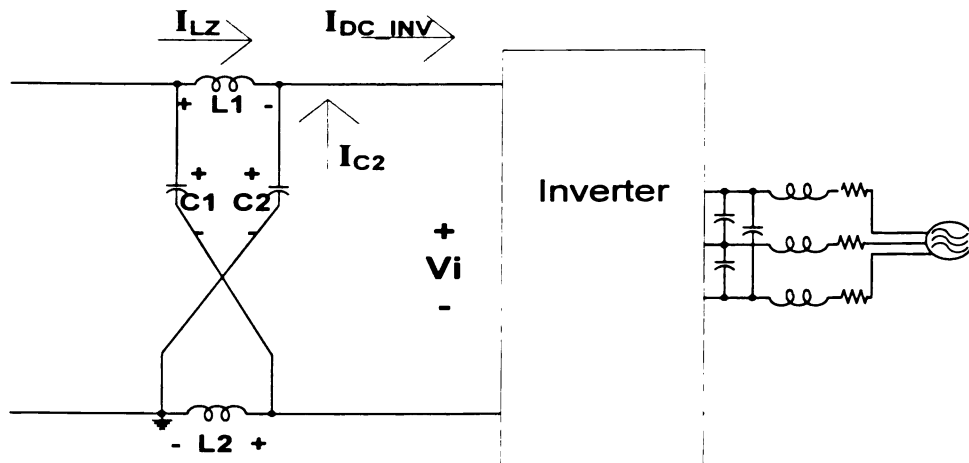


Figure 78 ILZ Average

Since I_C average = 0, then I_{LZ} average = I_{DC_INV} average. The Z network inductor current can not change instantaneously and is close to a constant over a switching cycle. I_{LZ} can be approximated as I_{LZ_avg} .

Also note that the inductor of the Z network delivers current to the traction motor only during the active state (not during the OCZ or SCZ states). If we let

\bar{I}_{DC_INV} be the average current in the DC rail that is being delivered to the traction motor inverter, than

$$I_{LZ_avg} \left(\frac{T_{ACT}}{T_S} \right) = I_{LZ_avg} \left(\frac{T_S - T_{SCZ-AVG} - T_{OCZ-TM}}{T_S} \right) = \bar{I}_{DC_INV}$$

Rearranging we can show,

$$I_{LZ_avg} = \bar{I}_{DC_INV} \left(\frac{T_S}{T_S - T_{SCZ-AVG} - T_{OCZ-TM}} \right).$$

So that we can determine I_{LZ_avg} , we now seek to find \bar{I}_{DC_INV} in terms of the traction motor power.

$$P_{DC} = P_{AC}$$

$$V_{DC_INV} * I_{DC_INV} = P_{3\phi-TM}$$

$$\left(\frac{V_{LL-TM} 2\sqrt{2}}{\sqrt{3}M} \right) * I_{DC_INV} = P_{3\phi-TM}$$

$$I_{DC_INV} = \left(\frac{P_{3\phi-TM} \sqrt{3}M}{V_{LL-TM} 2\sqrt{2}} \right)$$

Restating the equation from above,

$$I_{LZ_avg} = \bar{I}_{DC_INV} \left(\frac{T_S}{T_S - T_{SCZ-AVG} - T_{OCZ-TM}} \right)$$

And substituting,

$$I_{LZ_avg} = \left(\frac{P_{3\phi-TM} \sqrt{3}M}{V_{LL-TM} 2\sqrt{2}} \right) \left(\frac{T_S}{T_S - T_{SCZ-AVG} - T_{OCZ-TM}} \right)$$

Now we have all of the equations that we need to prepare a comparison by using the basic operating condition shown just below.

$$P_{\text{base}} = 200,000.$$

$$V_{\text{base (L-L)}} = 480$$

$$V_{\text{base DC}} = 480$$

$$I_{\text{base}} = 240.5$$

The following typical operating conditions are also defined.

M_G	1. pu
M_{TM}	1. pu
$P_{3\Phi-TM}$	1. pu
$P_{3\Phi-G}$	0.5 pu
$P_{O-BAT} = P_{DC/DC}$	0.5 pu
T_S	0.0001 s
V_{BAT}	0.75 pu
V_{LL-G}	0.5 pu
V_{LL-TM}	0.5 pu
ω_{motor}	314. rad/s
Θ	0.451 rad

Using these values, the following SDP evaluations are determined.

$$SDP_{AV-VSI-VSI} = 9.0$$

$$SDP_{AV-VSI-Z-CVI} = 9.0$$

$$SDP_{AV-CVI-Z-VSI} = 9.0$$

This shows the direct comparability of the Z network topologies against the

traditional Voltage Source topology. Yet the Z network topologies offer the ability to boost or buck voltage levels from one end of the DC link to the other. This improves the available options for maintaining different voltage levels at the generator and traction motor while independently controlling power flow to or from the generator, traction motor, and battery. The VSI-VSI topology is not able to allow different voltage levels at opposite ends of the DC link. The Z network topologies also enjoy an improvement in reliability due to both OCZ and SCZ switching states being allowed. To prevent destruction of the switching devices, these states are forbidden by the current source network and voltage source network, respectively. Below in fig. 78 it is shown that the SDP comparison of the topologies is very similar even when the Z network employs its unique ability to boost voltage levels. For fig. 78, the same parameters as above were observed, except that the traction motor voltage (V_{LL-TM}) was varied from 0.5 to 1.0 pu. That is, the generator voltage level was held at 0.5 pu while the traction motor voltage level was varied.

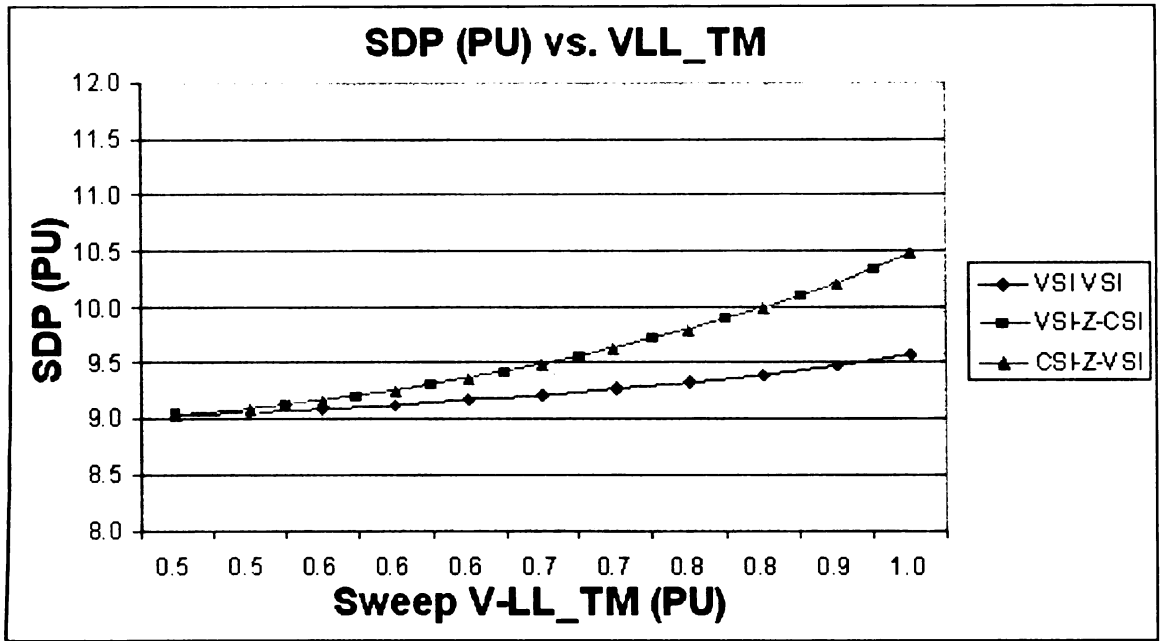


Figure 79 SDP Comparison

Perhaps the similarity between the comparisons is even more obvious if we display SDP on a normalized basis. Figure 79 shows this. From this graph, we see that the Z-Network topologies have an SDP of 1.17 at full boost as compared to an SDP of 1.06 for the non-Z-network topology.

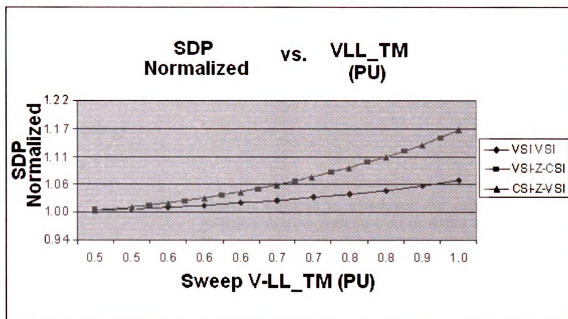


Figure 80 SDP (Normalized) Comparison

This change in voltage levels was accomplished by the Z-Network topologies while holding the modulation index of both the Generator and Traction Motor inverters at one. This is not possible with the VSI-VSI topology.

Maintaining the modulation index at one (100%) reduces voltage stress on the devices by allowing the DC Link voltage level to be kept at a minimum level for the corresponding output AC voltage levels. A modulation index of one also minimizes the harmonic losses in the generator and traction motor.[20]

A list is provided below to summarize the Pros and Cons of the topologies.

SUMMARY LIST

VSI-VSI topology

Pros:

- There is no need to coordinate the switch states of the generator inverter with the traction motor inverter.
- Non-reverse blocking switching devices can be used in both the generator and traction motor inverters.

Cons:

- Generator Inverter can only boost toward the DC Link.
- Generator Inverter can only buck toward the generator.
- An accidental shoot through would be destructive to the switching devices.

Z-Source topologies

Pros:

- This topology has the ability to both buck and boost voltage levels.
- This topology has the ability of maintaining different voltage levels at both ends of the topology. This provides an extra degree of control freedom which can be used to lower stress levels on the switching devices and reduce harmonics in the AC machines.
- There is no risk of shoot-through for the VSI which improves the dependability of this topology.
- There is no risk of open circuit for the CSI which improves the dependability of this topology.

Cons:

- A short circuit zero state of one inverter needs to coincide with an open circuit zero state of the other inverter, and vice versa.

4.8 Future Work

Much has been learned through the works sited above, and this has contributed greatly to this research. In the process of this work, it has been discovered that additional work is needed regarding the loss effects of the combination of inverters and AC machines. The work of others has shown much research about loss effects in power electronics, and much about loss effects in AC machines. A significantly lower amount of work has been done regarding the loss effects of the interaction of these two systems. The research that has been done in this area shows that significant progress may be possible through further research of these topics. Combining power electronics with AC machines has vastly improved the amount of control we have over various systems and this has allowed us to improve operations and conserve energy. However, the switching methods of the power electronic inverters cause harmonics in the AC machines and therefore iron losses. Changes in these switching methods, changes in the way that motors are controlled, and changes in the way that voltage levels are controlled by the power electronics may offer significant improvements over the presently existing technology.

It has been found that the harmonic content of the inverters are lowest at a modulation index of 100% and it is proposed here that a reduction in losses can be achieved by operating the inverters, which are driving the traction motors, at a modulation index of

100%. Including a DC/DC converter in the above topologies may reduce losses in the AC machines. See Figure 80 below.

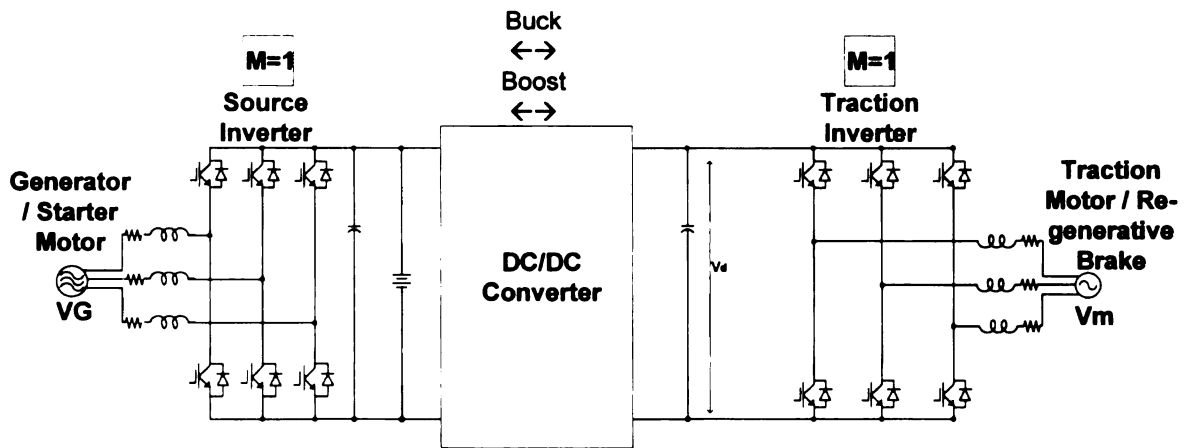


Figure 81 Proposed Topology

By placing a DC/DC converter in the DC link, the traction motor voltage magnitude is controlled by varying the DC link voltage level rather than by varying the modulation index of the inverter. The modulation index is held constant at 100% even while implementing constant volts/hertz operation of the traction motor. Several topologies should be considered.

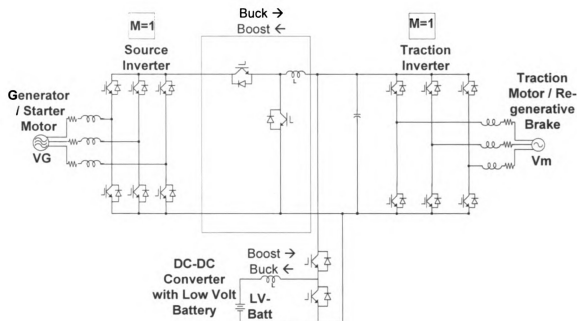


Figure 82 A Possible Implementation of the Proposed Topology Using Traditional Uni-Directional Buck/Boost Converters

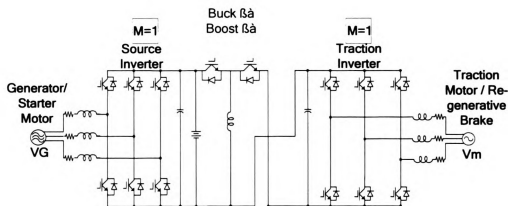
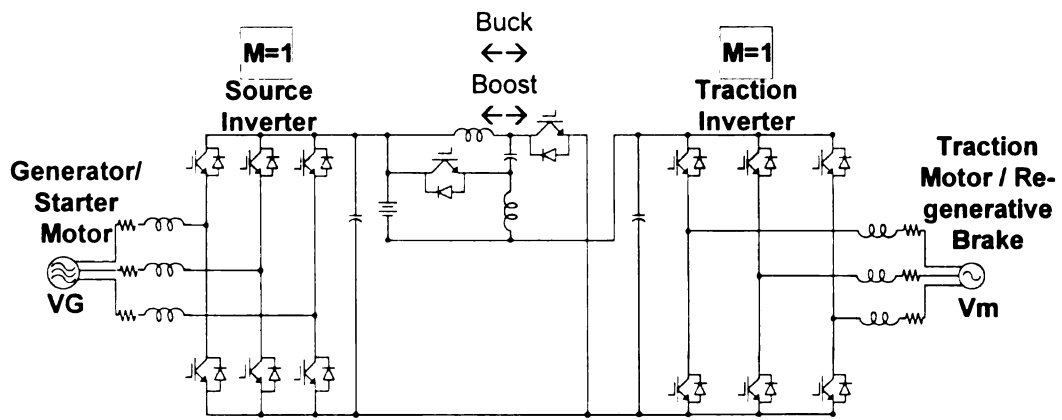


Figure 83 A Possible Implementation of the Proposed Topology Using Traditional Bi-Directional Buck/Boost Converter



**Figure 84 A Possible Implementation of the Proposed Topology
Using a Bi-Directional Quasi-Z-Source
Buck/Boost Converter**

REFERENCES

- [1] Bellis, Mary, "The History of the Automobile – Early Steam Powered Cars," October 14, 2007, <http://inventors.about.com/library/weekly/aacarssteama.htm>
- [2] New World Encyclopedia , "Internal Combustion Engine", May 05, 2009, http://www.newworldencyclopedia.org/entry/Internal_combustion_engine
- [3] M.J. Bradley, and Associates; *Report 59 Hybrid-Electric Transit Buses: Status, Issues, and Benefits*. Washington, D.C.: National Academy Press, 2000.
- [4] H. Moghbelli, K. Ganapavarapu, and R. Langari, "A comparative review of fuel cell vehicles (FCVs) and hybrid electric vehicles (HEVs) – Part II," in *Proc. SAE Future Transportation Technology Conf.*, Costa Mesa, CA, June 2003.
- [5] Syed, Fazal U.; Kuang, Ming L.; et. al. "Derivation and Experimental Validation of a Power-Split Hybrid Electric Vehicle Model." November 2006, IEEE Transactions on Vehicular Technology, Vol 55, No. 6
- [6] R. Thring; *Fuel Cells for Automotive Applications*. New York, NY: The American Society of Mechanical Engineers, 2004.
- [7] K. Thorborg; *Power Electronics*. London, U.K.: Prentice-Hall International (U.K.) Ltd., 1988.
- [8] A. Emadi, S. S. Williamson; "Fuel Cell Vehicles: Opportunities and Challenges," Grainger Power Electronics and Motor Drives Laboratory, Electric Power and Power Electronics Center, Illinois Institute of Technology, Chicago, IL, <http://www.ece.iit.edu/~emadi/>
- [9] M.H. Rashid; *Power Electronics*, 2nd ed. Englewood Cliffs, NJ: Prentice-Hall, 1993.
- [10] R. Erickson, D. Maksimovic; *Fundamentals of Power Electronics*, 2nd ed. Norwell, MA: Kluwer Academic Publishers, 2001.
- [11] G. Ledwich, "Pulse Width Modulation (PWM) Basics," website, 1998. http://www.powerdesigners.com/InfoWeb/design_center/articles/PWM/pwm.shtml
- [12] V. Onde; " ST92141 AC Motor Control Software Library Version 2.1 Update," AN1367 Application Note, STMicroelectronics, 2002.

- [13] D.A. Grant and J. A. Houldsworth: PWM AC Motor Drive Employing Ultrasonic Carrier. *IEE Conf. PE-VSD*, London, 1984, pp. 234-240.
- [14] V. Onde; “ ST92141 AC Motor Control Software Library Version 2.1 Update,” AN1367 Application Note, STMicroelectronics, 2002.
- [15] D.A. Grant and J. A. Houldsworth: PWM AC Motor Drive Employing Ultrasonic Carrier. *IEE Conf. PE-VSD*, London, 1984, pp. 234-240.
- [16] F. Z. Peng, “Z-Source Inverter,” *IEEE Transactions on Industry Applications*, vol. 39, No. 2, pp. 504-510, March/April 2003.
- [17] F. Z. Peng and Miaosen Shen, Zhaoming Qian, “Maximum Boost Control of the Z-source Inverter,” in *Proc. of IEEE PESC 2004*.
- [18] Miaosen Shen, Jin Wang, Alan Joseph, Fang Z. Peng, Leon M. Tolbert, and Donald J. Adams, “Maximum constant boost control of the Z source inverter.” in *Proc. IEEE IAS’04*, 2004, p.142.
- [19] Srinivas Iyer, “The Mean Time-to-Failure of some Special Series-Parallel Arrays”, *IEEE Transactions on Reliability*, Vol. 40, No. 1, 1991 April
- [20] Ruifang Liu, Chris Chunting Mi, David Wenzhong Gao, “Modeling of Iron Losses of Electrical machines and Transformers Fed by PWM Inverters”, *Power Engineering Society General Meeting, 2007, IEEE 24-28 June 2007* Pages: 1-7, digital object identifier 10.1109/PES.2007.385873
- [21] K. D. Holland; “Z-Source Inverter Control for Traction Drive of Fuel Cell – Battery Hybrid Vehicles,” Thesis presented to Michigan State University, Department of Electrical and Computer Engineering, August 26, 2005
- [22] Mohan, Ned; Underland, Tore M.; Robbins, William P.; “Power Electronics”, 2003 John Wiley & Son’s, Inc. , Hoboken, New Jersey
- [23] Sze, S.M.; Kwok, K. NG; “Physics of Semiconductor Devices”, 2007 John Wiley & Sons, Inc., Hoboken, New Jersey

MICHIGAN STATE UNIVERSITY LIBRARIES



3 1293 03063 5498